Contributions of Intrinsically Disordered Regions of Proteins to the Assembly of Ribonucleoprotein Granules

David S. W. Protter

B.A. Whitman College, 2010

A thesis submitted to the Faculty of the Graduate School of the University of Colorado in partial fulfillment of the requirement for the degree of Doctor of Philosophy

Department of Chemistry and Biochemistry

2017

This thesis entiled:

Contributions of Intrinsically Disordered Regions of Proteins to the Assembly of Ribonucleoprotein Granules

authored by David Stephen Warren Protter

has been approved for the Department of Chemistry and Biochemistry

---

Dr. Roy Parker, Committee Chair

Dr. Christopher Link, Second Reader

Date

The final copy of this thesis has been examined by the signatories, and we find that both the content and the form meet acceptable presentation standards of scholarly work in the above mentioned discipline.

Abstract

Protter, David Stephen Warren (Ph.D., Biochemistry)

Contributions of Intrinsically Disordered Regions of Proteins to the Assembly of Ribonucleoprotein Granules

Thesis directed by Professor Roy Parker.

Cells assemble large, non-membrane bound granules of protein and RNA, termed Ribonucleoprotein granules (RNP granules), often in response to a wide variety of cellular stresses. This behavior is conserved from yeast to mammals. Some RNP granules appear important in the stress response, while others are important for proper organismal development, and still others for control of RNA degradation and transport. Curiously, proteins found within granules are disproportionately likey to contain Intrinsically Disordered Regions. Here, I show that those disordered regions can often drive higher order assembly *in vitro* and contribute to granule assembly *in vivo*. I found that these domains can make it easier for proteins to undergo a process known as Liquid-Liquid Phase Separation in response to changes in ionic strength, wherein the protein of interest self-partitions into a concentrated liquid phase. The droplets that form mimic many of the behaviors of RNP granules in cells, such as recruitment of other IDR-containing proteins, assembly in response to RNA, and rapid exchange of contents with the surrounding medium. I also found that proteins that form these droplets tend to aggregate over time, turning the dynamic droplets into static structures.

Further, I identified several limitations to my *in vitro* model, most importantly the impairment of IDR-based phase separation in the presence of other proteins or cellular lysates. However, I also helped uncover the synergistic relationship between IDRs and the more well studied protein-protein and protein-RNA interactions that are important for granule assembly. I therefore propose an inclusive model of granule assembly which asserts that a wide variety of types of interactions are important, and that it is the sum-total of these interactions that determines whether or not a granule assembles.

Acknowledgements

I would like to thank the CU/NIH Biophysics Training Program for funding and valuable mentorship. I am sure the program will continue to help create exceptional researchers by pushing students to challenge their knowledge of biophysical techiques and principles.

I would like to acknowledge the many people who have had an impact on my time as a PhD student at CU Boulder. First, I would like to acknowledge the many wonderful graduate students I have had the pleasure of working with. I would especially like to thank Joe Cardiello and Briana Van Treeck for years of close friendship and support. Briana was especially understanding as I struggled through years of droplet formation assays, and I hope I have somewhat repaid her as she has found herself recently doing the same things. Joe has supported me emotionally through the hard times that come with research and life. It was awesome being housemates, and I hope we are all still close 10 years from now. No matter where I live you will both always be welcome in my home.

I would also like to acknowledge my teammates on Love Tractor, a team that was an important outlet for me when I was struggling emotionally with lab work. I also learned a tremendous amount about how to be a good person from this team, and I have tried my best to hold to the team tenants of maintaining positivity in the face of adversity, and remembering that there are many ways to measure success beyond the traditional metric of winning or losing. I would especially like to thank Jesse Kuroiwa, Stanly Strunk, and Dave Kamin for the years of hard work they put into making me a better player and making the team nationally competitive. Also Id like to thank Jack McShane for teaching me how to play defense and exercise more effectively, Scott Forrester for teaching me the value of being 65, and Stephanie Frost for teaching me how to say weird stuff but still sound cool. Thanks to Tyler Matheney for teaching me the importance of bicep curls in the squat rack.

I would like to thank Dr. Antony Cooper for whom I worked as an RA at the Garvan Institute of Medical Research, prior to applying to graduate school. Without his tutelage I doubt I would have applied to a doctorate program.

I would of course also like to thank Roy Parker for being a great mentor who taught me the importance of being 1) self-critical of ones own favorite model, and 2) being flexible and agile with ones scientific thinking. It would have been easy for both of us to commit to the popular and flashy model of IDR-driven phase separation being the main driver of granule assembly. However, Roy was always willing to listen to me when I was critical of that model, and of his own suggestions for experiments. I have learned how to be a more concise thinker, how to go for the jugular, and how to give the kind of talk that makes all your peers say wow, that was really clear and interesting! This was certainly not an easy project to maintain a surfeit of enthusiasm for, but Roy continually pointed out the importance of communicating what we had seen to the field at large, helping me to stay motivated. I would also like to thank the entire Parker Lab (especially Anne Webb, Denise Muhlrad, and Carolyn Decker) who made lab a fun and productive place. I would also like to thank Saumya Jain, Sarah Mitchel, and Robert Walters for endless advice.

Finally, I would like to thank my parents Ann and Andy, and my brother Michael, for always supporting me emotionally throughout the challenging time that is a PhD. Thanks for helping me choose to come to Colorado, thanks for appreciating my love of Ultimate and the outdoors, and thanks for keeping me in your thoughts even when I dont call home for weeks at a time.

Dedication

This thesis is dedicated to Dr. Rhonda Warr, who fought through a sexist culture in her home of Australia in the 1970s and 80s so that she could become a great scientist and a great mother, while she was afforded the chance.

Contents

List of Figures

1 Introduction

1.1 RNP Granules

A variety of non-membrane bound cellular compartments are termed Ribonucleoprotein granules (RNP granules) due to their high concentrations of protein and RNA. These include nuclear granules such as Cajal bodies, paraspeckles, and the nucleolus, as well as cytoplasmic granules such as stress granules and processing bodies (Spector, 2006). Other examples of RNP granules include neuronal granules and germ cell granules, which function in synaptic remodeling and maternal mRNA storage in early development (Barbarese et al., 2013; C. P. Brangwynne et al., 2009). RNP granules are generally dynamic and dependent on RNA for their assembly. Therefore, the formation of dynamic RNP granules to concentrate specific cellular components is a conserved strategy across multiple organisms and in different cellular compartments.

Stress granules and P-bodies are two conserved cytoplasmic mRNP granules that form from pools of untranslating mRNA (Anderson & Kedersha, 2009; J. R. Buchan & Parker, 2009; Parker & Sheth, 2007). Stress granules form from mRNAs stalled in translation initiation and contain various translation initiation factors, a variety of RNA binding proteins, and many non-RNA binding proteins (Jain et al., 2016). P-bodies contain mRNAs associated with translational repressors, and the mRNA decay machinery. mRNAs within P-bodies can be targeted for decapping and degradation but mRNAs can also be degraded outside of P-bodies (Aizer et al., 2014). P-bodies and stress granules can dock and/or overlap in both yeast and mammalian cells suggesting a dynamic mRNA cycle wherein mRNPs can be remodeled within these assemblies and exchange between stress granules and P-bodies ((J. R. Buchan, Muhlrad, & Parker, 2008; Kedersha et al., 2005); Figure 1). During RNP granule disassembly mRNPs within P-bodies and stress granules can return to translation or, in some cases, can be targeted for autophagy (**Figure 1**), which provides a second system for stress granule clearance (Bhattacharyya, Habermacher, Martine, Closs, & Filipowicz, 2006; Brengues, Teixeira, & Parker, 2005; J. Buchan,

Kolaitis, Taylor, & Parker, 2013).

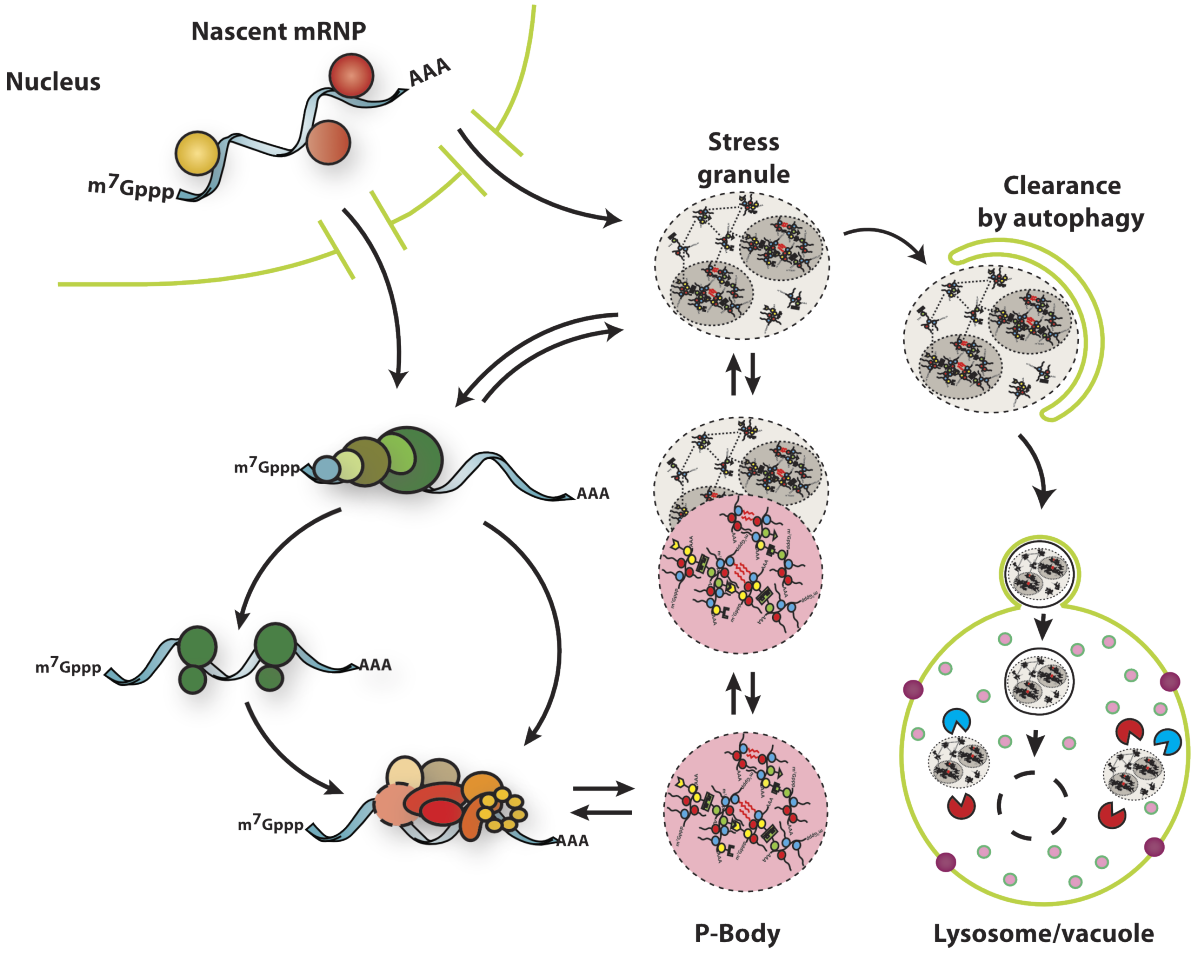

Figure 1: **Stress Granules Are Dynamic and Have Multiple Fates**
Stress granules form from untranslating messenger ribonucleoproteins (mRNPs). They can interact with P bodies, exchange components with the cytoplasm, and undergo autophagy.

Stress granules are of interest for four reasons. First, stress granule formation and dynamics can affect mRNA localization, translation and degradation, as well as signaling pathways and antiviral responses. Second, stress granules share many components with maternal mRNP and neuronal granules suggesting they reveal a conserved mechanism of mRNP compartmentalization (e.g (Barbee et al., 2006)). Third, mutations that increase stress granule formation and/or limit stress granule clearance are causative in some neurodegenerative diseases (Y. R. Li, King, Shorter, & Gitler, 2013; Ramaswami, Taylor, & Parker, 2013). Finally, as representative of non-membrane bound organelles, an understanding of their assembly and function illustrates an exciting new area of cell biology.

1.2 What are stress granules?

Three observations suggest stress granules represent assemblies of mRNPs stalled in translation initiation. First, stress granules form when translation initiation is inhibited either by drugs or by stress responses (Anderson & Kedersha, 2009). Similarly, stress granule-like RNP granules exist in neurons and embryos where there are significant pools of untranslating mRNPs (Martin & Ephrussi, 2009). Second, stress granules fail to form when mRNAs are trapped in polysomes, suggesting that mRNAs associated with ribosomes are unable to enter stress granules. Third, stress granules are observed to contain translation initiation factors (J. R. Buchan & Parker, 2009), and specific mRNAs that are stalled in steps of translation initiation such as TOP mRNAs (Damgaard & Lykke-Andersen, 2011).

Stress granules contain a diverse proteome. Based on proteomic analysis of stable sub-structures within stress granules referred to as "cores" (see below), ~50% of stress granule components are a subset of RNA binding proteins (Jain et al., 2016). Stress granule components that do not bind RNA are presumably recruited to stress granules through protein-protein interactions. Such non-RNA binding proteins include post-translation modification enzymes, metabolic enzymes, and protein or RNA remodeling complexes, which can affect stress granule assembly and disassembly (see below). Stress granules also contain key components of signaling pathways ((J. R. Buchan, 2014; Jain et al., 2016) which highlight how the formation of stress granules can alter signaling pathways. Also, see below.). An overlapping group of proteins form aggregates during extreme heat stress in yeast and some of those aggregating proteins are shown to be components of stress granules (Cherkasov et al., 2015; Wallace et al., 2015). These, and other, experiments show that the composition of stress granules can vary under different conditions revealing that they are both complex and variable assemblies (J. R. Buchan & Parker, 2009).

Stress granules are not uniform structures and contain internal sub-structures as judged by either electron dense regions in EM micrographs, (Souquere et al., 2009) or as regions identified by super-resolution fluoresence microscopy with higher concentrations

of proteins and mRNAs (Jain et al., 2016). These structures are referred to as "cores", and can be biochemically purified (Jain et al., 2016). This suggests that stress granules have two distinct layers (**Figure 1**), a core structure that is surrounded by a less concentrated, and potentially more dynamic shell. These two regions of stress granules may have different components, functions and dynamics.

Four examples suggest substructure within RNP granules is a general principle. First, the nucleolus contains dense fibrillarin cores as a substructure (C. P. Brangwynne, Mitchison, & Hyman, 2011). Second, *C. elegans* P granules show spatial orientation when bound to the nuclear pore, forming a consistent "tripartite sandwich." (Sheth, Pitt, Dennis, & Priess, 2010) Third, lattice-light sheet microscopy on P-granules in live *C. elegans* reveals substructures (J. T. Wang et al., 2015). Finally, FISH on *Drosophila* germline granules reveals foci of specific mRNAs implying a sub-granular organizing principle (Little, Sinsimer, Lee, Wieschaus, & Gavis, 2015).

Stress granules are dynamic structures. In mammalian cells, stress granules undergo fusion, fission and flow in the cytosol (Kedersha et al., 2005). Moreover, by FRAP, most components of stress granules exchange rapidly with half-times for recovery of less than 30 seconds (reviewed in (J. R. Buchan & Parker, 2009)). Interestingly, these FRAP experiments have also revealed an "immobile pool" of protein that does not exchange on a similar timescale suggesting that a subset of the molecules within stress granule components exchange very slowly. One intriguing possibility is that components in the shell structure can exchange rapidly, while stress granule components in the core layer may be less dynamic (Jain et al., 2016).

1.3 Interactions influencing stress granule assembly

Stress granules assemble when untranslating mRNPs interact through protein-protein interactions between mRNA binding proteins (Figure 2a). Analyses of the proteomes of yeast and mammalian stress granule cores identified a dense network of protein-protein interactions between stress granule components that could contribute in redundant manners to stress granule formation (Jain et al., 2016). For example, in both mammals and

yeast, Atx2/Pbp1, or TIA1/Pub1 proteins promote, but are not absolutely required for, stress granule assembly (J. R. Buchan et al., 2008; Gilks et al., 2004). The redundancy of interactions suggests that stress granule formation under different conditions can occur by different interactions. For example, the paralogs G3BP1 and G3BP2 play important roles in stress granule formation in mammalian cells in oxidative stress, both by self-interaction,(Tourriere, 2003) and by interaction with the caprin RNA binding protein (Solomon et al., 2007). However, during osmotic stress G3BP1/2 and caprin are not required for stress granule formation (Kedersha et al., 2016). Similarly, in yeast Gtr1, Rps1b, and Hgh1 promote stress granule formation during glucose starvation, but suppress stress granule formation during heat shock (X. Yang et al., 2014). Therefore, granule assembly is highly redundant, and the mechanism of assembly can be context specific. This is interesting because it suggests that granules can assemble differently in response to specific cellular conditions, and that stress granules may have different functions for different stresses.

Protein methylation, phosphorylation and glycosylation influence stress granule assembly, presumably by altering specific protein-protein interactions. For instance, phosphorylation of G3BP impairs its ability to multimerize, which impairs granule assembly (Tourriere, 2003). Similarly, granule disassembly during recovery is promoted by the phosphorylation of the granule protein Grb7 (Tsai, Ho, & Wei, 2008), and the DYRK3 kinase (Wippich et al., 2013). Many stress granule proteins contain RGG motifs that are sites of arginine methylation (Nott et al., 2015). This methylation can impact stress granules through the recruitment of Tudor domains. For example, the Tudor domain of TDRD3 is both sufficient and necessary for the recruitment of that protein to stress granules, and point mutants that impair TDRD3 binding to methylated arginine impair its localization to stress granules (Goulet, Boisvenue, Mokas, Mazroui, & Cote, 2008). O-Glc-NAc glycosylation of proteins also enhances stress granule formation (Ohn, Kedersha, Hickman, & Tisdale, 2008). Based on over-expression and inhibitor studies, acetylation and parylation have also been suggested to play a role in stress granule assembly in mammalian cells (Kwon, Zhang, & Matthias, 2007; Leung et al., 2011).

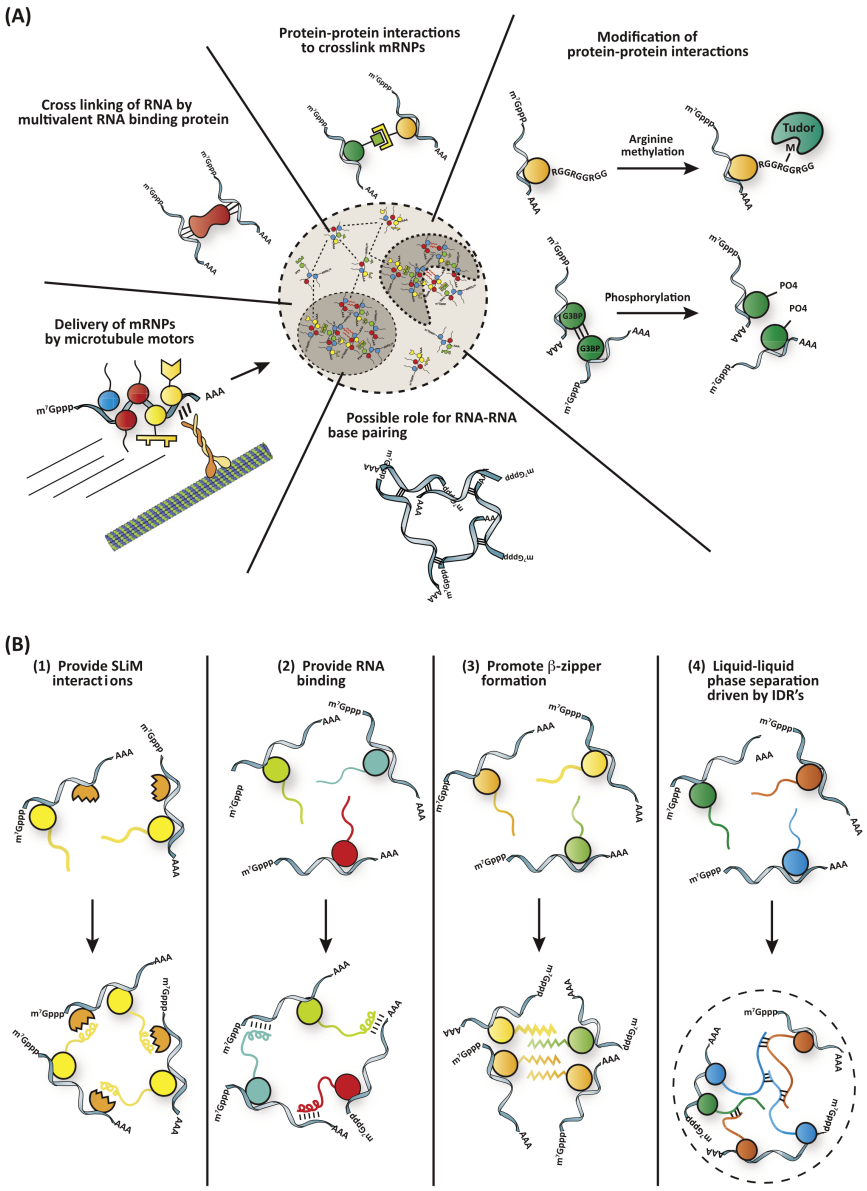

Figure 2: **Intermolecular interactions that drive RNP granule assembly**

(A) A diverse set of macromolecular interactions contribute to granule assembly

(B) Various ways in which Intrinsically Disordered Regions could contribute to granule assembly

1.4 Stress Granule Assembly: Possible roles for Intrinsically disordered domains

Given the dynamic behavior of RNP granules in cells, and the behavior of RNP granule components in vitro, a current model is that many RNP granules are liquid-liquid phase separations (LLPS) driven by dynamic and promiscuous interactions between IDRs (Elbaum-Garfinkle et al., 2015; Kroschwald et al., 2015; Lin, Protter, Rosen, & Parker, 2015; Molliex et al., 2015; Nott et al., 2015). A LLPS occurs when a molecule, or mixture of molecules, forms a network of multivalent weak interactions, which allows those molecules to concentrate into a separate phase. When applied to stress granules this model for assembly consists of three separate aspects worthy of discussion.

One issue is whether stress granules represent a phase separation wherein multivalent interactions between their components leads to the formation of a higher order structure. By definition, any assembly larger than a dimer requires multivalent interactions for its formation. Moreover, stress granules appear to form through the cross linking of untranslated mRNAs that can provide a scaffold for multiple mRNA binding proteins, thereby allowing each mRNP multivalent interactions and stress granule formation. Thus, stress granules can certainly be thought of as forming by phase separation, or as a multivalent assembly. Because of this nature, stress granules will have two interesting properties. First, because of the diversity of interactions promoting their formation, stress granules will not be specifically defined, and the interactions between components can vary, and even be rearranging. In addition, macromolecules below a certain size should enter, diffuse within, and exit stress granules. This principle is illustrated wherein 40 kDa, but not 155 kDa, dextrans can diffuse into the related P-granules in nematodes (Updike, Hachey, Kreher, & Strome, 2011).

Importantly, the liquid-like nature of an assembly is not due to its formation by phase separation. Indeed, protein crystals are also formed by phase separation. The material properties of the assembly are derived from the relative strengths of the interactions holding them together. Macromolecules interacting with slow off-rates will phase separate

into a solid, while interactions with fast off-rates will lead to liquid assemblies.

Another issue is how prevalent the role is for intrinsically disordered regions of proteins in stress granule formation, which is based on the following observations. First, many RNA binding proteins found in RNP granules contain intrinsically disordered regions (IDRs), also referred to as low complexity sequences (LCS), and containing the more narrowly defined prion-like domains (PrLD, which are identified by amino acid composition similar to fungal prion proteins predicted to have high cross-beta zipper forming abilities (Decker, Teixeira, & Parker, 2007; Kato et al., 2012; Reijns, Alexander, Spiller, & Beggs, 2008). Second, the IDR/prion-like-domain of the human TIA-1 protein promotes stress granule formation and can be substituted with the prion-like domain of the yeast Sup35 protein (Gilks et al., 2004). Although other evidence that IDRs affecting stress granule formation is limited, IDRs do affect other RNP granules. Specifically, assembly of P-granules in *C. elegans* requires an FG repeat region on the PGL proteins,(Hanazawa, Yonetani, & Sugimoto, 2011) the IDR of RBM14 is required for paraspeckle assembly, (Hennig et al., 2015) and P-body assembly in yeast is promoted by PrLDs on Lsm4 and several other P-body components (Decker et al., 2007; Reijns et al., 2008). However, since components of stress granules show a dense network of defined protein-protein interactions (Jain et al., 2016), a reasonable hypothesis is that stress granules form by a number of different protein-protein interactions, some of which involve IDRs.

The final issue to consider is whether stress granules are held together by weak promiscuous interactions of IDRs. In principle, IDRs could play four possible roles in stress granule assembly (**Figure 2B**). First, IDRs could provide access to Short Linear Motifs (SLiMs), short protein sequences that typically fit into binding sites on other well-folded domains. Precedent for IDRs functioning as important sites of SLiMs comes from the analysis of P-bodies, where many SLiMs in IDRs contribute to P-body assembly (Jonas & Izaurralde, 2013). Second, IDRs can contain regions that bind RNA (Lin et al., 2015; Molliex et al., 2015) and therefore might provide additional interactions between mRNPs in granules. Third, since IDRs can often form amyloid-like fibers in vitro, including both hetero- and homotypic interactions, perhaps IDRs function to stabilize granules by the

formation of cross-strand beta zippers (Guo et al., 2011; Hanazawa et al., 2011; Kato et al., 2012; Lin et al., 2015; Reijns et al., 2008).

A fourth manner by which IDRs might affect RNP granule assembly is through weak dynamic interactions between IDRs, which then promote a liquid-liquid phase separation (LLPS), which has gathered support from the observation that many IDRs from RNP granule components undergo LLPS *in vitro* , including the RNP granule components hnRNPA1, (Lin et al., 2015; Molliex et al., 2015) Ddx4,(Nott et al., 2015) LAF-1,(Elbaum-Garfinkle et al., 2015) and FUS (Patel et al., 2015). Interestingly, LLPS triggered by IDRs in vitro are initially dynamic and liquid-like, consistent with their formation through numerous weak interactions, but over time the high concentration of IDRs within the LLPS can promote the formation of stronger interactions, including amyloid-like structures (Lin et al., 2015; Molliex et al., 2015; Patel et al., 2015; Xiang et al., 2015; H. Zhang et al., 2015).

One complication with considering stress granules as a simple LLPS is that they contain stable core substructures, which implies more stable interactions are also present (Jain et al., 2016). Given this, there are two models for how LLPS could contribute to stress granule formation (**Figure 3A,B**) in the context of stable substructure. In one model, stress granules form first by a LLPS through weak dynamic interactions,(Lin et al., 2015; Molliex et al., 2015; Patel et al., 2015) and the high concentration of components in such a LLPS promotes the formation of the core structures, analogous to the formation of amyloid fibers in LLPS in vitro (Lin et al., 2015; Molliex et al., 2015; Patel et al., 2015).

Alternatively, since IDRs can be promiscuous in their interactions, we favor a model wherein mRNPs first condense into stable core structures through strong, specific interactions, and then the high local concentration of IDRs on stress granule components would trigger a LLPS (see below). This may explain the dynamic shell structure surrounding the cores (Jain et al., 2016).

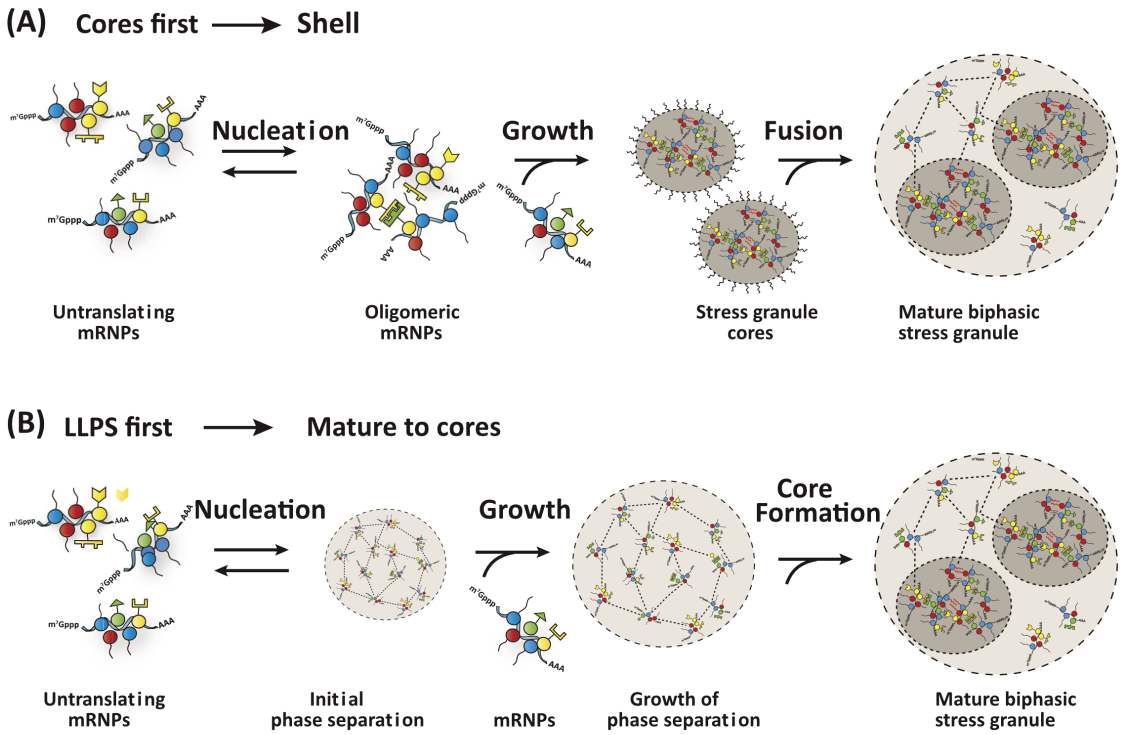

Figure 3: **Two models for discrete phases of stress granule assembly**

Stress granules can by hypothesized to undergo three phases of assembly:

(A) In the Cores First model, cores precede assembly of large stress granules. The first phase of assembly is the nucleation of translationally repressed RNPs into oligomers. The second phase of assembly is growth of these oligomers into larger assemblies by addition of more translationally repressed RNPs. The third phase of assembly is fusion of these core assemblies and recruitment of the dynamic shell to form the large, microscopically visible granules typically observed in cells. Some of the stability of cores may be due to amyloid interactions, as indicated by squiggly red lines.

(B) In the LLPS First model, the formation of large stress granules precedes core assembly. The first phase of this model is the nucleation of translationally repressed RNPs into initial phase separated droplets, held together by weak dynamics interactions. The second phase is growth of initial droplets by the addition of translationally repressed RNPs. The third phase of assembly is core formation within phase separated granules due to the high local concentration of proteins within the droplets. In this model, the formation of cores may be driven in part by amyloid interactions, as indicated by squiggly red lines.

1.5 Multiple phases of stress granule assembly

One can identify multiple steps in stress granule assembly (**Figure 3**). In the most parsimonious model, nucleation occurs wherein we hypothesize the formation of oligomeric assemblies of untranslating mRNPs, whose assembly can be controlled by post-translational modifications and/or RNP remodelers. For example, defects in the CCT chaperonin complex give more stress granules in yeast, which is consistent with the CCT complex limiting nucleation, either by remodeling interactions between mRNPs, or by limiting misfolded proteins, which in some contexts can overlap and potentially seed stress granule formation (Cherkasov et al., 2013, 2015; Jain et al., 2016; Kroschwald et al., 2015; Wallace et al., 2015). Second, the nucleated states then grow by the joining of additional mRNPs to form small stress granules of ˜200 nm in both yeast and mammals (Jain et al., 2016). Under some conditions, the oligomeric seeds of stress granules may form by transitions in mRNP composition that occur at P-bodies. This is suggested by the observation that stress granules tending to form after and on P-bodies in yeast during glucose deprivation, and the observation that some stress granules in mammalian cells appear to grow out of P-bodies (J. R. Buchan et al., 2008). In mammals, a third step occurs wherein, in a microtubule transport-dependent manner, (Chernov et al., 2009; Loschi, Leishman, Berardone, & Boccaccio, 2009; Nadezhdina, Lomakin, Shpilman, Chudinova, & Ivanov, 2010) smaller stress granules merge and form higher order assemblies with stable core structures surrounded by a more dynamic and less concentrated "shell" structure.

1.6 Dynamics, disassembly and clearnance of stress granules

Stress granules are dynamic structures and exhibit liquid-like behavior, rapid exchange rates of components, disassembly into translating mRNPs, and clearance by autophagy. Several lines of evidence now suggest a model where the dynamics of stress granules arises, at least in part, by ATP dependent remodeling complexes. For example, acute pharmacological impairment of ATP production eliminates stress granule movement, fusion and fission (Jain et al., 2016). Moreover, ATP depletion increases the pools of G3BP that

fails to recover after photobleaching, (Jain et al., 2016) suggesting that at least some of the protein exchange is dependent on ATP. Interesting, some G3BP protein does still recover, which could either be due to residual ATP in the cell, or could suggest that some G3BP is recruited to stress granules by interactions with intrinsically high off rates.

The ATP dependence of granule dynamics supports a general model of dynamic RNP assemblies as "active liquids", where the energy of ATP driven remodeling events keeps the assembly in a dynamic state (C. P. Brangwynne et al., 2011). In this view, stress granule proteins and mRNA can form stable interactions that are disrupted by ATPases. During stress, when concentrations of granule components like non-translating RNA are high, ATPases transiently disrupt such interactions and thereby contribute to fast exchange rates. During recovery this disruption leads to disassembly. Potentially, residual material is then subject to autophagy. The ATPases involved in stress granule dynamics are likely to include complexes that directly affect interactions within stress granules such as protein chaperones and RNA helicases (**Figure 4**), as well as those affecting cellular transport, such as microtubule dependent motors (Chernov et al., 2009; Loschi et al., 2009; Nadezhdina et al., 2010).

Several observations argue RNA/DNA helicases, which utilize the energy of ATP hydrolysis to either unwind DNA/RNA or to displace proteins bound to nucleic acids, also play roles in controlling stress granule assembly and disassembly (**Figure 4**). Stress granules contain a variety of different helicases including many members of the common DEAD-box helicase family (Jain et al., 2016). Moreover, the DEAD box helicases Ded1 (mammalian orthologue: DDX3) is a conserved component of stress granules and promotes stress granule assembly (Hilliker, Gao, Jankowsky, & Parker, 2011). However, mutations in Ded1 that block its ATPase activity trap mRNAs in stress granules and lead to the inhibition of translation, indicating an important role for ATP hydrolysis in the release of mRNAs back into the cytosol. Similarly, the exchange rate of the RHAU DEAD box from mammalian stress granules is slowed dramatically by cis acting mutations in the ATPase active site (Chalupnikova et al., 2008).

The MCM and Rvb complexes are conserved components of stress granules, and affect

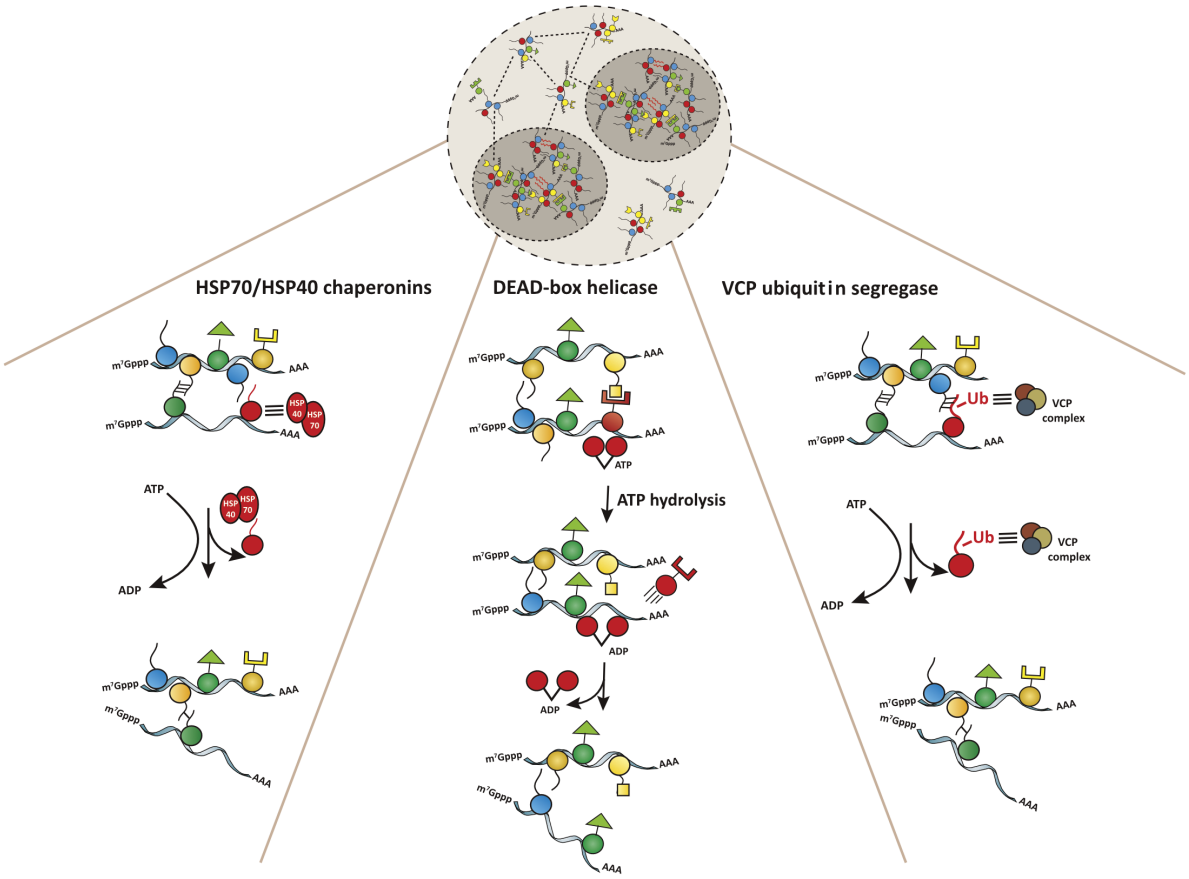

Figure 4: **Various ATPases impact granule assembly**
Heat shock proteins, helicases, and VCP all impact stress granule assembly by remodeling specific interactions utilizing the energy of ATP hydrolysis.

the rate of clearance of stress granules from cells. The key observation is that loss of function of either the MCM or Rvb complexes leads to an increased rate of stress granule disassembly during stress recovery in both yeast and mammalian cells (Jain et al., 2016). Since the MCM complex is known to act on DNA and function in DNA replication (Bell & Botchan, 2013) a role in stress granules would be a novel function for this complex. The Rvb complex also primarily acts on DNA but has been seen to affect snoRNA biogenesis and even function in translation control of HIV transcripts, which may be related to how it affects stress granules (Mu et al., 2015). Since helicases would generally be expected to disassemble RNA-protein assemblies, it remains to be determined how these helicases function to increase the stability of stress granules.

The AAA-ATPase VCP/Cdc48 appears to remodel stress granules in a manner that promotes their targeting to autophagy, and may also affect their disassembly. The key

observation is that inhibition of VCP/Cdc48 function in yeast or mammals leads to the accumulation of stress granules in the cytosol, as well as a reduction in stress granules that can be trapped in intravacuolar vesicles (J. Buchan et al., 2013). VCP/Cdc48 is an ubiquitin segregase and uses the energy of ATP hydrolysis to extract ubiquinated proteins from complexes (Meyer & Weihl, 2014). Thus one hypothesis is that VCP/Cdc48 may potentially extract some ubiquinated protein from stress granules and that process can, at a minimum, allow stress granules to be targeted for autophagy (**Figure 4**).

A number of protein chaperones affects stress granule assembly or disassembly. For example, inhibition of Hsp70 function in yeast or mammals leads to either increased stress granule formation and/or delayed disassembly of stress granules (Cherkasov et al., 2013; Mazroui, Di Marco, Kaufman, & Gallouzi, 2007; Walters, Muhlrad, Garcia, & Parker, 2015). Moreover, both Hsp70 and Hsp40 proteins can localize to stress granules in yeast and mammalian cells (Cherkasov et al., 2013; Kroschwald et al., 2015; Mazroui et al., 2007; Walters et al., 2015). Interestingly, in yeast different Hsp40 proteins, which often provide substrate specificity to Hsp70s, affect stress granules in different manners. Ydj1 plays a role in disassembling stress granules to promote new translation, while Sis1 functions to trigger stress granules entering autophagy (Wallace et al., 2015). This implies that different remodeling complexes can lead to different fates of stress granule components.

Under extreme heat shock conditions, the Hsp104 chaperone is also required for stress granule disassembly and timely resumption of translation (Cherkasov et al., 2013; Kroschwald et al., 2015). Interestingly, under extreme heat shock in yeast and Drosophila cells, stress granules appear to overlap with unfolded proteins, and this interaction is limited by Hsp104 (Cherkasov et al., 2013). One interpretation of this observation is that under extreme heat shock IDRs within stress granules are prone to misfolded and thereby interact with other misfolded proteins. Interactions between misfolded proteins and stress granules could suggest that in some contexts mutations causing misfolded proteins might enhance stress granule formation, and/or that stress granule formation might stimulate proteins misfolding, which might contribute to some pathologies (Vanderweyde et al.,

2012).

1.7 RNP Granules as "Active" Liquid may be a general principle

The concept of RNP granules as an active liquid, with ATP dependent remodeling complexes driving their observed liquidity is a general principle. For example, nucleoli require ATP for their own liquid-like behavior, and are 10 –fold less dynamic when ATP is depleted (C. P. Brangwynne et al., 2011). Similarly, germline RNP processing bodies in *C. elegans* form solid, crystalline-like aggregates when the helicase CGH-1 is non-functional (DDX6 in humans) (Hubstenberger, Noble, Cameron, & Evans, 2013). The ability of cells to modulate RNP granule assembly, disassembly, and dynamics via ATPases gives cells multiple points of regulation over granule dynamics, as well as leading to hyper-stable granules under conditions where stability may be advantageous, such as acute energy depletion.

1.8 Functions of stress granules

Stress granule formation is expected to affect biological reactions in two manners. First, due to the high local concentration of components, equilibriums of interacting molecules will shift towards associated states. For example, during viral infections stress granules recruit numerous antiviral proteins including RIG-1, PKR, OAS, and RNaseL, stimulating their activation, and thereby enhance induction of the innate immune response and viral resistance (Onomoto et al., 2012; Reineke, Kedersha, Langereis, van Kuppeveld, & Lloyd, 2015; Reineke & Lloyd, 2015) . Given this function, many viruses employ mechanisms to block stress granule induction including proteolytic cleavage of G3BP (Reineke & Lloyd, 2013). Stress granule formation might also promote the interaction of mRNAs with translation factors, and thereby enhance the formation of translation initiation complexes (J. R. Buchan et al., 2008).

A second manner by which stress granules may affect biological reactions is by limiting the interactions of sequestered components with the bulk cytosol. In this manner, stress

granules have been proposed to modulate signaling pathways by sequestering components of TOR, RACK1, or TRAF2 signaling pathways (Arimoto, Fukuda, Imajoh-Ohmi, Saito, & Takekawa, 2008; W. J. Kim, Back, Kim, Ryu, & Jang, 2005; Takahara & Maeda, 2012; Thedieck et al., 2013). Because stress granules also sequester numerous proteins involved in RNA physiology and/or metabolism, the formation of stress granules is likely to have broad affects on the physiology of cells. However, it should be noted that how stress granule assembly fully affects either the regulation of mRNA function, and/or other aspects of cell physiology remains to be established.

1.9 Stress granules in disease

Mutations that affect stress granule formation, or persistence, contribute to the formation of several degenerative diseases including ALS, FTLD, and some myopathies (Y. R. Li et al., 2013; Ramaswami et al., 2013). Strikingly, in many cases the mutations are in RNA binding proteins (e.g. hnRNPA1, FUS, TDP-43, Atx2, TIA1) which increase their self-assembly properties *in vitro*, and in cells lead to the formation of stress granule-like assemblies in the absence of stress. How related these pathogenic assemblies are to stress granules remains to be seen (Klar et al., 2013; Ramaswami et al., 2013). Moreover, mutations in VCP, an AAA-ATPase ubiquitin segregase, both inhibit the clearance of stress granules (J. Buchan et al., 2013) and trigger the same family of diseases as hyper-assembly mutations in RNA binding proteins (Johnson et al., 2010; Kimonis et al., 2008). Consistent with autophagy being important in clearing stress granules, mutations in other proteins that can affect autophagy (optineurin, ubiquilin-2, DNAJb6, and p62) also lead to neuro- or muscular degenerative diseases (Cipolat Mis, Brajkovic, Frattini, Di Fonzo, & Corti, 2016; S. Li et al., 2016; Walters et al., 2015). Moreover, because patient biopsies from these diseases often contain aggregates including various stress granule components and RNA (Y. R. Li et al., 2013; Ramaswami et al., 2013), an emerging model is that persistent stress granules trigger a series of events that leads to cell death.

One appealing model is that the persistence of stress granules in these diseases increases the probability of prion-like domains on stress granule components forming very

stable beta-amyloid structures, which might be largely irreversible in cells (Y. R. Li et al., 2013; Ramaswami et al., 2013). Consistent with that possibility, several groups have recently shown that when stress granule components undergo a LLPS in vitro, which generates a high local concentration, they show an increased tendency to form amyloid-like fibers (Lin et al., 2015; Molliex et al., 2015; Patel et al., 2015). The accumulation of such hyper-stable stress granule-like assemblies might then trigger cell death by altering regulation of RNA biogenesis and function, misregulation of signaling pathways, and/or triggering defects in axonal or nuclear-cytoplasmic transport of mRNPs (Freibaum et al., 2015; S.-C. Ling, Polymenidou, & Cleveland, 2013; Ramaswami et al., 2013; K. Zhang et al., 2015).

Stress granules also seem to be involved in both tumor progression and treatment (reviewed in (Anderson, Kedersha, & Ivanov, 2015)). For example, many chemotherapeutic agents promote stress granule formation (Adjibade et al., 2015; Kaehler, Isensee, Hucho, Lehrach, & Krobitsch, 2014). Moreover, mutations in DDX3 promoting the WNT subclass of pediatric medulloblastoma inhibit the ATPase activity of DDX3, which would be expected to trap mRNPs in stress granules based on analogous mutations in the yeast ortholog Ded1 (Hilliker et al., 2011). Similarly, YB-1 overexpression upregulates G3BP levels in human sarcomas, correlates with poor survival and in mouse models G3BP promotes metastasis (Somasekharan et al., 2015). Given the diversity of mechanisms by which stress granules can affect cell signaling and survival under stress conditions, one anticipates that stress granule formation will have multiple roles in both tumor progression and the outcome of chemotherapeutic treatments.

2 Formation and Maturation of Phase-Separated Liquid Droplets by RNA-Binding Proteins

2.1 Project Background

The work presented in the chapter stemmed from observations that RNP granules can behave like liquid droplets (C. P. Brangwynne et al., 2009) and that multivalent proteins can form similar droplets *in vitro* (P. Li et al., 2012). Our lab was invited to undertake a collaboration with Ron Vale (UCSF), Amy Gladfelter (UNC, Dartmouth), Michael Rosen (UTSW), Jim Wilhelm (UCSD), and Cliff Brangwynne (Princeton) to explore how proteins from RNP granules and R NA might form higher order assemblies. This work was highly collaborative in nature, with members from each lab working side-by-side for six weeks at the Marine Biology Laboratory in Woods Hole, MA. Each student brought a set of tools to share and work with. I contributed a large number of purified proteins for *in vitro* experimentation. Work over the summer exploring the ability of intrinsically disordered proteins to undergo liquid-liquid phase separation, as well as enhance the LLPS of multivalent RNA-binding proteins, became the kernel of a collaborative paper between the Parker lab and the Rosen lab published in *Molecular Cell* (Lin et al., 2015).

In that paper, which follows, I purified and performed experiments with SNAP-IDR constructs and SNAP-hnRNPA1 (and variants) constructs (**Figures 5, 13, 15**). Yuan Lin performed the other experiments, utilizing PTB-IDR constructs. I contributed heavily to the intellectual progress of the collaborative project both in frequent meetings with my advisor, and in discussions held with Yuan Lin and Michael Rosen. The manuscript was primarily written by Dr. Rosen and Dr. Parker, with significant contributions from both Yuan and me. The manuscript was heavily and repeatedly edited by both myself and Yuan. I would also like to thank Dr. Saumya Jain for his unflagging intellectual input at Woods Hole and over the course of preparing the paper.

2.2 Introduction

Introduction

Eukaryotic cells contain many organelles that are not bounded by membranes. Many of these structures are enriched in RNA and proteins, and play roles in controlling, assembling and/or processing various RNA-protein complexes. Such organelles are generically referred to as RNP granules and include, but are not limited to, the nucleolus, Cajal bodies, stress granules and P-bodies (Spector, 2006). Electron microscopy and refractive index studies showed that RNP granules have higher protein concentration than the surrounding cytoplasm or nucleoplasm, and appear to be heterogeneous in nature (Handwerger, Cordero, & Gall, 2005; Souquere et al., 2009; Z. Yang, 2004). Fluorescence recovery after photobleaching (FRAP) analyses showed that proteins can associate, dissociate and move within RNP granules on timescales of seconds to minutes, although there is variability from structure to structure and protein to protein (Buchan and Parker, 2009). Recent live cell imaging has suggested that P-granules and the nucleolus behave as phase separated liquids, being round in shape, undergoing cycles of fusion and fission, and distorting in response to shear forces (C. P. Brangwynne et al., 2009, 2011; S. Weber & Brangwynne, 2015; J. T. Wang et al., 2015) .

A variety of molecular interactions are known to be important for the formation of RNP granules and/or the recruitment of molecules into them. Granule assembly typically requires a pool of RNA molecules, which can bind to the RNA binding domains of numerous granule proteins (e.g. (Teixeira, Sheth, Valencia-Sanchez, Brengues, & Parker, 2005; J. R. Buchan & Parker, 2009). Redundant protein-protein interactions are also necessary for formation of the micron-scale structures observed by light microscopy. Such interactions include those between well-folded domains, as in Edc3 dimerization in yeast P-body assembly (S. H. M. Ling et al., 2008; Decker et al., 2007) or G3BP oligomerization to promote mammalian stress granule assembly (Tourriere, 2003), as well as between short linear motifs (SLiMs) in disordered regions of RNA binding proteins and other well-folded domains (reviewed in (Jonas & Izaurralde, 2013)). Some proteins, such as Dcp2

in P-bodies, contain multiple SLiMs, suggesting these interactions can crosslink multiple complexes and play a role in driving the formation of higher order assemblies that nucleate large structures *in vivo*, and phase separation in model systems *in vitro* (Fromm et al., 2014; P. Li et al., 2012).

RNP granule proteins often contain both RNA binding domains as well as sequences that have been variously termed prion-related, prion-like, low complexity or intrinsically disordered (here, we will use the most generic term, intrinsically disordered region, IDR). These sequences were originally identified by their similarity to those of the known prions, human prion protein and Sup35p (Gilks et al., 2004; Reijns et al., 2008; Decker et al., 2007), but also include those containing repeated G/S-F/Y-G/S motifs (Kato et al., 2012; Nott et al., 2015; Updike et al., 2011; King, Gitler, & Shorter, 2012; Sun et al., 2011). A variety of data have shown that these sequences can also be important for targeting to, and/or formation of, RNP granules. Genetic experiments showed that a prion-like domain of Tia1 is important in targeting Tia1 to mammalian stress granules (Gilks et al., 2004). Similarly, P-bodies in yeast assemble through redundant interactions of the Edc3 protein and by a prion domain of Lsm4 (Decker et al., 2007). The P-granules in C. elegans are dependent on the Pgl family of proteins for their assembly, which contain an XFG repeat structure (Updike et al., 2011). In addition, the RNA binding protein Fus localizes to yeast and mammalian stress granules through its N-terminal IDR, and mutation of tyrosines in multiple GYG motifs in this region prevents this accumulation (Sun et al., 2011; Kato et al., 2012). Finally, the formation of a subcellular mRNP compartment in the fungus Ashbya is driven by a polyQ region in the Whi3 protein (C. F. Lee, Brangwynne, Gharakhani, Hyman, & Jlicher, 2013).

It remains unresolved how IDRs promote RNP targeting and formation. Some of these sequences can drive aggregation *in vivo* (Reijns et al., 2008). *In vitro*, several are known to form amyloid-like fibers (Sun et al., 2011; Kato et al., 2012; H. J. Kim et al., 2013). The IDR of Fus forms filament-containing hydrogels *in vitro*, and recruitment of Fus IDR mutants into these hydrogels correlates with recruitment into stress granules in cells (Kato et al., 2012). More detailed analyses showed that these Fus filaments con-

tain cross-beta structure, similar to classical amyloid filaments formed by the amyloid beta protein (Kato et al., 2012). Additionally, the Fus hydrogels can retain mRNAs known to reside in RNP granules in cells, leading to a model that granules may consist of fiber-containing hydrogels (Kato et al., 2012; Han et al., 2012). A potentially alternative model is based on the observation that certain proteins and protein complexes can undergo liquid-liquid phase separation (LLPS), producing structures with physical behaviors similar to P granules and nucleoli (e.g. being round, dynamic, highly concentrated in protein, undergoing fusion and deforming under stress). For example, the disordered protein elastin has been known for decades to undergo LLPS as an important first step in generating elastic extracellular filaments needed for tissue stability (Yeo, Keeley, & Weiss, 2011). Recently the IDR of Ddx4, a protein that resides in maternal mRNP granules referred to as nuage, was shown to undergo LLPS *in vitro* and in cells in a salt- and temperature-dependent manner (Nott et al., 2015). Phase separation of Ddx4 and elastin is thought to be driven by interactions between multiple, weakly adhesive elements of the proteins. In a related process, interactions between multivalent proteins and their multivalent ligands (both protein and RNA) can also produce LLPS, concomitant with assembly into large oligomers/polymers (P. Li et al., 2012) . In these systems, factors that increase crosslinking of the interacting species can promote LLPS (P. Li et al., 2012). Thus, one hypothesis is that for proteins containing both RNA binding domains and IDRs, RNA-protein and IDR-IDR interactions may act cooperatively to promote LLPS. In IDR-containing systems the relationship between the molecular interactions that promote phase separation and those that promote fiber formation remains unknown. In either model, traditional protein-protein interactions that generate discrete multi-component complexes will also contribute to granule formation.

In this work, we examine the phase separation behaviors of IDRs from a series of engineered and natural RNA binding proteins *in vitro*. We demonstrate that some RNA binding proteins, or their IDRs, can rapidly phase separate on their own to produce dynamic, liquid-like structures. Phase separation occurs at low salt concentrations for the free proteins, and at more physiological salt concentration in the presence of RNA. On a

slower time scale, the IDR elements mature to a less dynamic state (as assessed by FRAP) that appears to be more stable (as assessed by salt resistance). In some cases maturation occurs concomitant with formation of fibrous structures visible by light- and electron microscopy. Different IDRs can co-assemble into phase-separated droplets to different degrees, indicating the presence of heterotypic interactions. We also observe analogous phase separation, maturation and heterotypic interactions for the full length RNA binding protein, hnRNPA1. Our data suggest that multivalent and weak interactions among disordered regions on RNA binding proteins, coupled with RNA-protein interactions, could contribute to RNP granule assembly by promoting LLPS. Moreover, such a view joins phase separation and fiber formation into a unified model by positing that the progression from dynamic liquid to more stable fibers could be regulated in cells to produce structures with varying physical properties and chemical compositions, according to particular biological needs. This model could explain the observation that many ATP driven machines, which can control the assembly state of proteins, modulate the assembly and disassembly of stress granules (Wallace et al., 2015). Aberrant regulation could explain the basis for the formation of pathological stress granules in certain diseases.

2.3 Results

2.3.1 *General Strategy*

To systematically examine the biochemical behavior of IDRs *in vitro* we recombinantly produced a panel of six different IDRs taken from known components of RNP granules: Lsm4, which is known to play a role in P-body assembly in yeast (Decker et al., 2007); Tia1 and its yeast ortholog Pub1, whose IDR has been suggested to play a role in mammalian stress granule assembly (Gilks et al., 2004); TIF4632 (eIF4GII), a yeast translation initiation factor with an N-terminal IDR suggested to play a role in stress granule assembly in yeast (J. R. Buchan et al., 2008); as well as human hnRNPA1 and Fus, which are abundant RNA binding proteins that localize to, and can contribute to, stress granule assembly (Schwartz, Wang, Podell, & Cech, 2013; Guil, Long, & Caceres, 2006). To enable examination of the components by fluorescence microscopy, we fused all

proteins to an N-terminal SNAP tag, which was then coupled to the SNAP-Surface 488 or SNAP-Surface 649 fluorophores. In addition, in some cases the proteins were fused to PTB, an RNA binding protein involved in splicing that contains four RNA-binding RRM domains. We previously reported that interactions between PTB and a single-stranded RNA containing five RRM-binding elements resulted in phase separation (P. Li et al., 2012). This collection of reagents enabled us to compare various IDRs, RNA binding elements and the interplay between domain- and IDR-promoted phase separation. To determine whether the behaviors of these simple engineered systems are manifest in more complicated natural proteins, we also generated recombinant full-length hnRNPA1, a mammalian granule protein that contains both folded RNA binding domains and IDR elements. Below, we indicate the specific IDR element of a given protein with a subscripted IDR (e.g. $Pub1_{IDR}$), and use no indication for full-length proteins. We then examined whether these proteins could undergo LLPS either at low salt concentration, which can promote phase separation of some IDRs (Nott et al., 2015), or in the presence of RNA binding partners, and how the properties of the resulting droplets varied over time and between proteins.

2.3.2 *IDRs Can Undergo LLPS*

We initially asked whether IDRs alone can undergo LLPS when fused to the SNAP-tag. In all cases examined ($Pub1_{IDR}$, $eIF4GII_{IDR}$, $Lsm4_{IDR}$, $Tia1_{IDR}$, Fus_{IDR} and $hnRNPA1_{IDR}$), solutions of these proteins remained clear at room temperature under physiologic salt conditions (100-150 mM NaCl). When the solutions were examined by light microscopy, only small, diffraction-limited puncta were observed settled onto the glass slide surface, which appear to represent a low level of aggregated protein. However, when the NaCl concentration was diluted to 37.5 mM, solutions of $hnRNPA1_{IDR}$, $eIF4GII_{IDR}$, and Fus_{IDR} (6-33 µM protein, see Figure 1 legend) became opalescent, and brightly fluorescent, micron sized spherical structures were observed in solution by light microscopy. Over time, these structures settled onto the slide, where they sometimes spread into irregular shapes (**Figure 5B**). These structures appeared to be phase separated liquids based on several

criteria. They: a) were spherical in solution, b) could flow and fuse (See (Lin et al., 2015) Movie S1), c) showed concentration dependence in their total volume (data not shown and see below), and d) disassembled rapidly when returned to high salt after 30' of low salt treatment (see below). Solutions of SNAP-Lsm4$_{IDR,}$ Pub1$_{IDR}$ and Tia1$_{IDR}$ either rapidly formed fiber-like structures (Lsm4) or remained as a single phase when fused to the SNAP tag at low salt. Thus, IDRs can alternatively form both fibers and phase-separated droplets under low salt conditions.

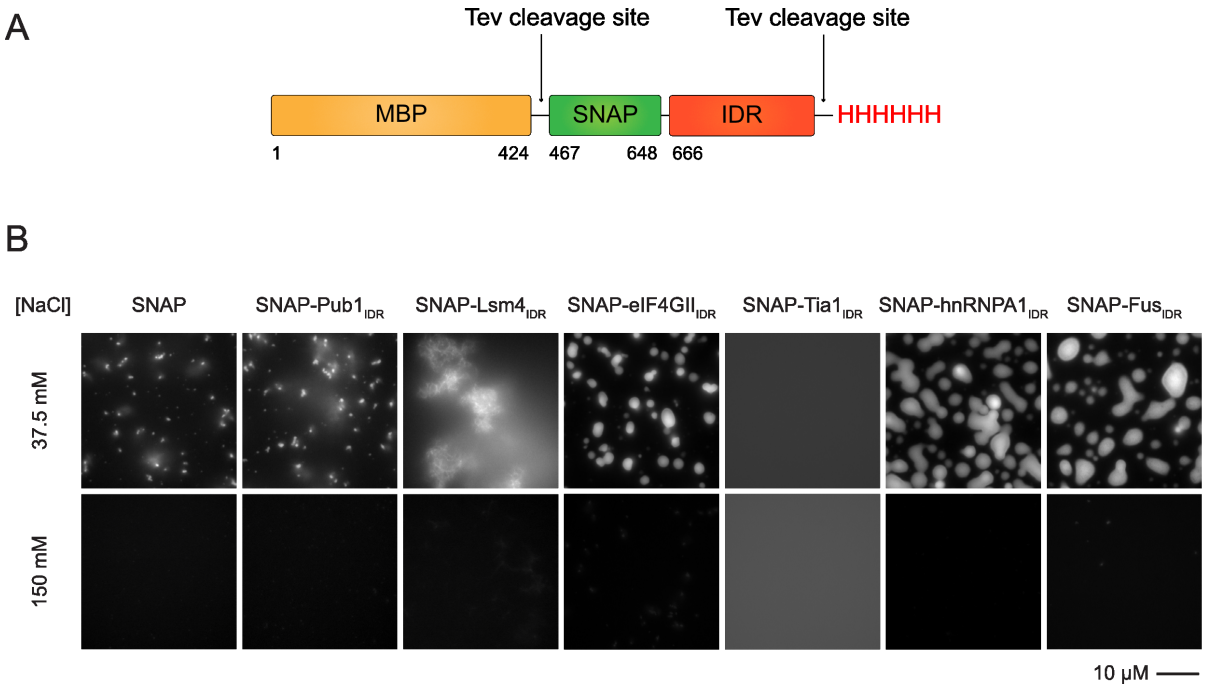

Figure 5: **Particular IDRs are sufficient to drive LLPS at low salt concentration**

(A) Schematic of SNAP-IDR proteins. MBP, maltose binding protein. SNAP, SNAP-tag used for fluorophore labeling. IDR, intrinsically disordered region. TEV protease removes MBP and His tags.

(B) Fluorescence microscopy images of the macroscopic structures formed by SNAP-IDRs at 37.5 and 150 mM NaCl. SNAP-hnRNPA1$_{IDR}$, 6.925 µM; SNAP-Fus$_{IDR}$, 10.75 µM; all the other proteins, 32.75 µM. Proteins were labeled with SNAP-Surface 649

To determine how intracellular crowding might affect LLPS driven by IDRs, we examined the hnRNPA1$_{IDR}$ in the presence of 10% PEG. We observed that in the presence of crowding agents hnRNPA1$_{IDR}$ underwent LLPS at 150 mM NaCl and at a concentration of 1 µM (**Figure 6B**), which is below the concentration of hnRNPA1 in cells (1.17x10^7 molecules per cell or approximately 5-10 µM; (Beck et al., 2011)). Thus crowding strongly

promotes LLPS of hnRNPA1$_{IDR}$ (compare conditions of **Figure 5B** and **6**).

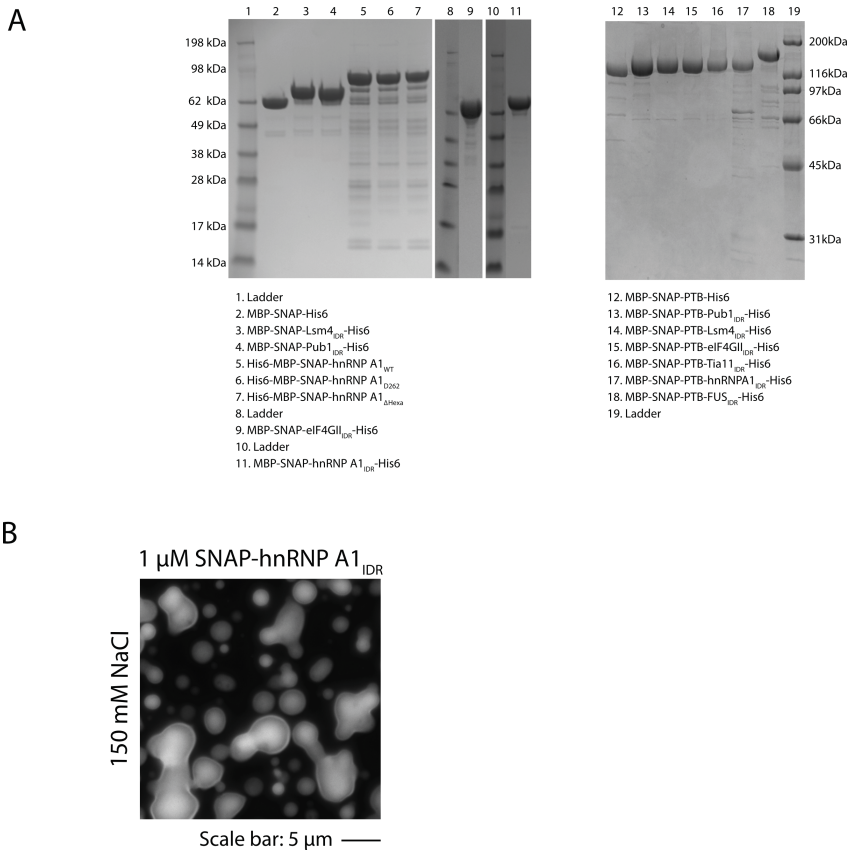

Figure 6: **Crowding agent promotes the LLPS of hnRNPA1$_{IDR}$**

(A) Coomassie blue stained SDS-PAGE gels of purified proteins used in this study.

(B) Fluorescent microscopy images of SNAP-Surface 488 labeled SNAP-hnRNPA1IDR forming droplets at low protein concentrations in the presence of 100 mg/ml PEG 3350

2.3.3 *RNA Can Promote LLPS of IDR Proteins*

In cells, RNP granule assembly is often dependent on the concentration of specific RNAs (Teixeira et al., 2005; J. R. Buchan & Parker, 2009). In addition, we previously showed that interactions between the four RNA-binding RRM domains of PTB and an RNA molecule containing multiple RRM-binding motifs can promote LLPS, independent of any IDR elements (P. Li et al., 2012). Thus, we asked whether RNA could promote LLPS in proteins containing both PTB and IDRs. At 100 mM NaCl and protein concentrations of 1.25-2.5 μM all six SNAP-PTB-IDR fusions rapidly phase separated upon addition of 0.4-

0.8 µM RNA, producing droplets that concentrated both molecules (**Figure 8** and **Figure 7A**, showing RNA enrichment). In contrast, SNAP-PTB only phase separated at 50 µM concentration in the presence of 2 µM RNA (not shown). Performing the experiment in the presence of 100 mg/ml BSA to mimic protein crowding effects within the cell, allowed the detection of RNA driven LLPS of the SNAP-PTB-Fus$_{IDR}$ at concentrations below 10 nM (**Figure 8D**)), which is below the cellular concentration of many of the abundant components of mRNP granules (Beck et al., 2011).

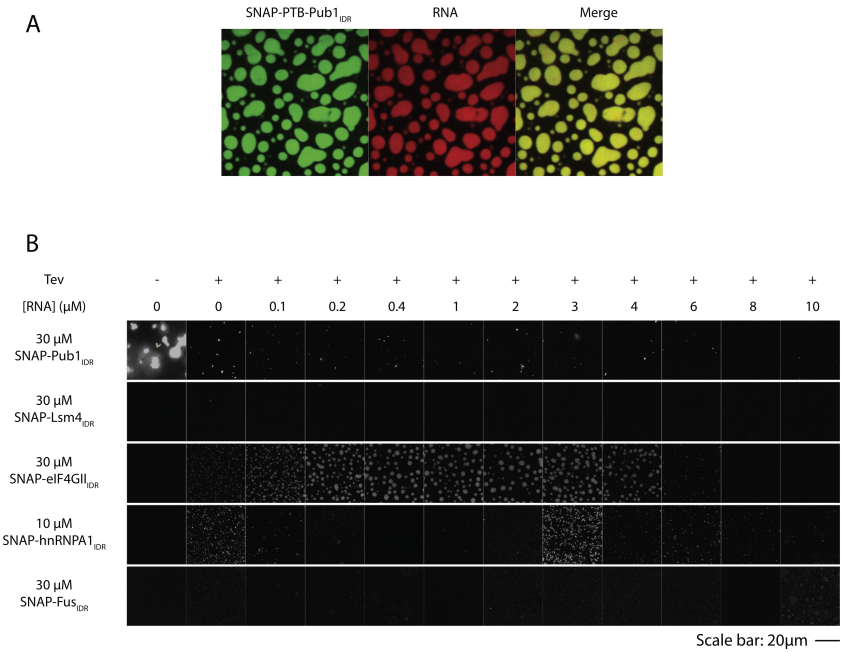

Figure 7: **RNA does not stimulate LLPS of most SNAP-IDR proteins lacking PTB**

(A) Cy3 labeled RNA (0.5 µM, red) and SNAP-PTB-Pub1IDR (3 µM, green) co-localize within liquid droplets at 100 mM NaCl

(B) Fluorescence microscopy images of SNAP-IDRs (at the indicated concentrations) titrated with RNA. Proteins are labeled with SNAP-Surface 649

To better understand how RNA promotes phase separation, we examined whether RNA could stimulate LLPS of the SNAP-IDR proteins lacking PTB. A range of RNA concentrations (0.1-10 µM) did not promote phase separation of the SNAP-IDR proteins, up to protein concentrations of 10 – 30 µM. The only exception to this behavior was provided by SNAP-eIF4GII$_{IDR}$, which did phase separate upon addition of RNA (**Figure 7 B**), and was able to bind RNA directly according to a gel shift assay (data not shown).

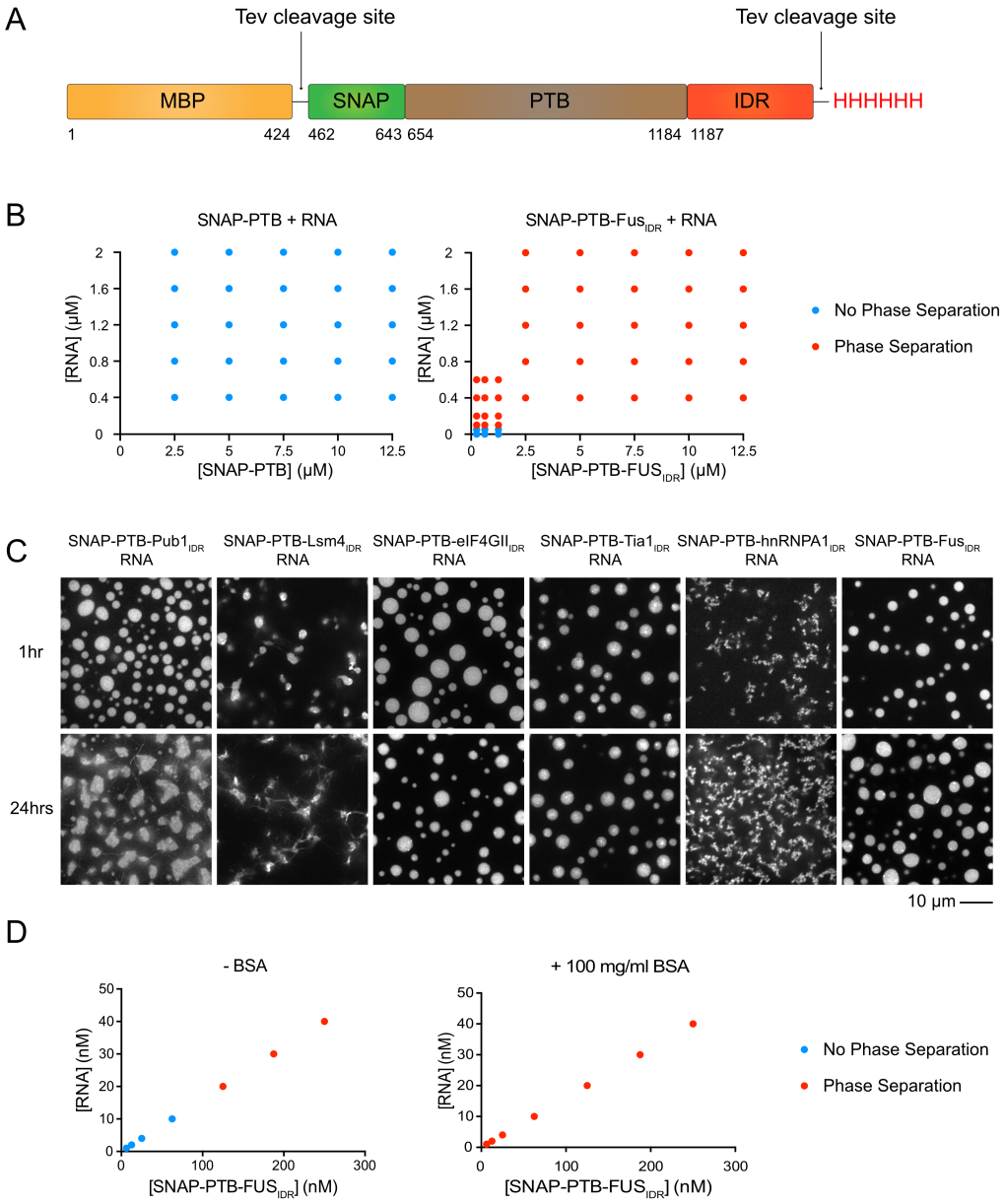

Figure 8: **RNA can promote LLPS of IDR proteins**

(A) Schematic of SNAP-PTB-IDR proteins. PTB, polypyrimidine tract-binding protein, containing four RRM RNA binding domains. TEV protease removes MBP and His tags

(B) Phase diagram of SNAP-PTB and SNAP-PTB-Fus_{IDR} plus RNA. Red dots indicate phase separation; blue dots indicate no phase separation

(C) Fluorescence microscopy images of the macroscopic structures formed at 100mM NaCl by SNAP-PTB-$4GII_{IDR}$ 1.25 µM and RNA 0.4 µM; SNAP-PTB-Fus_{IDR} 1.25 µM + RNA 0.4 µM; for the rest of droplets, SNAP-PTB-IDR 2.5 µM, RNA 0.8 µM. Proteins were labeled with SNAP-Surface 649. Images were taken at 1 hour and 24 hours after the initiation of phase separation by RNA addition

(D) Phase diagram of SNAP-PTB-Fus_{IDR} plus RNA in the absence and presence of 100 mg/ml bovine serum albumin (BSA)

Thus, for all proteins except eIF4GII, RNA-induced phase separation required both the IDR and RNA binding to PTB. We interpret these results as indicating that PTB-RNA and IDR-IDR interactions act synergistically to promote LLPS.

Although all six SNAP-PTB-IDR proteins phase separated with RNA, the resulting structures differed significantly in their morphologies (**Figure 8C**). At 1 hour after RNA addition, droplets formed by the $eIF4GII_{IDR}$, $Pub1_{IDR}$ and Fus_{IDR} fusions were relatively large, round, and separated into discrete structures. By contrast, the $Lsm4_{IDR}$, $Tia1_{IDR}$ and $hnRNPA1_{IDR}$ fusions created droplets that were smaller, and often attached to each other in long irregular chains, as though coalescence into larger structures had been aborted. These behaviors mirrored those observed for the SNAP-IDR structures induced by low salt, where SNAP-$eIF4GII_{IDR}$ formed liquid droplets, while SNAP-$Lsm4_{IDR}$ formed fibers (**Figure 5B**). Thus, different IDRs can create phase-separated droplets with different physical properties.

2.3.4 *Phase Separated Droplets Mature Over Time*

We next monitored the SNAP-PTB-IDR+RNA droplets over time after initiating their formation. In all cases, the droplets changed over time according to three measures. First, their gross appearance changed. When examined over 24 hours, droplets from most of the IDRs changed from round to irregularly shaped. Many also formed filamentous structures that extended outside of the droplet bodies, and became less homogeneously fluorescent (**Figure 8C**). The only exception to this behavior was SNAP-PTB-Fus_{IDR}, whose droplets remained round and homogeneous to 72 hours (data not shown). For

SNAP-PTB-Lsm4 $_{\text{IDR}}$ and SNAP-PTB- Tia1$_{\text{IDR}}$, formation of filaments was greatly accelerated by LLPS in a biochemical assay, where RNA addition caused most of the protein to become insoluble (and filamentous in nature in electron micrographs) after 24 hours, while most remained soluble in solutions without RNA (**Figure 10 A,B**). We also assessed the relative stability of the SNAP-PTB-Lsm4 $_{\text{IDR}}$ and SNAP-PTB- TIA1$_{\text{IDR}}$ fibers by the addition of SDS prior to centrifugation. We observed that the SNAP-PTB-Lsm4 $_{\text{IDR}}$ fibers were SDS resistant while the SNAP-PTB- Tia1$_{\text{IDR}}$ fibers were SDS sensitive (**Figure 9C**). This differential sensitivity to SDS indicates that IDRs will form fibers of different biochemical properties, tunable to their biological role.

A second property that changed over time was resistance of the phase-separated droplets to salt. Phase separation of SNAP-hnRNPA1$_{\text{IDR}}$ and SNAP-Fus$_{\text{IDR}}$ induced by low salt was largely reversible in the first 22 minutes after initiation. But with increasing time the remaining assemblies became salt resistant, with full resistance seen at 24 hours (**Figure 9A,B**).

A third key observation was that the dynamics of the SNAP-PTB-IDR + RNA droplets changed substantially over time as assessed by FRAP of the SNAP-Surface 649 label (**Figure 10D**). In the first hour after initiation, the fluorescence of a small region in the center of larger droplets would recover after photobleaching with half-lives ranging from 19 to 64 seconds, and recovery fractions ranging from 0.3 to 0.9. Over 14-48 hours the half-lives for each fusion protein increased and the fractional recoveries steadily decreased, such that fluorescence of most of the IDRs no longer recovered at the latest time point. The progression from dynamic to static reflected the changes in droplet morphology: droplets that remained rounder and longer remained dynamic longer (e.g. Fus and eIF4GII), and vice versa (e.g. Lsm4 and Tia1). Since droplets from both the IDRs alone and PTB-IDR + RNA showed similar changes in morphology, we attribute these effects primarily to the IDR elements rather than PTB or RNA. Our interpretation of these results is that the high concentration of the IDR in the phase separated droplets (370 µM and 310 µM for SNAP-PTB-Pub1$_{\text{IDR}}$ and SNAP-PTB-eIF4GII$_{\text{IDR}}$, respectively; **Figure 9D,E**) leads over time to the formation of kinetically trapped and

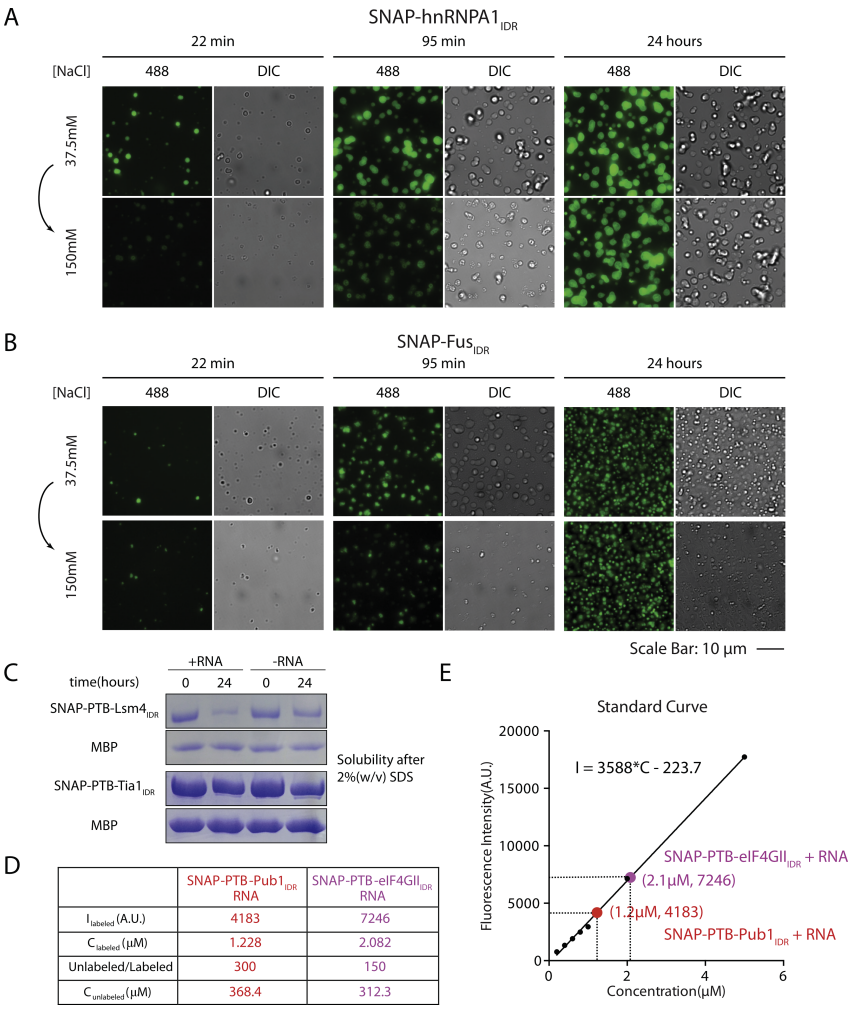

	SNAP-PTB-Pub1$_{IDR}$ RNA	SNAP-PTB-eIF4GII$_{IDR}$ RNA
$I_{labeled}$ (A.U.)	4183	7246
$C_{labeled}$ (µM)	1.228	2.082
Unlabeled/Labeled	300	150
$C_{unlabeled}$ (µM)	368.4	312.3

Figure 9: **Phase separated droplets of SNAP-IDRs mature over time**

(A) Fluorescence microscopy images of structures formed by SNAP-hnRNPA1$_{\mathrm{IDR}}$ (4 µM) at 37.5 mM NaCl. At indicated time points, NaCl was raised to 150 mM total concentration and structures that remained were imaged. Both fluorescent and DIC images were taken for better illustration. Images at each time point are shown with the same intensity scale

(B) Fluorescence microscopy images of structures formed by SNAP-Fus$_{\mathrm{IDR}}$ (10.75 µM) at 37.5 mM NaCl. At indicated time points, NaCl was raised to 150 mM total concentration and structures that remained were imaged. Both fluorescent and DIC images were taken for better illustration. Images at each time point are shown in the same intensity scale

(C) SDS-PAGE assays of the amount of SDS-soluble species present at different time points after the initiation of phase separation by addition of RNA. MBP-SNAP-PTB-Lsm4IDR (5 µM) or MBP-SNAP-PTB-TIA1$_{IDR}$ (5 µM) were mixed with RNA (1.6 µM) (phase separation) or buffer (no phase separation) and TEV protease. At the indicated times SDS was added to 2%,(w/v) followed by 5 minutes of centrifugation and filtration through an 0.22µmfilter. The supernatant was then loaded into the gel and stained with Coomassie Blue. TEV protease was present to remove MBP, which serves as an internal loading control

(D) The absolute concentrations of the fluorophore-labeled proteins within the liquid droplets were calculated from the droplet intensities according to the standard curve of a series of pure fluorophores at different concentrations. Droplets of SNAP-PTB-Pub1$_{IDR}$ (7.5 µM) plus RNA (2.4 µM) were doped with 25 nM fluorophore-labeled SNAP-PTB-Pub1$_{IDR}$; Droplets of SNAP-PTB-eIF4GII$_{IDR}$ (3.75 µM) plus RNA (1.2 µM) were doped with 25 nM fluorophore-labeled SNAP-PTB-eIF4GII$_{IDR}$. The proteins were labeled with SNAP-Surface 649

stable structures. This maturation may involve the formation of amyloid-like fibers, since the filamentous structures of SNAP-PTB-Lsm4$_{IDR}$ + RNA that become more numerous with time stained strongly with Thioflavin-T, (**Figure 10C**).

2.3.5 *Phase Separated Droplets Can Recruit IDRs Through Multiple Types of Interactions*

In vivo RNP granules contain both RNA and multiple proteins with IDRs. This raises the possibility that heterotypic interactions between IDRs, folded domains and/or RNA might recruit proteins with IDRs into these assemblies. To test this idea *in vitro*, we examined the ability of PTB-Fus$_{IDR}$ + RNA droplets to recruit GFP fusions of the other IDRs. GFP alone was not selectively recruited into, or excluded from, any of the droplets, with partition coefficients ({droplet concentration}/{bulk concentration}, quantified from fluorescence intensities related to a calibration curve) of approximately 1 in all cases. All of the GFP-IDR proteins were recruited into the PTB-Fus$_{IDR}$+RNA droplets, with partition coefficients ranging from approximately 3 to 12 (**Figure 11**). All proteins were also recruited into PTB+RNA droplets. But for GFP-Lsm4$_{IDR}$, GFP-Tia1$_{IDR}$ and GFP-Fus$_{IDR}$, recruitment into the PTB- Fus$_{IDR}$+RNA droplets was significantly higher (**Figure 11B**), suggesting that interactions dependent on the Fus$_{IDR}$ can enhance hetero- and homotypic recruitment of IDRs into the phase separated droplets. Consistent with Fus$_{IDR}$ promoting heterotypic recruitment, the difference between recruitment into PTB-Fus$_{IDR}$ + RNA droplets and PTB + RNA droplets was even larger for SNAP-IDR proteins

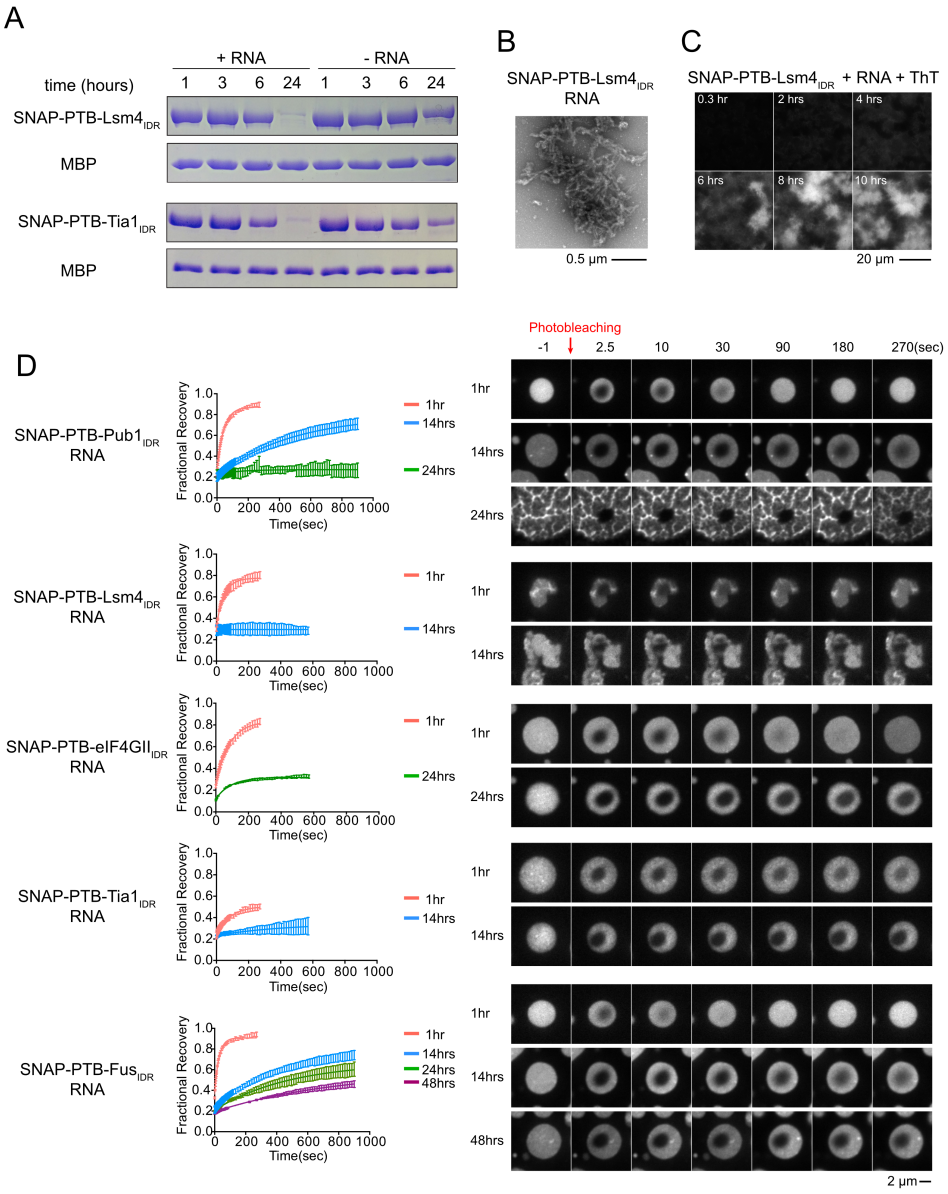

Figure 10: **Phase separated droplets of SNAP-PTB-IDRs plus RNA mature over time**

(A) SDS-PAGE of the high-salt soluble species present at different time points after the initiation of phase separation by RNA addition. MBP-SNAP-PTB-Lsm4$_{\text{IDR}}$ (5µM) or MBP-SNAP-PTB-TIA1$_{\text{IDR}}$ (5µM) were mixed with RNA (1.6µM) (phase separation) or buffer (no phase separation). At the indicated times, NaCl was raised to 500mM total concentration followed by 5 minutes of centrifugation, and the supernatant analyzed by SDS PAGE; gels were stained with coomassie blue. TEV protease was also present to remove MBP, which serves as an internal loading control

(B) Transmission electron micrographs of the high-salt insoluble species in a solution of SNAP-PTB-$Lsm4_{IDR}$ plus RNA after 24 hours incubation

(C) Representative images of increase over time in Thioflavin T (ThT) fluorescence for droplets of SNAP-PTB-$Lsm4_{IDR}$ (5 µM) plus RNA (1.6 µM) shown in the same intensity scale

(D) The liquid droplets of SNAP-PTB-IDR proteins plus RNA become less dynamic over time. Left panels show FRAP recovery curves. Data are reported as mean SD. Right panels show a representative droplet for each protein at different time points.

than for EGFP-IDR proteins (**Figure 12**).

The recruitment of GFP-$Pub1_{IDR}$, GFP-$Lsm4_{IDR}$ and GFP-$eIF4GII_{IDR}$ into the PTB + RNA droplets could be explained by weak interactions of these IDRs with RNA. Consistent with this possibility we note all of these IDRs have high predicted pI values (Pub1 11.5; Lsm4 11.0; eIF4GII, 9.6). Moreover, we observed by gel shift assays that $Lsm4_{IDR}$ and $eIF4GII_{IDR}$ had stable interactions with RNA (data not shown). Analogously, GFP-$Tia1_{IDR}$ and GFP-Fus_{IDR}, which both are acidic (IDR pI values of 5.8 and 4.7, respectively) may be recruited through interactions with PTB, which is quite basic (pI = 9.2). Taken together, these observations suggest that IDR containing proteins could be recruited to RNA-protein granules by both IDR dependent interactions and by other interactions, which could include binding to RNA.

2.3.6 *Natural RNP Granule Proteins Show the Same Behaviors as the Engineered Proteins*

Using a series of engineered proteins, we have able to systematically explore the behaviors of different IDRs in combination with different RNA binding domains. We found that A) the IDRs can undergo LLPS at low salt, B) LLPS by IDRs is promoted under physiologic salt conditions by RNA, C) the IDR-containing phase separated droplets mature over time to become less dynamic and D) droplets formed by one IDR can recruit other IDRs to different degrees. We next asked whether these same behaviors are also manifest in natural RNA binding proteins.

hnRNPA1 is a component of stress granules in mammalian cells (Guil et al., 2006), whose mutations can be causative in inclusion body myopathies such as ALS and FTLD, and can increase stress granule formation (H. J. Kim et al., 2013). The protein is com-

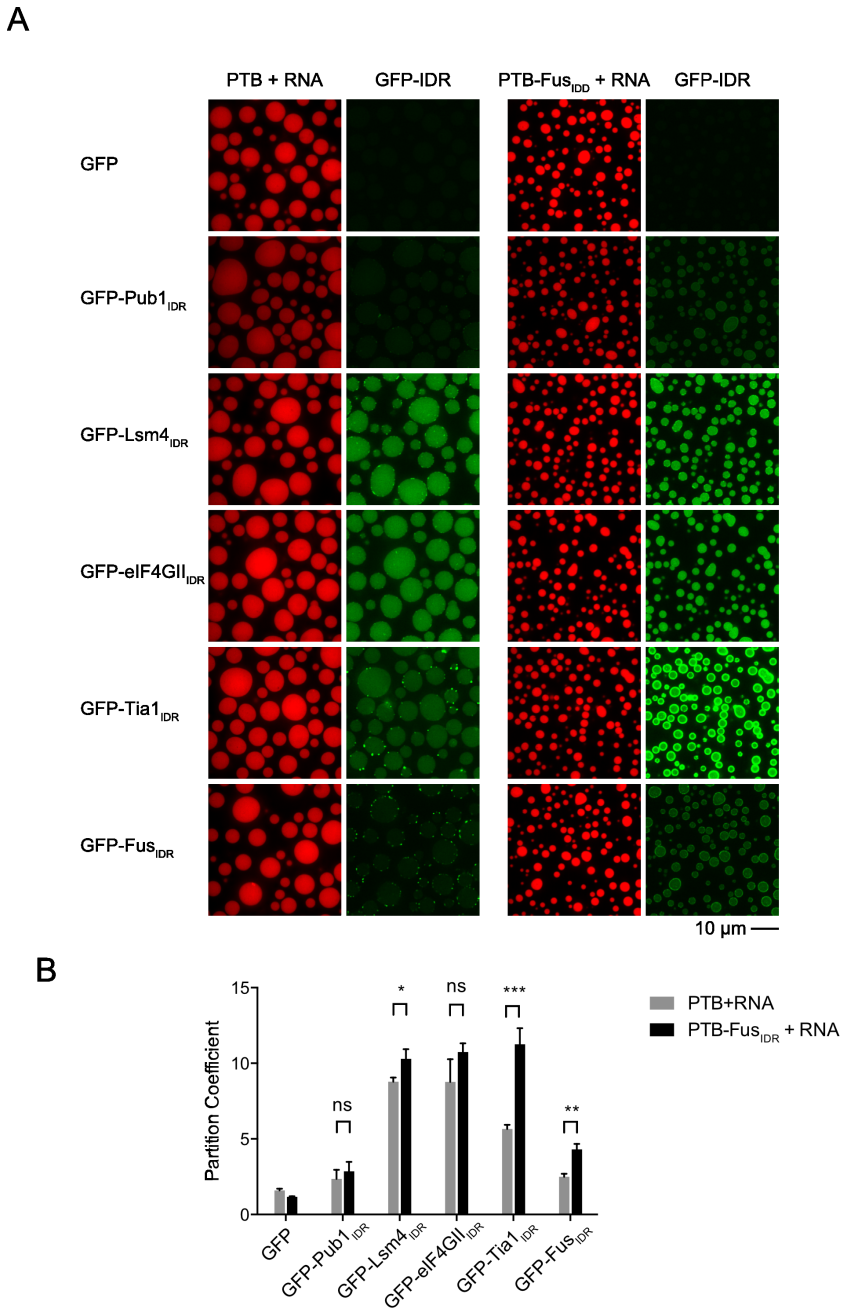

Figure 11: **IDR-dependent phase separated droplets recruit heterotypic IDRs**

(A) Representative images showing the partitioning of GFP-IDR probes (100nM, green) into liquid droplets (red) of PTB or PTB-Fus$_{IDR}$ plus Cy3-labeled RNA

(B) Quantification of the GFP-IDR partition coefficients in experiments from panel A. The partition coefficients are plotted as mean ± SD, from three independent measurements each of which averaged all the droplets across four random slide regions. ns, not significant, $p > 0.05$; *, $p < 0.05$; **, $p < 0.01$; ***, $p < 0.001$. p-values were determined by unpaired t-test

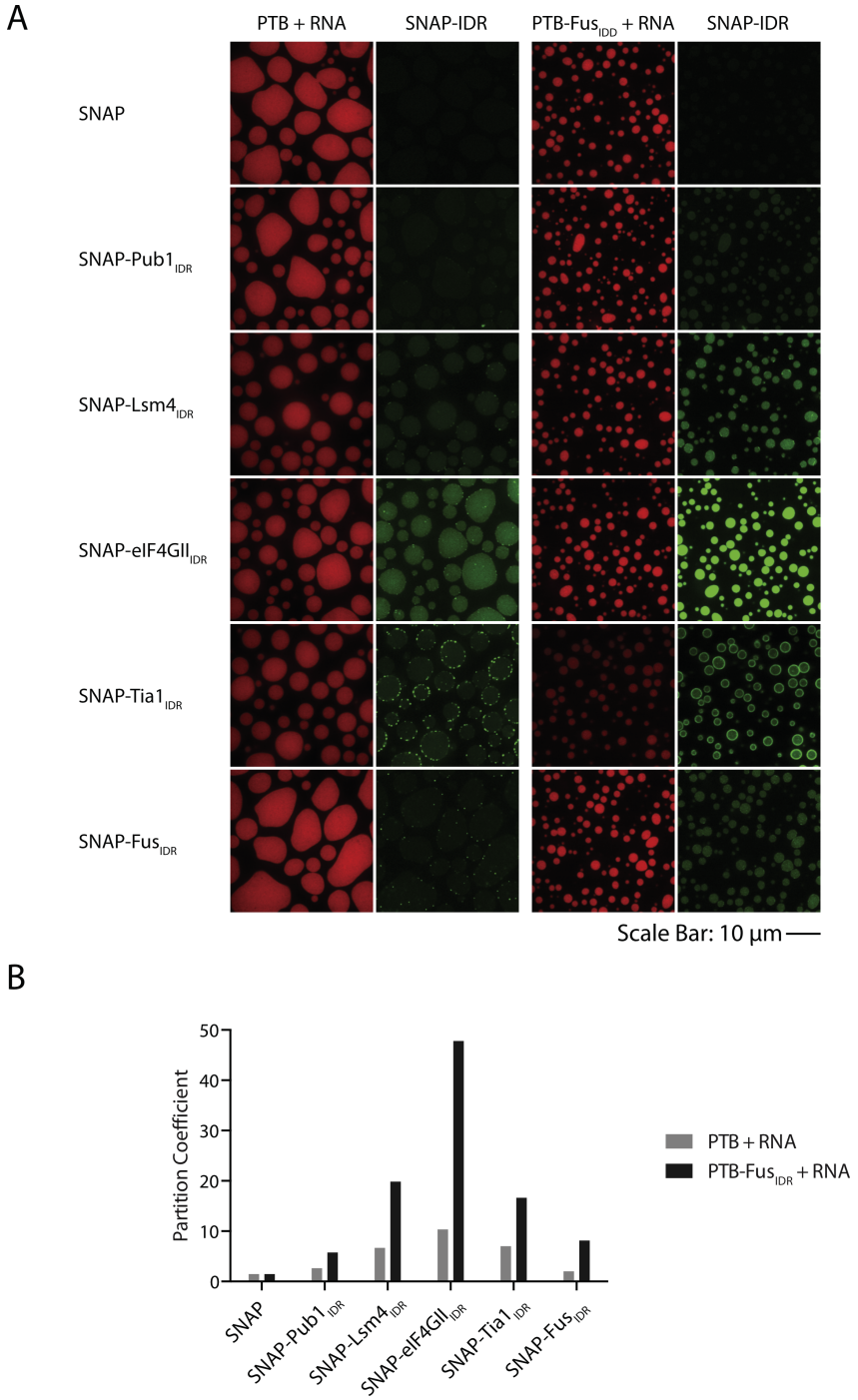

Figure 12: **IDR dependent phase separated droplets recruit SNAP-IDR probes**

(A) Representative images showing the partitioning of SNAP-IDR probes (100 nM, labeled with SNAP-Surface 488, green) into the liquid droplets (red) of PTB or PTB-FUS$_{\mathrm{IDR}}$ plus Cy3-labeled RNA

(B) Quantification of the SNAP-IDR partition coefficients in experiments from panel A

posed of two N-terminal RNA-binding RRM domains, and an ˜200 residue C-terminal IDR that is enriched in G/S-Y/F-G/S elements (**Figure 13A**). We expressed full-length hnRNPA1 in *E. coli* with an N-terminal SNAP-tag and purified it to homogeneity. Under physiologic salt conditions (150 mM NaCl), the protein was soluble and existed as a single-phase solution up to concentrations as high as 300 µM at room temperature. However, upon transfer to low salt (37.5 mM NaCl), SNAP-hnRNPA1 rapidly coalesced into micron sized, brightly fluorescent spherical structures at concentrations above 13.5 µM (**Figure 13B**). As with the engineered proteins, these structures were spherical, could flow and fuse (See (Lin et al., 2015) Movie S3), were concentration dependent (**Figure 13B**) and disassembled rapidly when returned to high salt after 30 minutes of low salt treatment, indicating that they were phase separated liquids (**Figure 13C**). This phase separation was dependent on the IDR since an hnRNPA1 construct lacking this C-terminal element ($\text{hnRNPA1}_{\Delta\text{IDR}}$) did not phase separate under salt and protein concentrations where the full-length protein generated droplets (**Figure 13B**). Similar to the model systems, we observed that macromolecular crowding in the presence of PEG led to LLPS of full length hnRNPA1 under physiological concentrations of protein as low as 1 µM at 37.5 mM NaCl (**Figure 14A**). Thus, hnRNPA1 can undergo IDR-dependent LLPS on its own at low ionic strength.

The phase separated hnRNPA1 droplets also matured over time. When examined from 27 minutes to 73 hours after initiation of LLPS in low salt, the droplets changed from uniformly round and homogeneously fluorescent to irregularly shaped and heterogeneously fluorescent (**Figure 13C, top row**) . Further, while phase separation was largely reversible by returning to high salt after 27 minutes, with increasing time the remaining assemblies became salt resistant (**Figure 13C, second row**). Thus, as with the engineered systems, the phase separated hnRNPA1 droplets become more stable over time. Since the IDR of hnRNPA1 is known to form amyloid-like filaments (Kato et al., 2012; H. J. Kim et al., 2013), it seems likely that formation of amyloid fibers contributes to this maturation of the droplets over time. We note that our data showing that hnRNPA1 can phase separate, and that phase separation promotes formation of structures

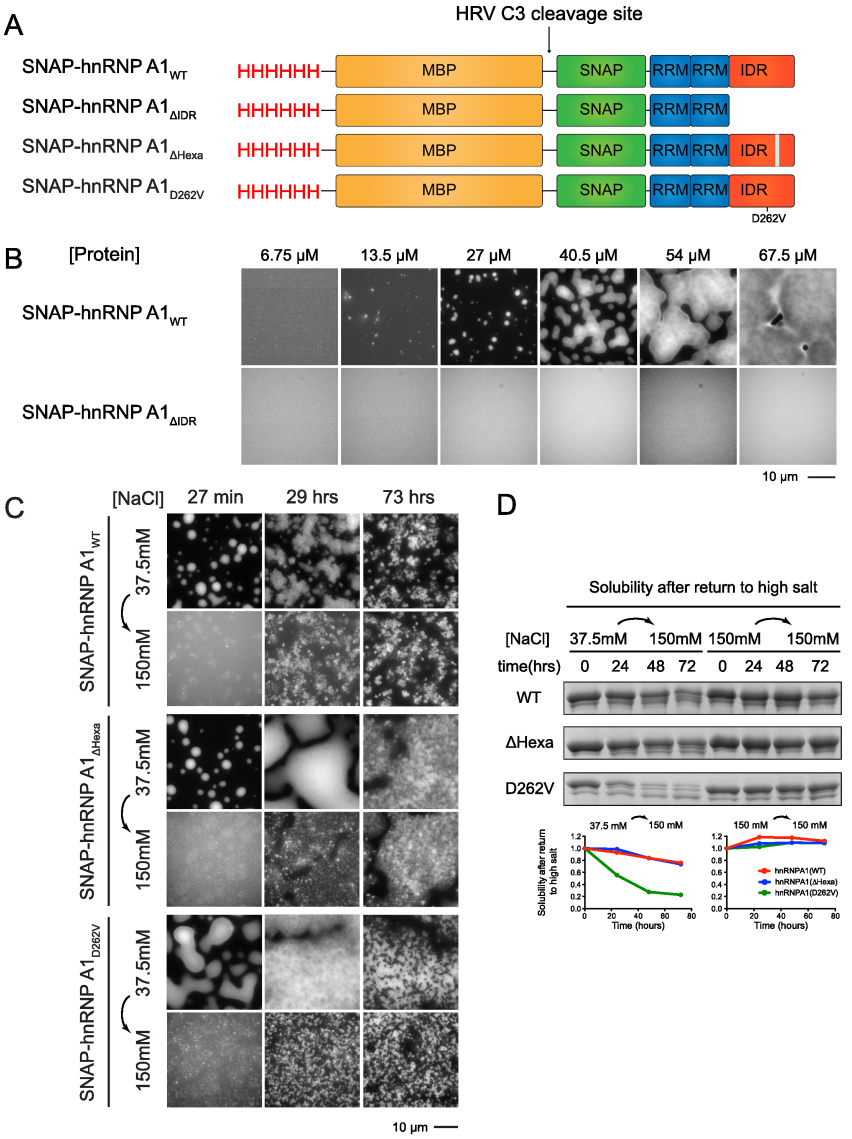

Figure 13: **Full-length hnRNPA1 undergoes IDR-dependent phase separation**

(A) Schematic of domain architecture of SNAP-hnRNPA1 proteins. HRVC3 removes His and MBP tags

(B) Fluorescence microscopy images of the macroscopic structures formed by SNAP-hnRNPA1$_{\mathrm{WT}}$ or SNAP-hnRNPA1$_{\Delta\mathrm{IDR}}$ at 37.5 mM NaCl, Images are shown in different intensity scale to highlight morphological changes

(C) Fluorescence microscopy images of structures formed by hnRNPA1WT, hnRNPA1$_{\Delta\mathrm{Hexa}}$, and hnRNPA1$_{\mathrm{D262V}}$ (all 25 μM) at 37.5 mM NaCl. At indicated time points, NaCl was raised to 150 mM total concentration and structures that remained were imaged. Images are shown in different intensity scale to highlight morphological changes

(D) SDS-PAGE assays of the amount of high-salt soluble species present at different time points after the initiation of phase separation at 37.5 mM NaCl. hnRNPA1$_{\mathrm{WT}}$, hnRNPA1$_{\Delta\mathrm{Hexa}}$, and hnRNPA1$_{\mathrm{D262V}}$ (all 25 μM) were incubated at 37.5 mM NaCl for the indicated time period before raising total NaCl concentration to 150 mM followed by centrifugation. The supernatant was then analyzed by SDS-PAGE with Coomassie staining. Quantification of the relative intensities of the bands is shown in the lower panel

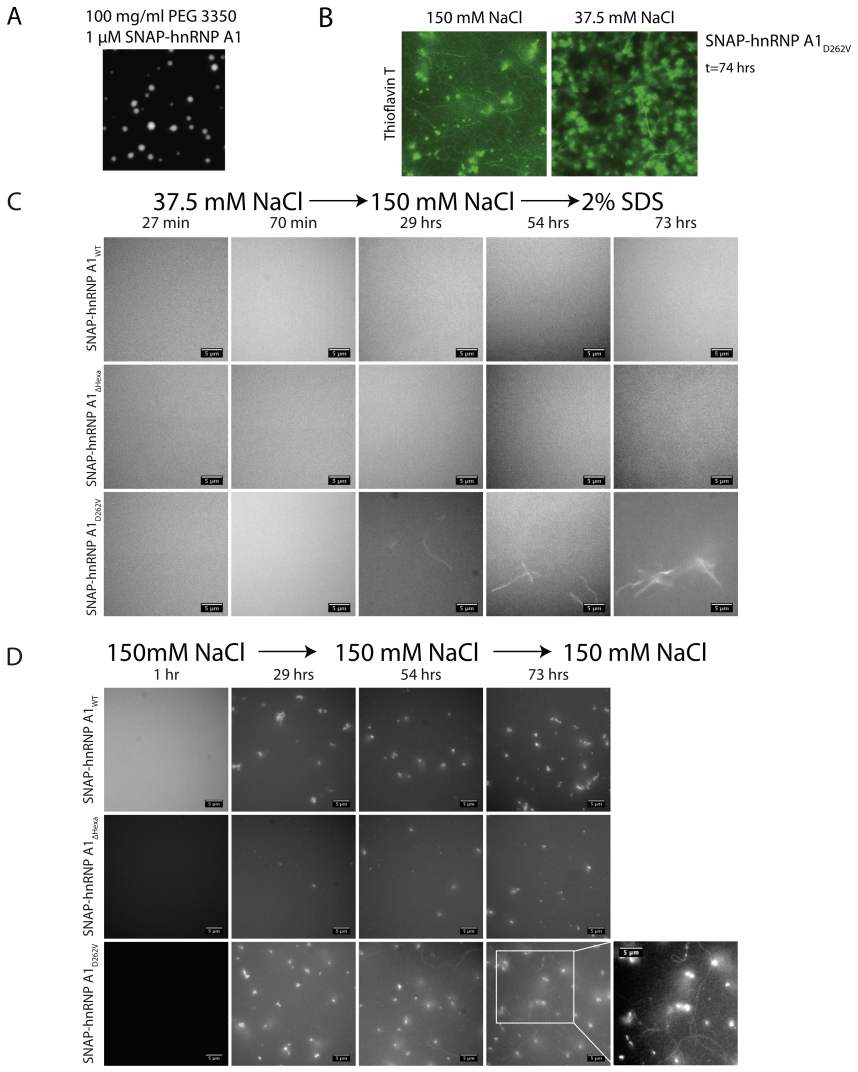

Figure 14: **hnRNPA1$_{\mathbf{D262V}}$ mutant forms SDS-resistant fibers**

(A) Fluorescent microscopy images of SNAP-Surface 488 labeled SNAP-hnRNPA1$_{\mathrm{WT}}$ forming droplets at low protein concentrations in the presence of 100mg/ml PEG 3350

(B) Fluorescence microscopy images of SNAP-hnRNPA1$_{\mathrm{WT}}$ (25 µM) forming Thioflavin T-stained fibers. Fibers were observed in both low salt (37.5 mM NaCl) and high salt (150 mM NaCl) after incubation

(C) Fluorescence microscopy images of SDS-resistant structures formed by SNAP-hnRNPA1$_{\mathrm{WT}}$, SNAP-hnRNPA1$_{\mathrm{Hexa}}$ and SNAP-hnRNPA1$_{\mathrm{D262V}}$ (all 25 µM) present at different time points after initiation of phase separation at 37.5 mM NaCl. At the indicated time points NaCl was raised to a final concentration of 150 mM and SDS was then added to a final concentration of 2% (w/v). The structures that remained were imaged

(D) Fluorescence microscopy images of structures formed by SNAP-hnRNPA1$_{\mathrm{WT}}$, SNAP-hnRNPA1$_{\mathrm{Hexa}}$ and SNAP-hnRNPA1$_{\mathrm{D262V}}$ (all 25 µM) after incubation for the indicated time at 150 mM NaCl

that likely resemble amyloids have also been described (Molliex et al., 2015).

To better understand the relationship between fiber formation and phase separation by hnRNPA1, we examined how mutations that affect the propensity of the protein to form amyloid structures (H. J. Kim et al., 2013) affect phase separation and droplet maturation. A hexapeptide deletion of hnRNPA1 ($hnRNPA1_{Hexa}$) removes the predicted amyloid-forming region of the protein and abolishes hnRNPA1 fiber formation *in vitro* (H. J. Kim et al., 2013). Oppositely, a mutation in the amyloid core (D262V) is known to induce ALS-like neurodegeneration *in vivo* and amyloid hyper-assembly *in vitro* (H. J. Kim et al., 2013). We observed that both the variants of $hnRNPA1_{\Delta Hexa}$ and $hnRNPA1_{D262V}$ produced droplets similarly to wild-type hnRNPA1, indicating that the ability to phase separate is not strictly coupled to amyloid formation (**Figure 13C**). Interestingly, $hnRNPA1_{D262V}$ became salt resistant much faster than the wild-type and the Δhexapeptide hypo-assembly mutant (**Figure 13D**). Consistent with the ability of $hnRNPA1_{D262V}$ to form amyloid fibers, we observed that SDS-resistant fibers were visible after 29 hours in solutions containing the $hnRNPA1_{D262V}$ droplets (**Figure 14C**). Similar fibers were also seen in the $hnRNPA1_{D262V}$ protein preparation with continued incubation at high salt where no phase separation occurs, but only after 54 hours (**Figure 14D**). Thus, phase separation is not required to generate fibers, although as in the engineered systems it appears to increase the rate of fiber formation, presumably due to the high concentration of protein in the droplets. Consistent with these hnRNPA1 fibers having amyloid-like features, fibers formed in either high or low salt stained positive with Thioflavin-T (**Figure 14B**).

Like the model systems, we also observed that phase separated droplets of hnRNPA1 could recruit other IDRs. Specifically, the GFP-Fus_{IDR}, GFP-$eIF4GII_{IDR}$ and GFP-$Lsm4_{IDR}$ proteins were similarly recruited into droplets produced from the hnRNPA1 protein in low salt, while GFP alone was not (**Figure 15A,B**). This indicates that the heterotypic recruitment of IDR proteins into droplets can occur in a protein dependent manner.

Initial attempts to observe LLPS upon RNA addition to hnRNPA1 under physio-

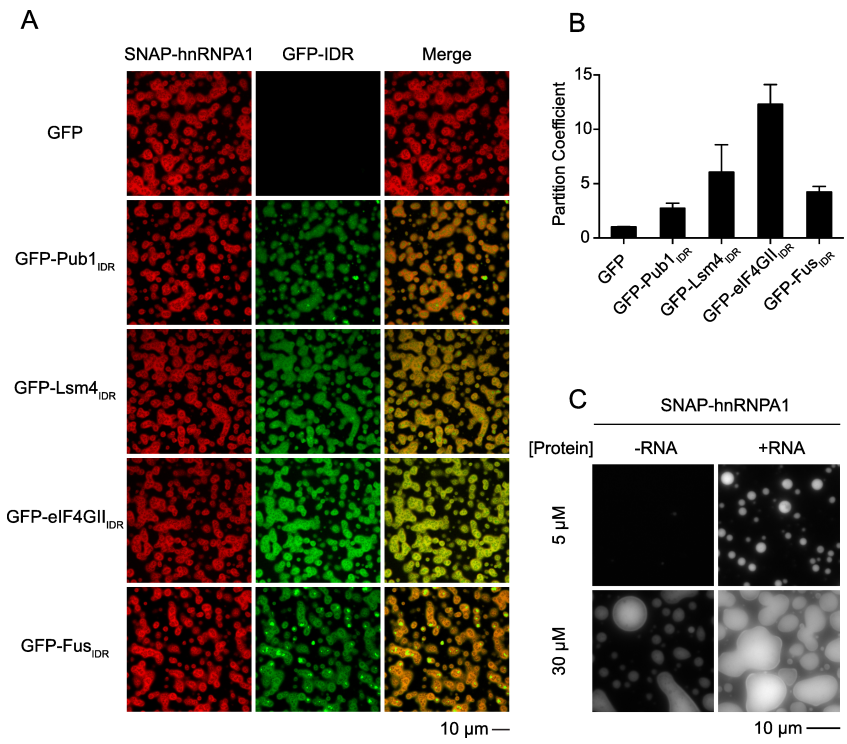

Figure 15: **Phase separated droplets of full-length hnRNPA1 recruit GFP-IDRs and are promoted by RNA**

(A) Images showing the partitioning of GFP-IDR probes (100 nM, green) into the liquid droplets (red) of SNAP-hnRNPA1 (30 µM) at 37.5 mM NaCl. SNAP-hnRNPA1 was labeled with SNAP-Surface 649

(B) Quantification of the GFP-IDR partition coefficients in experiments from panel A. The partition coefficients are plotted as mean ± SD, from three measurements each of which averaged all the droplets across three slide regions

(C) Fluorescence microscopy images of SNAP-hnRNPA1 (2 or 20 µM) with or without RNA(2: 1 molar ratio of 5XA1 RNA : hnRNPA1) at 175 mM NaCl, 100 mg/ml PEG 3350

logic salt conditions were unsuccessful. However, if we added PEG as a crowding agent, we observed phase separation of hnRNPA1 without RNA at high protein concentrations (**Figure 15C**), and stimulation of LLPS with RNA addition at lower protein concentrations (**Figure 15C**), demonstrating that RNA can promote LLPS of hnRNPA1. Similar results were observed with Ficoll as a crowding agent (**Figure 16A,B**).

Thus, the basic behaviors that we have observed for droplet formation, maturation and partitioning are common among a large group of engineered and natural RNA binding proteins, suggesting they are likely common to proteins of this type that contain both RNA binding domains and IDRs. The implications of these behaviors for the formation and regulation of RNA granules are discussed below.

2.4 Discussion

2.4.1 *Disordered Regions Can Promote Phase Separation*

Several observations demonstrate that IDRs on a number of RNA binding proteins can promote phase separation. First, the IDR elements of hnRNPA1, eIF4GII, Fus, TIA1 and Pub1 are sufficient to promote LLPS at low salt when fused to a SNAP-reporter protein (**Figure 5**). Second, full length hnRNPA1 also undergoes LLPS at low salt, which is dependent on its C-terminal IDR region (**Figure 13B**), observations also made by Molliex et al., (Molliex et al., 2015). When IDRs are fused to the PTB RNA binding protein, LLPS can be induced by RNA at lower protein concentrations than PTB alone at physiologic salt concentration. In the presence of crowding agents LLPS occurs at protein concentrations similar to those measured for a number of RNA granule proteins *in vivo* (Beck et al., 2011), indicating these transitions are occurring in a biologically relevant concentration regime. For all of the IDRs except that of eIF4GII this effect is specific to PTB-RNA binding, as RNA does not induce phase separation of the IDRs alone.

These observations suggest that PTB-RNA and IDR-IDR interactions act synergistically to promote LLPS. How might this occur? Both interaction modes are effectively

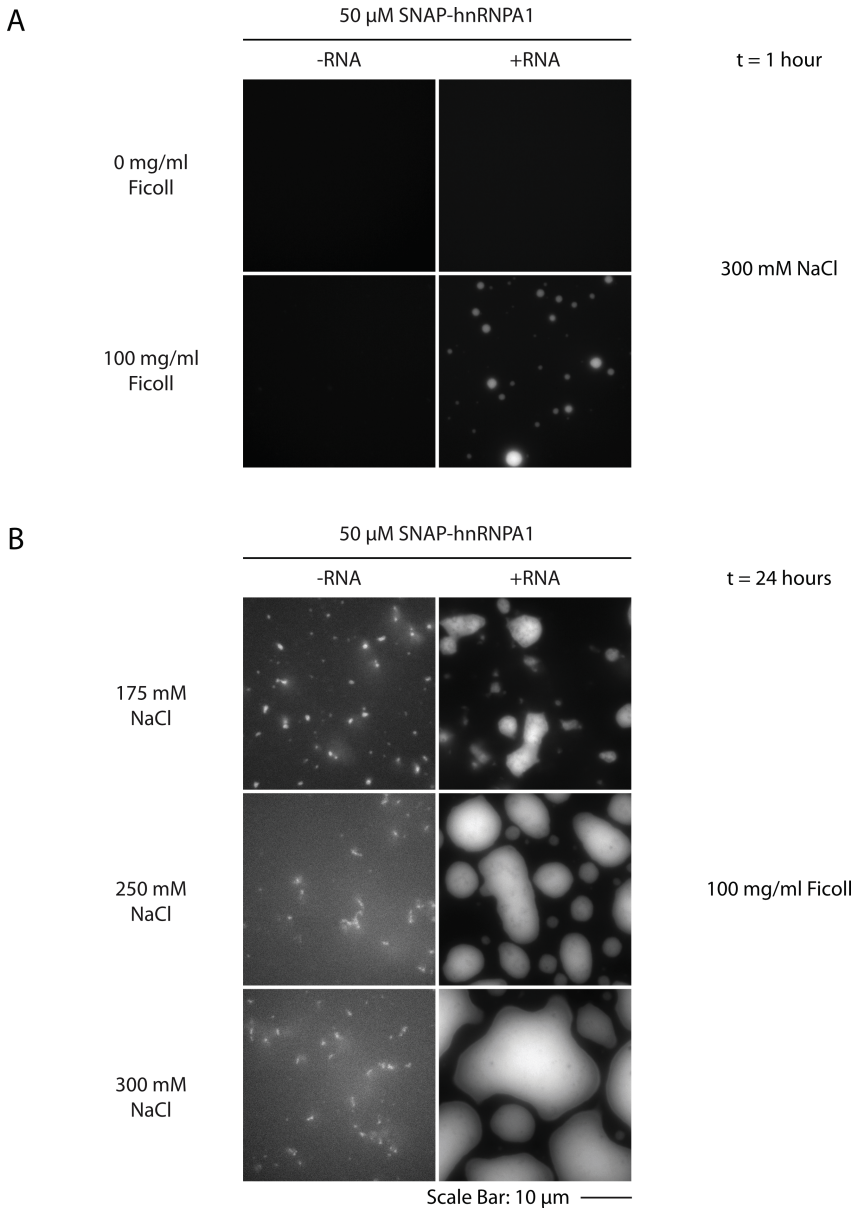

Figure 16: **Both RNA and Ficoll promote LLPS of full-Length hnRNPA1**

(A) Fluorescence microscopy images of SNAP-hnRNPA1 (50 µM) with or without RNA (100 µM) in the presence or absence of 100 mg/ml Ficoll at 300 mM NaCl.

(B) Fluorescence microscopy images of SNAP-hnRNPA1 (50 µM) with or without RNA(100µM) at indicated salt concentrations. 100 mg/ml Ficoll.

multivalent, the former through binding of multiple RRM domains to repeated nucleotide motifs (P. Li et al., 2012), and the latter presumably through weak binding of multiple sequence motifs in the disordered chains to each other (Nott et al., 2015). This property enables each to promote oligomerization and concomitant phase separation (P. Li et al., 2012). In PTB-IDR fusion proteins, the two interaction modes, since they involve different regions of the molecule, act together to produce larger oligomeric structures than either would alone, at a given concentration. Since oligomers become less soluble as they grow larger (Flory, 1953), this effect would promote LLPS at lower concentrations. Analogous behaviors are seen for very simple proteins such as the gamma-crystalins, whose crosslinked oligomers undergo LLPS at progressively lower concentrations as their size increases (Pande et al., 1995; Asherie et al., 1998), and also for crosslinked polymers (Semenov & Rubinstein, 1998). This suggests that RNP granule assembly in cells will be driven in part by mRNA providing multivalent sites for RNA binding proteins and then hetero- and homo-typic interactions between IDRs on these proteins to work in concert to create oligomers generated from two inherent forms of multivalency.

2.4.2 *IDR Dependent Phase Separated Droplets Mature to a Less Dynamic State.*

Several observations indicate that the phase-separated droplets promoted by IDRs change their biochemical nature over time and mature to more stable, less dynamic assemblies. First, the droplets generated by the engineered proteins and full-length hnRNPA1 are initially reversible with high salt, but over time change to a more granular consistency and become resistant to salt disassembly (**Figures 10, 9** and **13**) (Figures 3, S3 and 5). Second, FRAP experiments reveal that SNAP-PTB-IDR+RNA droplets become less dynamic over time (**Figure 10C**). Third, over time many of the IDR proteins form filaments that can be observed by light- and/or electron microscopy (**Figures 8C** and **10B**). For SNAP-PTB-Lsm4 $_{\text{IDR}}$, SNAP-PTB-Tia1 $_{\text{IDR}}$ and full length hnRNPA1 (**Figures 10A** and **13D**) filaments form more rapidly in phase separated solutions, likely due to the high concentration of molecules in the droplets, which by analogy to various amyloid

systems is expected to accelerate nucleation and growth (Eisenberg and Junker, 2012). Since these fibers stain with Thioflavin-T and are, at least in some cases, SDS resistant (**Figures 9C and 14C**) , the simplest interpretation is that they are amyloid-like. Together, these results suggest that maturation results at least partially from the formation of amyloid-like fibers.

Our data indicate that under the same biochemical conditions, IDRs can form two types of homotypic interactions, those that lead to initial phase separation, which are multivalent and dynamic, and those that form more slowly, which are more stable and structurally organized. One possibility is that these different interactions contribute initially to RNP granule assembly by triggering LLPS, and also subsequently by the formation of more stable fiber-like structures (or assemblies thereof). The fibers could be kept short in cells by competing disassembly machineries (Walters et al., 2015). These stronger interactions could give stability to the granules once formed, while extreme fiber formation could become pathological. Further experiments will be necessary to determine whether the different interaction modes involve the same or different chemical elements in the various IDR chains.

2.4.3 *IDR Dependent Phase Separated Droplets Recruit Other IDR Proteins.*

Several observations demonstrate that phase separated droplets promoted by one IDR can effectively recruit proteins containing the same, or different IDRs. First, PTB-Fus_{IDR}+RNA droplets effectively recruit GFP-IDR and SNAP-IDR molecules (**Figure 11** and **12**). IDR recruitment appears to depend on a combination of interactions with PTB/RNA and also the Fus IDR. Second, hnRNPA1 droplets generated in low salt effectively recruit the IDRs of Lsm4, Pub1, eIF4GII and Fus (**Figure 15**). The ability of a given phase separated droplet to recruit diverse IDRs could be relevant to cells by providing a mechanism for the assembly of multiple RNA binding proteins with IDR domains into a single mRNP granule. Moreover, the presence of heterotypic interactions between IDRs on RNA binding proteins might also increase the relevant concentration

available to trigger phase separation *in vivo*.

2.4.4 A Model for RNP Granule Assembly

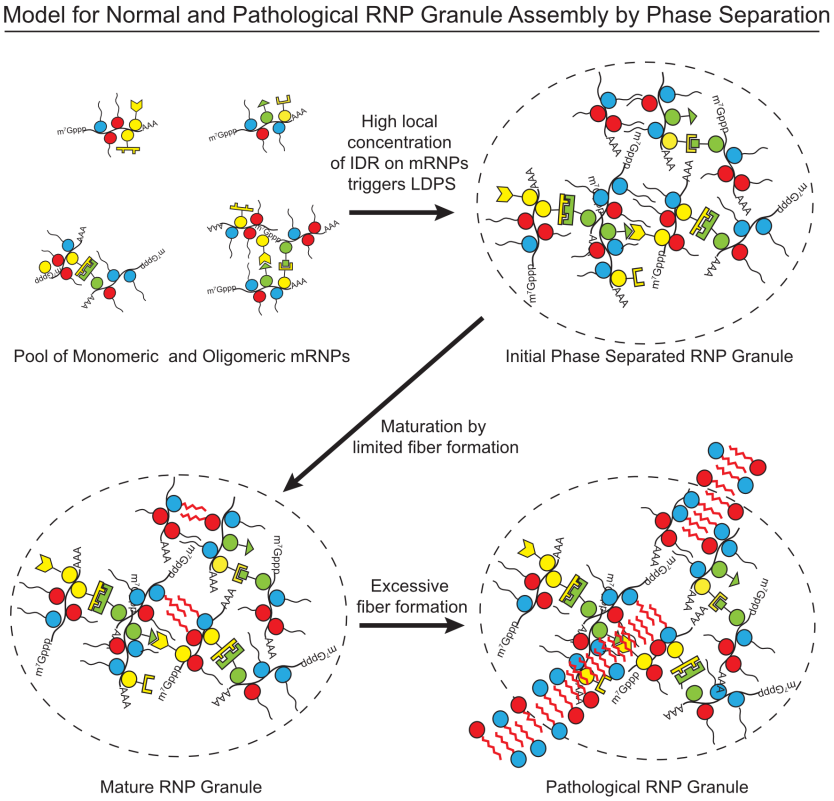

Figure 17: **Possible model for how phase separation contributes to RNP granule assembly**

Previous data have argued that RNP granules may form through LLPS in cells (C. P. Brangwynne et al., 2009, 2011; Nott et al., 2015; Elbaum-Garfinkle et al., 2015). Our data suggest a molecular mechanism by which this phase separation could be promoted by molecules known to reside in these structures. That is, phase separation could be promoted by the combined interactions of defined RNA binding domains, IDR elements and RNA. IDR interactions and multivalent RNA-protein interactions can each drive LLPS alone, but could act synergistically for the many proteins that contain both elements. Since IDR interactions may be of relatively low specificity, it seems likely that any mechanism that brought IDR elements together could promote LLPS. For example, the high concentration of heterotypic IDRs on an assembled mRNP, or mRNPs

oligomerized by traditional protein-protein interactions, could create a high local IDR concentration to initiate phase separation (**Figure 17**). Similarly high local concentrations of RNPs (and accompanying IDRs) could occur at sites of RNP biogenesis (as in the nucleolus), or at locations targeted by specific transport mechanisms. The latter would be consistent with evidence that motors play important roles in the assembly of stress granules (Loschi et al., 2009). The liquid-like structures formed by these processes would be distinct from traditional macromolecular assemblies in at least two important ways. First, and most significantly, unlike canonical multicomponent complexes (e.g. the ribosome) a granule formed by LLPS would not be stereochemically defined across its length. Rather, beyond the scale of its individual components, which could be individual proteins or protein-RNA assemblies, the elements would be largely randomly organized. Moreover, the arrangement of components will change, likely rapidly, with time. Importantly, though, our data on droplet maturation suggest that the degree and length scale of order could be controlled through regulation of the fibrillization of IDRs (see below). Second, our data suggest that while proteins and RNA are very highly concentrated in droplets, the structures are still >90 % water by mass (based on protein concentrations 300 µM), unlike assemblies of folded proteins which typically exclude water, and even protein crystals which are often 30-50 % water. RNP granules in cells are similarly only somewhat more dense that the surrounding cytosol (Handwerger et al., 2005), and studies of molecular diffusion in P-granules in nematodes have suggested that while 155 kDa dextrans are excluded from granules, 40 kDa particles are not excluded (Updike et al., 2011). Together, these properties conspire to enable molecules to be concentrated within granules, but move rapidly and freely within them. The degree to which the physical environment of a granule affects the biochemical processes that occur within it remains an exciting open question.

Initially the macromolecular interactions within the phase separated droplets are transient, and without long-range structural organization, affording the droplets liquid-like properties. But the high protein concentrations within the phase-separated droplets would increase additional protein-protein interactions, including accelerating the natural

tendency of IDRs to form amyloid-like fibers. This would naturally lead over time to more static structures that behave as solids. In cells, the balance between disordered, dynamic liquid and ordered, more static fibers is likely regulated to produce a range of RNP granules with different physical and chemical properties according to specific functional needs. More generally, the ability of LLPS to rapidly generate a concentrated biochemical compartment within cells that favors downstream interactions is likely to be a fundamental principle of these transitions, which cells use in numerous contexts to rapidly establish and then maintain cellular structures.

The lengths and/or numbers of fibers within a granule could be controlled through factors that enhance or inhibit fiber nucleation and growth, or that actively disassemble fibers, such as the ATP-driven disaggregase machines VCP/Cdc48 and Hsp70/Hsp40 complexes, which are known to control RNA granule lifetimes and turnover (J. Buchan et al., 2013; Walters et al., 2015). When this regulation is aberrant, for example due to mutations that increase fiber propensity or decrease disaggregase activity, fiber formation can become extreme, leading to disease. Such a model could explain how increased or prolonged stress granules can promote the formation of pathological aggregates that occur in various degenerative diseases (Ramaswami et al., 2013; Y. R. Li et al., 2013). It could also explain why many ATP driven machines play a role in modulating stress granule dynamics (Walters et al., 2015). The unique ability of IDRs to populate highly distinct structural and dynamic states under physiologic conditions would make them uniquely suited to control the physical and chemical properties of RNP granules, perhaps explaining the abundance of IDR elements in RNA binding proteins.

2.5 Materials and Methods

Materials

Expression plasmids for all the recombinant proteins were constructed based on the pMal-c2 vector (NEB), except for full length hnRNPA1 and related mutants, which were built into a modified pet11a vector (Novagen)(see also Supplemental Experimental Pro-

cedures). Proteins were expressed in *Escherichia coli* BL21(DE3) and purified with Ni and/or amylose resin . Proteins of SNAP-PTB-IDRs were further purified through a Superdex200 column. The extinction coefficients at 280 nm were obtained from ExPASy ProtParam (`http://web.expasy.org/protparam/`) and used to calculate protein concentrations from A280 values obtained on NanoDrop spectrophotometers. Proteins were fluorescently-labeled with SNAP-Surface 488 or SNAP-Surface 649 (NEB) according to the manufacturer's protocols.

Droplet Assembly

For SNAP-IDRs and SNAP-hnRNPA1 (˜2% fluorescently labeled), droplet assembly was initiated by diluting the solutions to 37.5 mM NaCl, 20 mM Tris pH 7.4, 1 mM DTT. For SNAP-PTB-IDRs, proteins and RNA were mixed at the indicated concentrations (including 100 nM SNAP-PTB-IDRs labeled with SNAP-Surface 649) in 100 mM NaCl, 20 mM imidazole pH 7.0, 1 mM DTT, 10% glycerol. The N-terminal purification tags of SNAP-hnRNPA1 were removed by HRV C3 protease (EMD Milipore) during the dye conjugation step. The N-terminal MBP and C-terminal His tags of SNAP-IDRs and SNAP-PTB-IDRs were cleaved during droplet assembly with TEV protease (Promega ProTEV). Reactions were placed in glass-bottom chambers which were pre-coated with 3% BSA and washed three times with H_2O before use Thioflavin T incorporation was measured by including 10-25 µM of the reagent in droplet forming reactions. Imaging parameters are found in the Supplemental Experimental Procedures.

Fluorescence Microscopy

All images of SNAP-IDR and SNAP-hnRNPA1 were acquired on a DeltaVision epi-fluoresence microscope, equipped with a SCMOS camera and LED illumination. The EGFP-IDR recruitment assay was performed on a Nikon AR1 LSM confocal microscope. All images of SNAP-PTB-IDR were acquired on a Leica-based spinning disk confocal microscope (EMCCD digital camera, ImagEM X2, Hamamatsu; confocal scanner unit, CSU-X1, Yokogawa).

Fluorescence Recovery After Photobleaching

Fluorescence recovery after photobleaching (FRAP) experiments were performed on the same spinning disk confocal microscope mentioned above. The SNAP-tag containing proteins were labeled with SNAP-Surface 649 and bleached with full laser power for 30 iterations using a 405 nm laser line. The droplets were $>$ 5 µm in diameter and the bleaching area was ˜ 2 µm in diameter. Time-lapse images were acquired at 637 nm. Images were processed in ImageJ. Background intensity was subtracted and an image of a homogeneous solution was used to correct for uneven illumination. At each time point, the averaged fluorescence intensity within the bleaching spot was also divided by the intensity of a neighboring unbleached area of the same size to correct for changes in illumination during the time course of imaging. The corrected intensities within the bleaching spot during recovery were fit to a single exponential growth curve to yield the half time and the ratio of recovery ($[I_{max}\text{-}I_{min}]/[I_0\text{-}I_{min}]$) using GraphPad Prism 5 (GraphPad Software). Data are reported as mean SEM, n 2.

SDS-PAGE Assay for High-Salt Soluble Species in Droplets

Identical samples were prepared to contain 5 µM MBP-SNAP-PTB-Lsm4 (or 5 µM MBP-SNAP-PTB-TIA1) plus 1.6 µM RNA(phase separation) or buffer(no phase separation). TEV protease was present to remove MBP, which served as an internal loading control. At the indicated time points, NaCl was raised to 500 mM total concentration to disassemble the droplets. After incubation for 1 minute followed by centrifugation at 15,000 g for 5 minutes, the supernatant was carefully removed and loaded on an SDS-PAGE gel. Gels were stained with coomassie blue. The pellet was examined by TEM (see below). For SNAP-hnRNPA1$_{WT}$, SNAP-hnRNPA1$_{Hexa}$, SNAP-hnRNPA1$_{D262V}$, 25 µM proteins were first treated with HRV C3 at room temperature for 5 hours to cleave MBP completely. The proteins were diluted to 37.5 mM NaCl to initiate phase separation. At indicated time points, NaCl was raised to 150 mM total concentration. After incubation for 5 minutes followed by centrifugation at 15,000 g for 5 minutes, the supernatant was carefully removed and loaded on an SDS-PAGE gel. Gels were stained with coomassie blue. The intensities of the bands were measured in Image J and normalized

by the intensities of the internal control, MBP.

Transmission Electron Microscopy

The pellet after high salt wash (see previous section) at 24 hours was resuspended in buffer (100 mM NaCl, 20 mM imidazole pH 7.0, 1 mM DTT) by brief sonication, and directly transferred to a TEM grid (FCF300-Cu grid, Electron Microscopy Sciences) and stained with 5 µl of 1% (w/v) PTA (phosphotungstic acid, pH adjusted to 8.0 with NaOH) for 1 minute. After the removal of the PTA solution, the grid was air-dried. The images were obtained on FEI Tecnai transmission electron microscope.

IDR Recruitment Assay

Partitioning of EGFP-IDRs into droplets of PTB or PTB-Fus$_{IDR}$ + RNA

Droplets were formed in glass bottomed chambers by either 10 µM PTB plus 3.2 µM RNA (note that PTB phase separates at lower concentrations than SNAP-PTB) or 1.25 µM PTB-Fus$_{\mathrm{IDR}}$ plus 0.4 µM RNA. In both cases, droplets were labeled with 10 nM 3'-Cy3 RNA and 100 nM GFP-IDR was used as probe. TEV protease was present to remove MBP tag. After a 1 hour incubation, images were acquired using the spinning disk confocal microscope mentioned above at 637 nm and 561 nm simultaneously. Background intensity was subtracted and an image of a homogeneous solution was used to correct for uneven illumination. Droplet intensities were measured by averaging the intensities at the center (with diameter 2.5 µM smaller than that of the droplets) of droplets (˜50-100 total number) from at least three different areas. For bulk intensities, identical samples were prepared in microcentrifuge tubes for 1 hour and centrifuged at 21,130 g for 5 minutes. The supernatants were transferred to glass-bottom chamber and the intensities were measured identically. Intensities were converted to concentrations through a GFP standard curve. The partition coefficient is defined as $[\mathrm{GFP}]_{\mathrm{droplet}}$ / $[\mathrm{GFP}]_{\mathrm{bulk}}$, and shown as mean SD from three measurements. P values were obtained using the unpaired t-test. A representative image for each condition was chosen and the same brightness and contrast were used to show the relative intensities.

Partitioning of EGFP-IDRs into Droplets of SNAP-hnRNPA1$_{FL}$

Fluorescently tagged 30 µM SNAP-hnRNPA1 (SNAP-Surface 649) with purification tags removed was mixed with 100 nM GFP-IDR or GFP alone in the presence of TEV protease (Promega ProTEV) to remove the N and C terminal purification tags from GFP constructs. Samples were incubated for 30 minutes at room temperature to allow for cleavage of purification tags prior to droplet assembly. Samples were diluted with 20 mM Tris pH 7.4 to indicated protein and salt concentrations. Of each reaction ,3 aliquots were plated into passivated glass-bottomed 96 well plates (3 % BSA, 15 minutes, washed 3X with ddH2O) (PerkinsElmer Glass-Bottomed ViewPlate). After 45 minutes the other half of the reaction was centrifuged at 16,300 g for 3 minutes, and 3 aliquots of the supernatant were transfered to the 96 well plate. Droplet and supernatant wells were imaged with different instrument parameters due to the small dynamic range of the Nikon AR1 LSM Confocal microscope used. Small FUS aggregates were excluded from the droplet region. The reported relative enrichment is defined as $I_{droplet}$ / $I_{bulk.}$

3 Intrinsically Disordered Regions Contribute Promiscuous Interactions for RNP Granule Assembly

3.1 Project Background

The work presented in this chapter stemmed from the observation that BSA tended to disrupt IDR-driven droplet assembly. I made this observation while testing different crowding agents in an attempt to make our droplets occur at buffer conditions mimicking the cell. I proposed that IDRs did not seem sufficient to drive higher-order assemblies in cells. Dr. Parker and I soon realized that other unpublished observations from other lab members supported this hypothesis. Briana Van Treeck had observed that IDRs from a variety of RNP granule components were insufficient to localize GFP or mCherry to P-bodies in *S. cerevisiae*. Conversely, Bhalchandra Rao had observed that under conditions where P-body assembly was already impaired, the IDR of Dhh1 was required for P-body assembly in *S. cerevisiae*. We therefore developed a model wherein the IDRs of RNP granules contribute weak interactions that are not sufficient for granule assembly, but can still contribute important binding energy for the formation of higher-order assemblies. We came to the difficult conclusion that the generic IDR-LLPS experiments often used in the literature to suggest that a protein contributes to granule assembly were likely not accurately representing the behavior of these proteins in cells. This is especially clear when one considers the exterme effect that yeast lysates had on LLPS of our model proteins. Therefore, we do not believe using the simple ability of a protein to undergo LLPS as a single component *in vitro* as evidence for contribution to RNP granule assembly. This work is currently under re-submission at eLife.

To this work, which follows, I contributed significant intellectual input, proposing the idea that IDRs are not sufficient for granule assembly and suggesting the inclusion of Brianas work. I performed a variety of *in vitro* and one *in vivo* experiments that

were not included in the final manuscript (**Figures 27 and 28**), as well as the *in vitro* experiments that became **Figures 18, 19, and 21**. Yuan Lin provided data for Figure 22 using tools he developed for our previous collaboration, while I performed image quantification on his data. Briana Van Treeck performed yeast experiments examining the IDR contribution to granule localization (**Figure 23**). Bhalchandra Rao performed p-body rescue experiments (**Figure 24**) in yeast for which I helped determine which IDRs to use for rescue, as well as to construct plasmids. I also wrote Python scripts to identify foci and quantify the data.

3.2 Introduction

Eukaryotic cells contain a variety of non-membrane bound RNA-protein assemblies, collectively referred to as RNP granules. Such RNP granules include the nucleolus and Cajal body in the nucleus, as well as stress granules and P-bodies in the cytosol (Spector, 2006). RNP granules are generally highly dynamic, as judged by FRAP of their protein components, and exhibit liquid-like behaviors, such as flowing, fusing, and rapid reorganization of internal components (C. P. Brangwynne, 2013; C. P. Brangwynne et al., 2009). RNP granules are thought to assemble through a process referred to as liquid-liquid phase separation (LLPS) wherein RNA molecules provide binding sites for RNA binding proteins that interact with themselves or other RNA binding proteins to create a larger multivalent assembly (Elbaum-Garfinkle et al., 2015; Feric et al., 2016; Kaiser, Intine, & Dundr, 2008; Mitrea et al., 2016; Nott et al., 2015; Pak et al., 2016; Patel et al., 2015; Riback et al., 2017; S. C. Weber & Brangwynne, 2012; H. Zhang et al., 2015). Some of the interactions that drive RNP granule assembly are well defined interactions between folded proteins, or folded protein domains and short linear motifs (SLiMs) (Decker et al., 2007; Jonas & Izaurralde, 2013; Kedersha et al., 2016; S. H. M. Ling et al., 2008; Mitrea et al., 2016; Tourriere, 2003). Since these interactions require folded protein structures and/or extended linear motifs that interact in a stereospecific manner, we refer to these interactions as specific interactions.

The IDRs of RNA binding proteins have been highlighted as drivers of RNP granule assembly for three reasons. First, genetics indicate that IDRs can be important for assembly of RNP granules or localization of granule components (Decker et al., 2007; Feric et al., 2016; Gilks et al., 2004; Hennig et al., 2015; Kato et al., 2012). Second, RNP granules are often enriched in proteins with IDRs (Decker et al., 2007; Jain et al., 2016; Kato et al., 2012; Kedersha, Ivanov, & Anderson, 2013; Reijns et al., 2008). Finally, IDRs are often (but not always) both necessary and/or sufficient for LLPS of granule proteins *in vitro*, forming structures that resemble RNP granules *in vivo* (Elbaum-Garfinkle et al., 2015; Lin et al., 2015; Molliex et al., 2015; Nott et al., 2015; Patel et al., 2015; Smith et al., 2016; H. Zhang et al., 2015).

An unresolved issue is how IDRs contribute to RNP granule assembly, and how IDR based assembly mechanisms integrate with specific protein-protein and protein-RNA interactions to promote RNP granule formation. The literature suggests three non-mutually exclusive models by which IDRs could contribute to LLPS *in vitro* and RNP granule formation *in vivo*. First, some experiments *in vitro* suggest that IDRs promote LLPS via weak binding, utilizing electrostatic, cation-, dipole-dipole and - stacking interactions (C. Brangwynne, Tompa, & Pappu, 2015; Lin et al., 2015; Nott et al., 2015; Pak et al., 2016). Charge patterning also appears to play an important role, wherein like-charged amino acids are clustered together within an IDR. Scrambling these charges across the length of an IDR has been observed to impair LLPS both *in vitro* and *in vivo* (Nott et al., 2015; Pak et al., 2016). Because these interactions only require a few amino acids, and do not require any stereospecific arrangement, they would be anticipated to occur between an IDR and many other proteins, including other IDRs. Indeed, charge patterning specifically has been proposed to mediate interactions between IDRs and cellular proteins (Pak et al., 2016). For this reason, we refer to the above types of IDR interactions as nonspecific. These interactions will also be promiscuous, because they will be relatively indiscriminate with respect to binding partners. A second possibility is that elements within some IDRs interact in a specific manner involving local regions of secondary structure. For example, there is a correlation with how mutations in hnRNPA2

affect binding of its C-terminal disordered domain to beta-strand rich hydrogels, and the recruitment of those hnRNPA2 domain variants to LLPS of wild-type hnRNPA2 (Xiang et al., 2015). Similarly, a locally formed α-helix in TDP-43 can mediate LLPS through homotypic interactions (Conicella, Zerze, Mittal, & Fawzi, 2016). Finally, it is likely that a subset of IDRs are also promiscuous RNA binding proteins since they can be rich in positive charges, some IDRs can cross link to mRNA *in vivo* , and some IDRs can bind RNA *in vitro* (Lin et al., 2015; Lyons, Ricciardi, Guo, Kambach, & Marzluff, 2014; Mayeda, Munroe, Cceres, & Krainer, 1994; Molliex et al., 2015).

Given the promiscuous nature of IDR interactions, we hypothesized that such IDR based interactions alone would be susceptible to other highly abundant proteins in cells, and therefore insufficient to drive LLPS and the assembly of an RNP granule *in vivo*. In the context of the protein-rich cellular environment other proteins would compete for binding to the IDRs and thereby prevent their forming a defined assembly. Moreover, even the ability of some IDRs to form specific local structure based interactions might be impaired by competition with other proteins in the cell. Instead, to account for the contributions from both IDRs and specific interactions to RNP granule assembly, we hypothesized that IDRs would reinforce assemblies that contained specific assembly interactions. Effectively, specific interactions would concentrate the IDRs and strengthen their interactions through additive binding energies (Jencks, 1981), either biasing their promiscuous interactions toward components of the assembly, or promoting the formation of specific interactions between the IDRs. In this way, IDR-based interactions could contribute to the energetics of assembly.

Here we provide several observations that RNP granule assembly gains selectivity from specific protein-protein and protein-RNA interactions, and that promiscuous binding of IDRs to proteins and possibly RNA enhances these assemblies. First, we observe that LLPS driven by IDRs *in vitro* is inhibited by other proteins. Second, in cells we observe that IDRs of granule components are often neither required nor sufficient to target proteins to RNP granules. Third, we demonstrate that *in vitro* LLPS driven by specific protein-RNA interactions is enhanced by adding promiscuously interacting

IDRs, and the assembly of yeast P-bodies in cells is promoted by nonspecific IDRs in conjunction with specific interactions. Thus, RNP granules assemble primarily by specific interactions, which can be enhanced by IDRs capable of either promiscuous, or weak specific interactions based on small structural elements that become effective at high local concentrations. We suggest that this general assembly mechanism may be shared by other macromolecular complexes rich in IDRs.

3.3 Results

3.3.1 *Several proteins inhibit LLPS driven by IDRs* in vitro

We hypothesized that IDRs of RNA binding proteins might not be sufficient to drive LLPS in the presence of other proteins similar to the intracellular environment, despite the observation that such IDRs are capable of undergoing LLPS as purified proteins (Elbaum-Garfinkle et al., 2015; Lin et al., 2015; Molliex et al., 2015; Nott et al., 2015; Patel et al., 2015; Smith et al., 2016; H. Zhang et al., 2015). Our hypothesis was based on the observations that LLPS driven by IDRs *in vitro* are thought to occur by weak electrostatic, dipolar interactions as well as interactions involving aromatic groups (reviewed in (C. Brangwynne et al., 2015)). Since these interactions are nonspecific, they are likely relatively promiscuous and could, in principle, occur between an IDR and other IDRs or with many other proteins. Moreover, even IDRs that have homotypic interactions based on local structural elements might be sensitive to other proteins and be most efficient at forming such specific assemblies only when concentrated by specific interactions (Xiang et al., 2015; Conicella et al., 2016). Thus, we asked whether IDR driven LLPS *in vitro* would be inhibited in the presence of other polypeptides, which would be analogous to the interior of the cell.

To test whether an IDR can promote LLPS in the presence of other proteins, we induced LLPS of either full-length hnRNPA1$_{\Delta\text{hexa}}$ or only the hnRNPA1$_{\text{IDR}}$ region (amino acids 186 to 300, **Figure 18A**) by dilution into lower salt (37 mM NaCl) (Lin et al., 2015) in the presence of increasing amounts of bovine serum albumin (BSA). We used the Δhexa-peptide variant of the full-length hnRNPA1 protein as it is less prone to forming

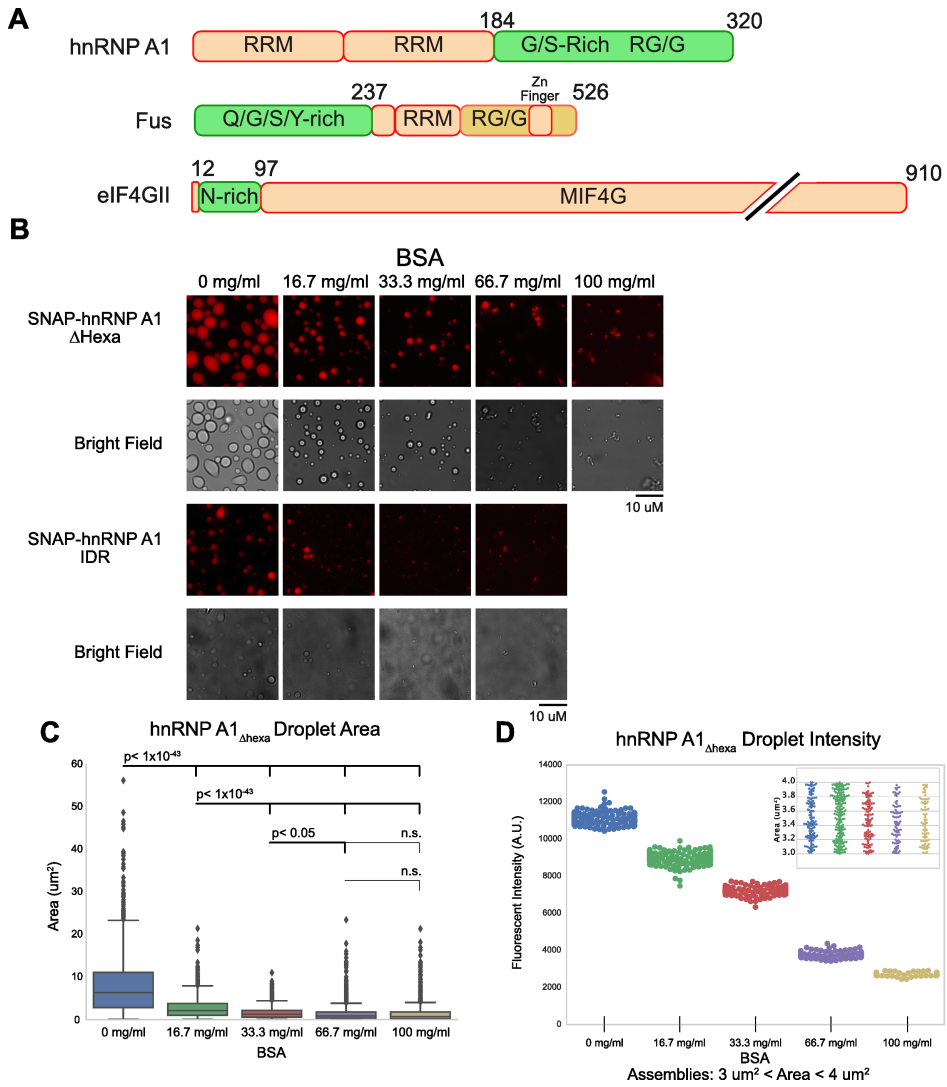

Figure 18: **Competitor proteins disrupt IDR-Driven phase separations**

(A) Domain structure of hnRNPA1, FUS, and eIF4GII

(B) Fluorescent and bright-field microscopy images of phase separated droplets formed at 37.5 mM NaCl by SNAP-hnRNPA1Δhexa and SNAP-hnRNPA1IDR with the indicated concentrations of BSA. Images are each independently scaled

(C) Quantification of structure size for hnRNPA1Δhexa from (B), significance calculated with Welch's t-test for unequal size and variance

(D) Quantification of the intensity of all structures between areas of 3µmand 4µmfor hnRNPA1Δhexa from (B). These subsets of droplets have roughly equal distributions of size (inset)

amyloid fibers during purification and analysis, and behaves similarly to the wild-type protein with regards to LLPS (Lin et al., 2015; Molliex et al., 2015). The fluorescently conjugatable SNAP tag was fused to both proteins to visualize droplets.

As the concentration of BSA increased, LLPS for both full-length SNAP-hnRNPA1$_{\Delta\text{hexa}}$ and the SNAP-hnRNPA1$_{\text{IDR}}$ was inhibited (**Figure 18B**). At higher BSA concentrations, we observed the formation of aggregated hnRNPA1$_{\Delta\text{hexa}}$ and hnRNPA1$_{\text{IDR}}$ that contrast with the liquid droplets seen in the absence of BSA (**Figure 18B**). As BSA concentrations increase, droplet sizes decrease and no large droplets form (**Figure 18C**). Interestingly, by looking at a subset of droplets of similar size across all BSA concentrations, we noticed that as BSA concentrations increased the intensities of hnRNPA1$_{\Delta\text{hexa}}$ droplets decreased (**Figure 18D**). The distribution of areas was approximately equal between samples (**Figure 18D inset**). The partition coefficient of LLPS (the ratio of protein within the concentrated phase versus within the dilute phase) is a measure of the equilibrium between the two states. Therefore, we interpret this decrease in intensity to mean that BSA shifts the phase separation equilibrium such that it is less favorable for hnRNPA1$_{\Delta\text{hexa}}$ to exist within the concentrated phase. At higher BSA concentrations the equilibrium shifts such that hnRNPA1$_{\Delta\text{hexa}}$ is below the critical concentration for LLPS. Thus, BSA is an inhibitor of LLPS driven by hnRNPA1 or its IDR alone under these conditions.

To determine if this inhibitory effect is unique to hnRNPA1 and BSA, we examined how BSA, lysozyme, and RNase A affected LLPS driven by the IDRs of hnRNPA1, FUS, or eIF4GII, all of which have been reported to undergo LLPS at low salt or low temperature (Lin et al., 2015; Molliex et al., 2015; Patel et al., 2015). We observed that LLPS of FUS$_{\text{IDR}}$ (amino acids 1-237), eIF4GII$_{\text{IDR}}$ (amino acids 13-97), or the hnRNPA1$_{\text{IDR}}$ (184-320) (**Figure 18A**) were also inhibited by the presence of BSA, lysozyme or RNase A (**Figure 19A**).

To more closely mimic the cellular environment, we examined whether IDRs or IDR containing proteins could undergo LLPS in the presence of yeast lysate, which had been previously depleted of small metabolites and exchanged into droplet-forming buffer via

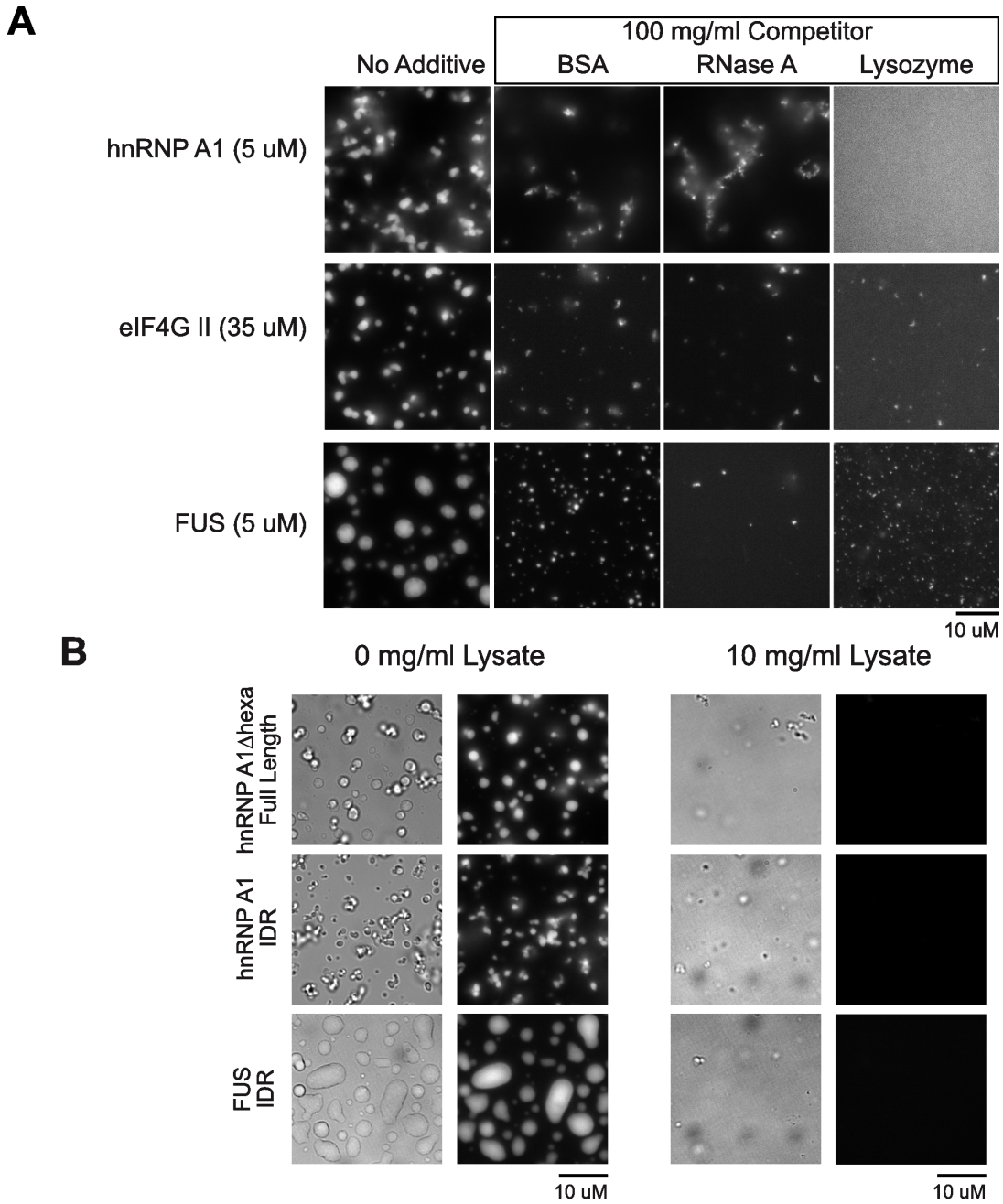

Figure 19: **Diverse globular proteins disrupt a variety of IDR-driven LLPS**

(A) Fluorescent microscopy images of phase separated droplets formed at 37.5 mM NaCl by hnRNPA1IDR, SNAP-FUSIDR, and SNAP-eIF4GIIIDR in the absence or presence of 100 mg/ml BSA, lysozyme, and RNase A.

(B) Fluorescent microscopy images of phase separated droplets formed at 37.5 mM NaCl by SNAP-hnRNPA1Δhexa, hnRNPA1IDR, and SNAP-FUSIDR, in the absence or presence of approximately 10 mg/ml yeast lysate.

desalting columns. We observed that LLPS of hnRNPA1$_{\Delta hexa}$, hnRNPA1$_{IDR}$, and FUS IDR are all strongly impaired in yeast lysates, which contained approximately 10 mg/ml protein (**Figure 19B**). Yeast lysates are our closest approximation of the cellular environment, and we find that even lysates 1/10th as concentrated as the cell (Milo, 2013) strongly impair LLPS of IDRs. Thus, phase separation of multiple IDRs is sensitive to competition from other molecules within the cell.

3.3.2 *Competitor proteins inhibit LLPS* in vitro *by interacting with IDRs*

What is the mechanism by which competitor proteins inhibit IDR-driven LLPS *in vitro*? One possibility is that BSA, lysozyme, and RNase A share some specific property or structural feature that inhibits LLPS of these IDRs. This is unlikely as BSA, lysozyme, and RNase A are structurally unrelated, and vary in size (66.4, 14.3, and 13.7 kDa respectively) and pI (5.3, 11.35, and 9.6, respectively). A second possibility is that any crowding agent will inhibit LLPS under these conditions. However, we observe that LLPS driven by hnRNPA1$_{IDR}$ is stimulated by the crowding agents Ficoll and PEG, with phase separation occurring at higher ionic strengths and lower protein concentrations than without crowding agents (**Figure 20**) (see also **Figure 6**).

A third possibility is that these competitor proteins compete for promiscuous interactions between IDRs and thereby disrupt LLPS. A prediction of this model is that at low concentrations, insufficient to block LLPS, the competitor proteins would be recruited into the phase separated droplets (due to interactions with the IDR). To test this possibility, we examined the recruitment of fluorescent BSA or lysozyme into droplets formed by IDRs. At low concentrations both proteins were recruited to IDR-driven droplets without disrupting the assemblies. For example, at 500 nM concentration FITC-BSA was strongly enriched in droplets of hnRNPA1$_{\Delta hexa}$ (**Figure 21A**). FITC-Lysozyme was also recruited (**Figure 21A**). Similarly, droplets of eIF4GII$_{IDR}$, hnRNPA1$_{IDR}$, and FUS$_{IDR}$ all recruited both FITC-BSA and FITC-lysozyme (**Figure 21B**). This suggests that these IDRs can interact with both BSA and lysozyme, consistent with the idea that competitor proteins could compete with the weak interactions that mediate LLPS.

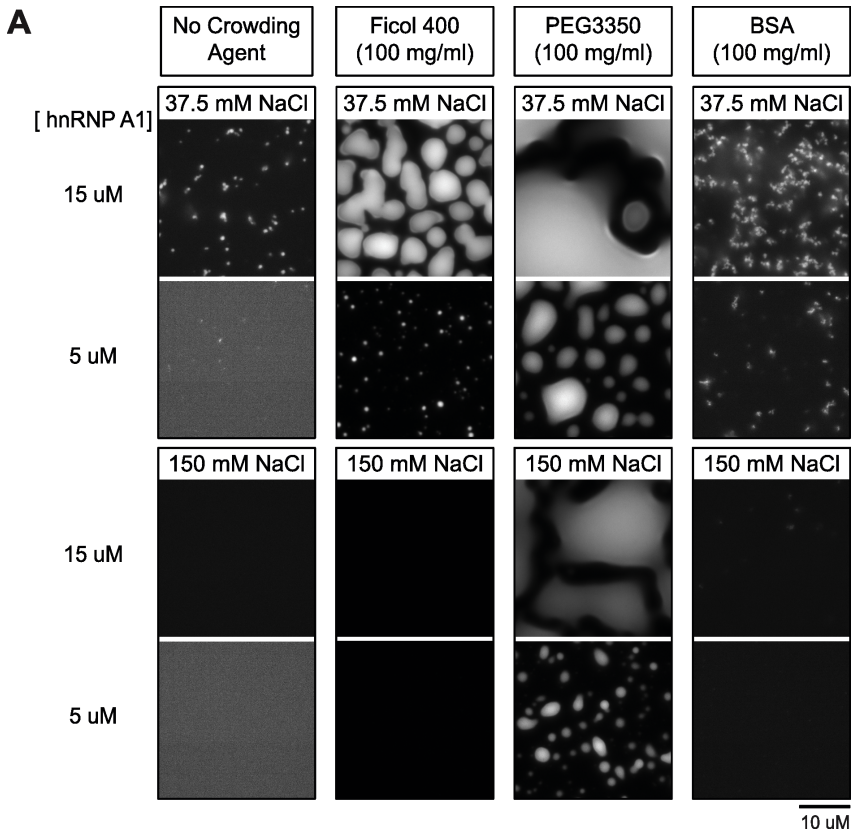

Figure 20: **Diverse effects of crowding agents and proteins on LLPS**

(A) Fluorescence microscope images of structures formed by SNAP-hnRNPA1 at either 150 mM NaCl or 37.5 mM NaCl in the absence or presence of 100 mg/ml Ficol 400, PEG 3350, or BSA. SNAP-hnRNPA1 concentrations were either 15 µM or 5 µM.

The above evidence suggests that competitor proteins can interact with IDRs, both because these proteins are recruited into phase-separated droplets and because they inhibit LLPS at higher concentrations. Since these proteins were chosen at random and have diverse physical properties, and LLPS is also inhibited by metabolite-depleted cell lysates, we suggest that IDRs by themselves are likely to be susceptible to such nonspecific interactions in the more complex cellular environment. Therefore, in many cases, promiscuous interactions of IDRs are unlikely to be sufficient for RNP granule assembly in cells.

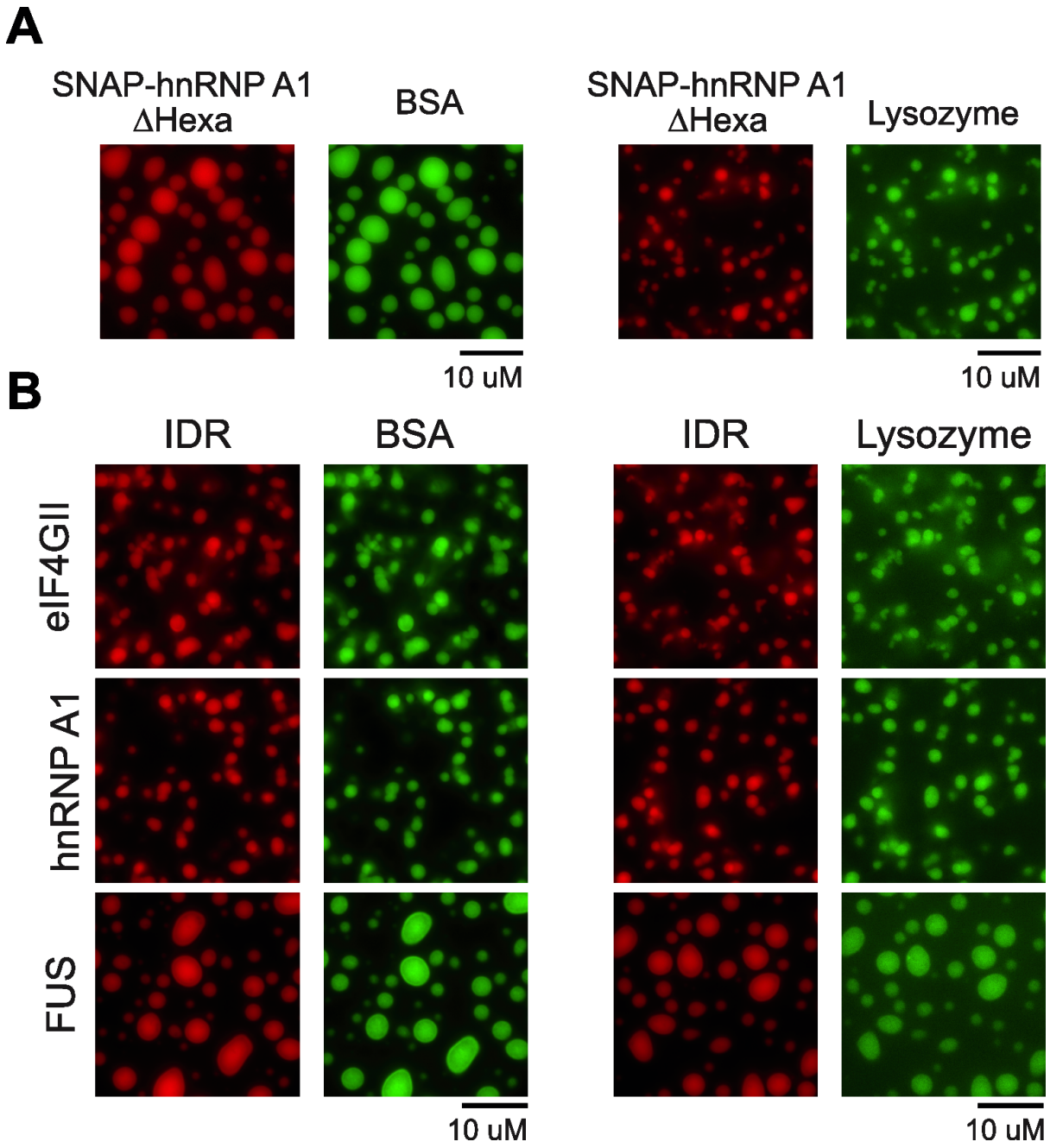

Figure 21: **Globular proteins are recruited to IDR-driven LLPS droplets**

(A) Fluorescence microscopy images of phase separated droplets formed at 37.5 mM NaCl by 25 µM SNAP-hnRNPA1$_{\Delta hexa}$ (red) and 500 nM FITC-labeled BSA (green) or FITC-labeled Lysozyme.

(B) Fluorescence microscopy images of phase separated droplets formed by SNAP-eIF4GII$_{IDR}$ (35 µM), SNAP-hnRNPA1$_{IDR}$ (5.25 µM), or SNAP-FUS$_{IDR}$ (5 µM) in the presence of either 10 nM FITC-BSA or 100 nM FITC-Lysozyme.

3.3.3 *IDRs can enhance LLPS driven by specific interactions in the presence of competitor proteins*

The *in vitro* results above suggest that IDR-IDR interactions are susceptible to competition by the complex protein mixture in the cell. However, IDRs are enriched in RNP granule proteins (Decker et al., 2007; Jain et al., 2016; Kato et al., 2012; King et al., 2012; Reijns et al., 2008), and IDRs can play a role in RNP granule assembly (e.g. (Decker et al., 2007; Gilks et al., 2004; P. Wang et al., 2014)). In some cases, IDRs contain SLiMs that are important for assembly of RNP granules (reviewed in (Jonas & Izaurralde, 2013)). However, since there are cases wherein one IDR can functionally substitute for another in RNP granule assembly (Decker et al., 2007; Gilks et al., 2004), a more generic role for IDRs in RNP granule assembly is also likely.

We hypothesized that IDRs in proteins that also make specific interactions could provide promiscuous, nonspecific interactions that stabilize an RNP granule by acting together with the specific interactions. By concentrating the IDRs through specific interactions, promiscuous IDR-based interactions are biased to other components of the assembly. In this model, specific interactions and nonspecific interactions both donate binding energy that promotes LLPS. This model makes two predictions that we first tested *in vitro*.

First, the model predicts that LLPSs driven by specific interactions should be less susceptible to the interference from other competitor proteins, and may even be enhanced, given that high concentrations of such proteins can serve as crowding agents. Consistent with this view, we have shown that the LLPS driven by the specific interaction of an RNA binding protein, poly-pyrimidine tract binding protein (PTB), with RNA is promoted by BSA (Lin et al., 2015), an observation reproduced here. For example, while SNAP-tagged PTB and RNA showed limited assembly when mixed together at concentrations of 20 μM and 1.6 μM, respectively, the addition of 100 mg/ml BSA induced robust phase separation at these concentrations (**Figure 22A**). Consistent with this effect being due to molecular crowding, the PTB-RNA LLPS is also stimulated by PEG or Ficoll, two additional crowding agents (**Figure 22A**). Thus, the specific PTB-RNA interactions are

not outcompeted by BSA, allowing the crowding effect of BSA to dominate.

A second prediction of the model is that while IDRs alone are not sufficient to drive phase separation in the presence of competitor proteins, IDRs would contribute binding energy to phase separation driven by specific interactions, decreasing the threshold concentration of assembly. To test this prediction, we examined how IDRs affect PTB-RNA phase separation in the presence of competitor proteins. For example, 4 µM PTB and 0.32 µM RNA do not phase separate in 100 mg/ml BSA. However, we observed LLPS with identical concentrations of RNA and PTB, when the PTB was fused to either the FUS or Pub1 IDR (**Figure 22B**). PTB fused to either IDR showed an increase in both the number and size of the assemblies visualized (**Figure 22C**). Therefore, weak interactions of IDRs can enhance phase separation in the presence of competitor proteins, when present in molecules that also contain specific interactions which are less susceptible to competition from cellular macromolecules.

3.4 IDRs are often neither sufficient nor necessary *in vivo* to target components to RNP granules

An assembly mechanism for RNP granules driven by specific interactions aided by promiscuous interactions of IDRs has predictions for how components would be recruited to RNP granules. Specifically, one would predict that generally IDRs would not be sufficient to target a protein to an RNP granule, unless they contained a specific SLiM. Moreover, IDRs would not be required for recruitment to a granule, although they could affect the partition coefficient (the concentration of a component within versus outside of a granule).

To examine how IDRs of yeast proteins affect their targeting to P-bodies, we examined if IDRs within Lsm4, Dhh1, Pop2, and Ccr4 (**Figure 23A**) were necessary and/or sufficient for their recruitment into P-bodies. The IDRs of Lsm4, Dhh1, Pop2, and Ccr4 were fused separately to either GFP or mCherry. IDR-fusion proteins were expressed in yeast co-expressing a chromosomally GFP-tagged P-body component or containing a secondary plasmid containing a mCherry tagged P-body component. P-bodies were induced by glucose deprivation for 15 minutes, and the percentage of P-bodies containing the IDR

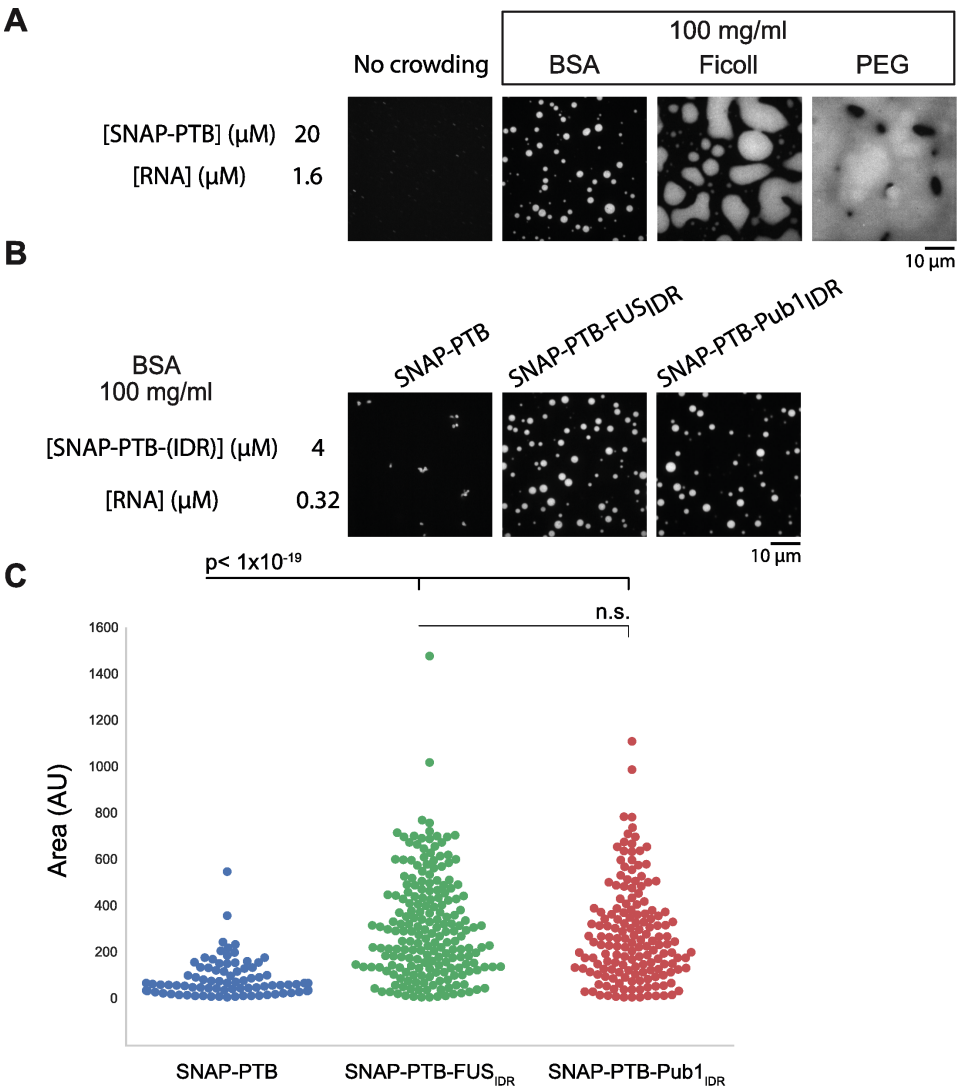

Figure 22: **IDRs enhance LLPS of PTB plus RNA in the presence of BSA**

(A) Fluorescent microscopy images of phase separated droplets formed by SNAP-PTB and RNA in the presence or absence of 100 mg/ml BSA, Ficoll, or PEG.

(B) Fluorescent microscopy images of 4 μM SNAP-PTB, SNAP-PTB-FUS_{IDR}, or SNAP-PTB-$Pub1_{IDR}$ plus 0.32 μM RNA assemblies in the presence or absence of 100 mg/ml BSA.

(C) Quantification of assembly area for (B), with arbitrary units. Significance calculated with Welch's t-test for unequal size and variance.

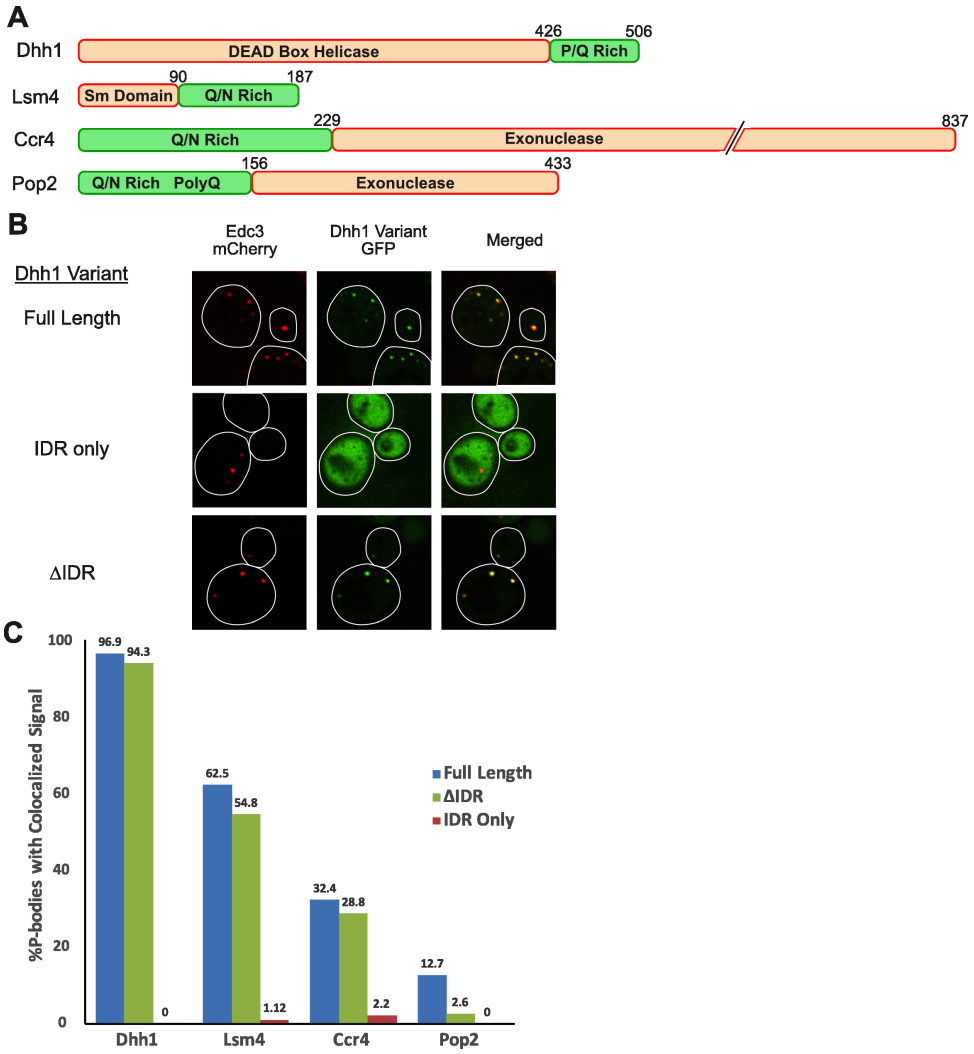

Figure 23: **IDRs are neither sufficient nor required for P-body localization**

(A) Domain structures of the yeast proteins Dhh1, Lsm4, Ccr4 and Pop2

(B) Dhh1-GFP variant fusions were expressed in Edc3-mCherry expressing yeast. After 10 minutes of glucose deprivation to induce P-bodies, cells were visualized by fluorescence microscopy. Representative images are presented.

(C) Quantification of the percentage of P-bodies that exhibited colocalization with the expressed fusion protein. GFP was fused to the N-terminus of Dhh1, Ccr4, and Pop2 variants. These variants were cotransformed with Edc3-mCherry. mCherry was fused to the C-terminus of the Lsm4 variants, which were expressed in cells encoding genomically-tagged Dcp2-GFP. Dhh1$_{\Delta IDR}$ 1-427, Dhh1 IDR 427-506; Ccr4$_{\Delta IDR}$ 148-837, Ccr4 IDR 1-229; Pop2$_{\Delta IDR}$ 147-433, Pop2 IDR 1-156; Lsm4$_{\Delta IDR}$ 1-90, Lsm4 IDR 91-187. (>100 foci counted per condition)

fusion protein was counted. For example, clear enrichment in P-bodies was detectable for full length Lsm4 (**Figure 23B**). However, the Lsm4 IDR was not sufficient for P-body localization (**Figure 23B**). Similarly, the IDRs of Dhh1, Pop2, and Ccr4, were insufficient for recruitment to P-bodies (**Figure 23C**). We then removed these IDRs from their full-length proteins, and found that deletion of the IDRs in Lsm4, Dhh1, Ccr4 had little to no effect on their recruitment to P-bodies (**Figure 23B,C**). However, for the already poorly localized Pop2, deletion of the IDR did have a noticeable impact on localization (**Figure 23C**). Thus, the IDRs of Lsm4, Dhh1, Ccr4, and Pop2 are not sufficient their recruitment into P-bodies, but may contribute in cases where recruitment is already poor such as Pop2.

3.5 IDRs can enhance LLPS driven by specific interactions in cells

The observations above suggest cellular assemblies such as RNP granules may form with assembly primarily driven by a set of specific interactions, with the prevalence of IDR regions in such assemblies contributing either a second set of promiscuous nonspecific interactions that would enhance assembly, or having specific interactions with themselves that require high local concentrations to form. Reported observations suggest, however, that some IDRs noticeably contribute to RNP granule assembly in genetic backgrounds that limit assembly. One example of this phenomenon is the previous observation that the C-terminal IDR of Lsm4 is not required for P-body assembly normally, but plays a role in a strain lacking the P-body scaffold protein Edc3 (Decker et al., 2007).

To determine if this may be a more general phenomenon, we examined how the C-terminal IDR of the yeast Dhh1 protein promotes P-body formation. In *edc3*Δ *lsm4*ΔC yeast strains, which lack visible P bodies, P-body formation can be partially rescued by the addition of a single copy plasmid providing an extra copy of the Dhh1 gene, which through specific interactions with RNA and Pat1 enhances P-body assembly (Rao et al., 2017, submitted). Overexpression of Dhh1 in an *edc3*Δ *lsm4*ΔC background creates a cellular context where P-bodies are just above the threshold for assembly. Dhh1 also

has a C-terminal P/Q rich IDR (**Figure 22**). To determine whether this C-terminal IDR contributes to P-body assembly, we compared the ability of full length Dhh1 and a Dhh1ΔIDR truncation (1-427), which lacks the C-terminal IDR (residues 428 to 506), to rescue P-body formation in an *edc3*Δ *lsm4*Δ*C* strain.

We found that wild-type Dhh1 rescues P-body formation in the *edc3*Δ *lsm4*Δ*C* strain, yet the Dhh1ΔIDR variant fails to do so (**Figure 24A,B**), despite being expressed at levels similar to the full-length protein (**Figure 25A**). This demonstrates that the C-terminal IDR of Dhh1, while not required for P-body formation normally, can contribute additional interactions that enhance the formation of P-bodies when granule assembly is partially impaired.

In principle, the Dhh1-IDR could provide a specific interaction, perhaps containing a SLiM, or a promiscuous interaction as we observed for several IDRs *in vitro*. If the Dhh1-IDR makes a specific interaction, then it should not be functionally replaceable by other IDRs capable of promiscuous interactions. Alternatively, if this IDR simply provides additional promiscuous interactions then any IDR capable of such interactions should functionally replace the Dhh1-IDR in promoting P-body assembly. To distinguish between these possibilities, we determined whether the IDRs of human Lsm4, a P-body component, as well as the IDRs of two human stress granule components, hnRNPA1, and the N-terminal domain of FUS, could replace the function of the Dhh1 IDR. We also tested the disordered regions of two Late-Embryogenesis Abundant (LEA) - like proteins, which are proposed to provide desiccation protection by interacting promiscuously with proteins in the cell, potentially in lieu of water (Hand, Menze, Toner, Boswell, & Moore, 2011). We utilized the IDRs of human proteins because these are very unlikely to contain specific binding partners in yeast.

All three granule-component IDRs complemented the P-body assembly defect seen in the Dhh1-ΔIDR construct (**Figure 24B**). Additionally, 2 LEA-like protein (LEA Group 3 – like from the brine shrimp *Artemia franciscana,* "LEA-G3," and LEA Group2 – like from the nematode *Steinernema carpocapsae*, "LEA-SC") IDRs also rescued the assembly defect (**Figure 24C**). Addition of these IDRs does not cause appreciable assembly of large

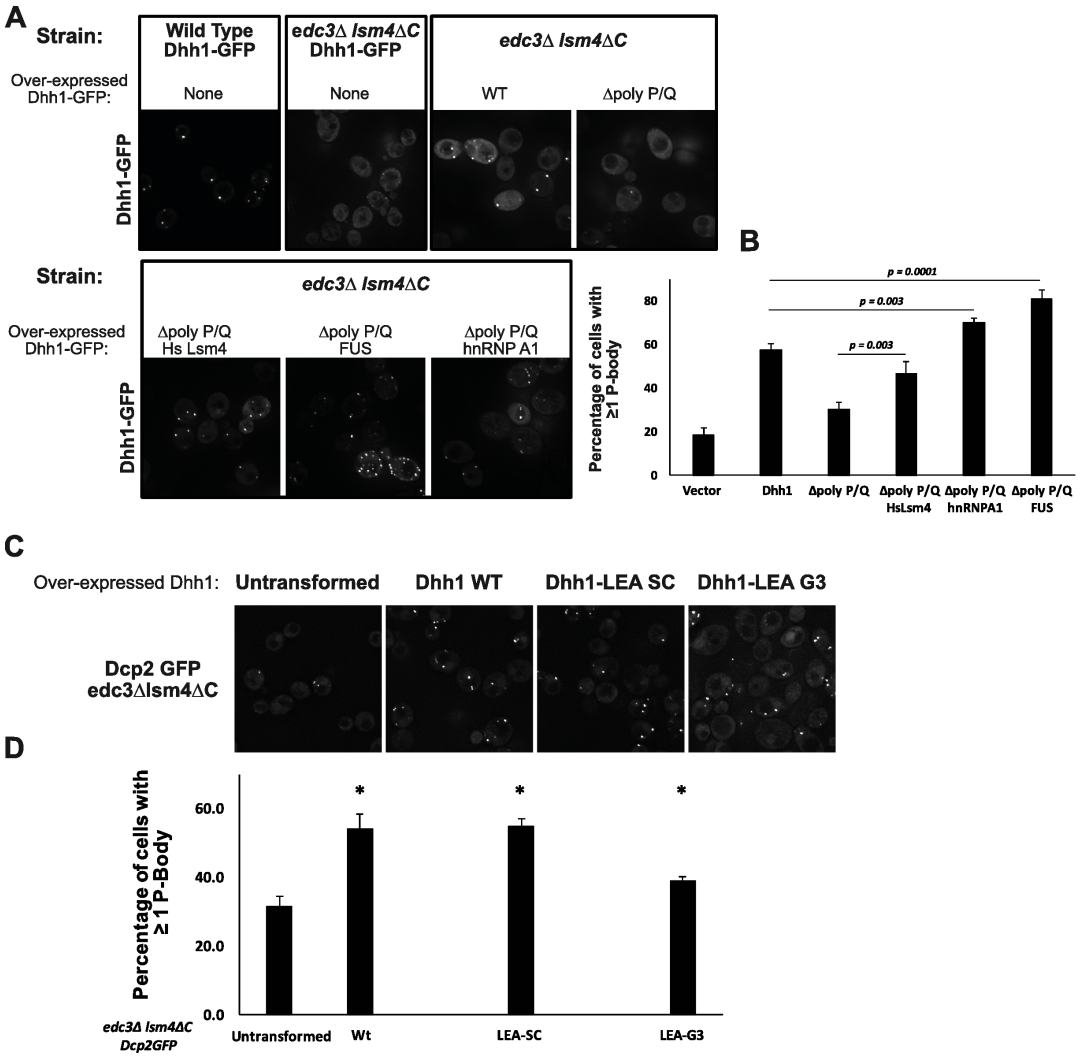

Figure 24: **Specific interactions can synergize with promiscuous nonspecific interactions to drive assembly**

(A) Fluorescent microscopy images of cells expressing Dhh1-GFP, either genomically or as a plasmid-expressed Dhh1-GFP variant. Cells were deprived of glucose for 10 minutes to induced P-body assembly.

(B) Quantification of (A), depicting the percentage of cells containing at least one P-body. (Student's t-test, 3 biological replicates)

(C) Fluorescent microscopy images of cells expressing Dhh1 LEA variants or wild-type Dhh1. Cells were deprived of glucose for 10 minutes to induced P-body assembly, and visualized by genomically GFP-tagged Dcp2.

(D) Quantification of (C), depicting the percentage of cells containing at least one P-body. (Student's t-test, 3 biological replicates, * $p < 0.05$)

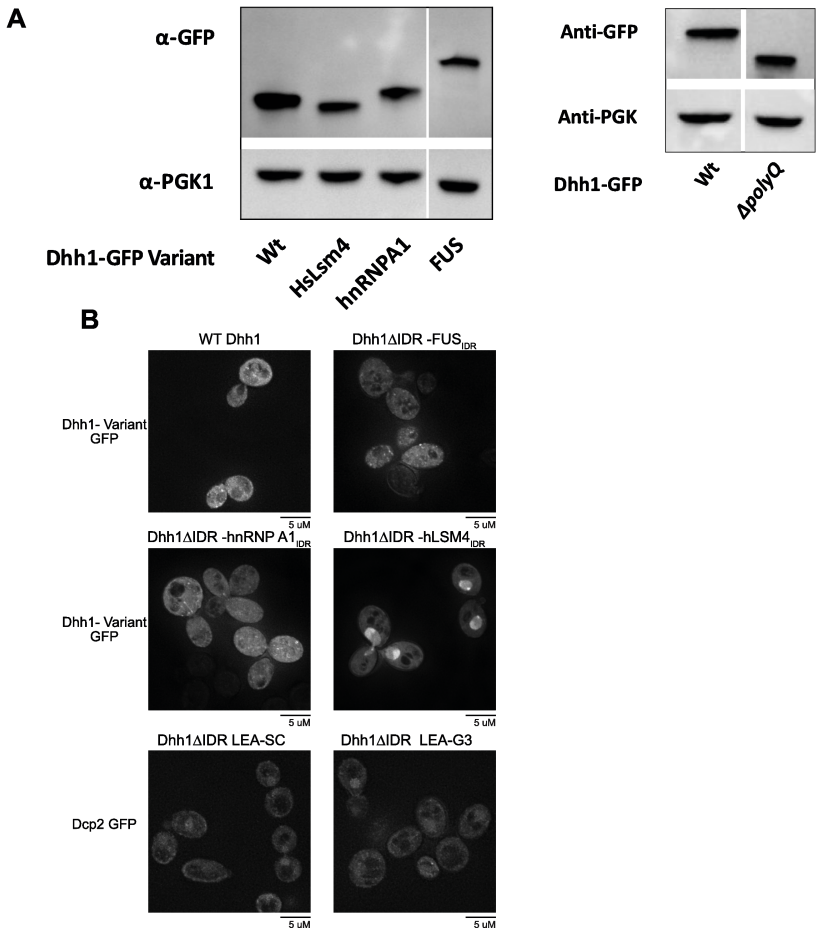

Figure 25: **Dhh1 IDR fusions do not form large assemblies in the absence of stress**

(A) Western blot of Dhh1 variant expression

(B) Fluorescent microscopy images of cells expressing Dhh1-GFP, either genomically or as a plasmid-expressed Dhh1-GFP variant. Cells were growing under log phase growth conditions just prior to imaging.

structures without glucose deprivation (**Figure 25B**), demonstrating these assemblies are indeed P-bodies and not a different constitutive aggregate. These results argue that the Dhh1 IDR does not provide a specific interaction necessary for P-body assembly, as it can be replaced with a variety of other human IDRs. This result also demonstrates that multiple different IDRs can complement the Dhh1ΔIDR, consistent with promiscuous, nonspecific interactions of the IDRs contributing to RNP granule assembly in conjunction with specific interactions.

3.6 Discussion

RNP granules are cytoplasmic assemblies composed of specific groups of cellular proteins and RNA molecules (Jain et al., 2016) (Khong et al., 2017 in submission). In principle, a specific assembly could be assembled in three manners: a) solely a set of specific interactions with well defined, and limited binding partners; b) through a summation of promiscuous interactions, where the sum of this network of interactions for a given molecule would bias its assembly characteristics, or c) through a combination of specific and promiscuous interactions. This third potential mechanism is supported by genetic analyses of the interactions that drive RNP granule assembly as well as our own findings. Specific interactions can clearly be important for assembly. For example, Edc3 dimerization via its YjeF-N domain is important for P-body assembly in yeast (Decker et al., 2007). G3BP dimerization, as well as interactions with caprin, are important for mammalian stress granule assembly (Tourriere, 2003; Kedersha et al., 2016). Some specific interactions can involve SLiMs found in IDRs that specifically interact with well-folded domains of other RNA binding proteins (reviewed in (Jonas & Izaurralde, 2013)). One example of this phenomena is the disruption of Edc3 localization to P-bodies in yeast caused by deletion of or interference with specific SLiMs in Dcp2's C-terminal IDR, which interact with a surface of Edc3 (Fromm et al., 2012, 2014). Thus, specific interactions between RNA binding proteins play important roles in formation of P bodies and recruitment of molecules into them. However, we have also shown that promiscuous interactions can play a role in assembly.

A key contribution of this work is to provide evidence that at least some IDRs function to promote RNP granule assembly both in cells, and in model biochemical systems, through weak interactions that require being coupled to protein domains with specific interactions. First, examination of the FUS, hnRNPA1, and eIF4GII IDRs reveal that they all interact nonspecifically with generic proteins, and those proteins and yeast lysates disrupt their ability to undergo LLPS in isolation (**Figure 18 & 19**). However, when tethered to the PTB RNA binding protein, which phase separates in the presence of RNA, promiscuous IDRs can promote LLPS, even in the presence of competitor proteins (**Figure 22**). Third, the C-terminal P/Q rich IDR of Dhh1 promotes P-body assembly in yeast, and this domain can be replaced by the IDRs of human Lsm4, hnRNPA1, or FUS, or by specific LEA proteins from brine shrimp or nematodes (**Figure 24**). The contribution of such IDRs to assembly is likely due to the ability of IDRs to promote LLPS through a variety of weak promiscuous interactions including electrostatic, cation-, dipole-dipole and - stacking interactions (C. Brangwynne et al., 2015; Nott et al., 2015), which would be enhanced through effects analogous to avidity by coupled specific interactions of adjacent domains (Jencks, 1981).

Additional evidence exists that LLPS can be driven by combined specific and non-specific interactions. For example, even very high expression levels of hnRNPA1-Cry2 or DDX4-Cry2 fusion proteins do not phase separate in cells, unless the Cry2 protein is first triggered to assemble through specific light activated interactions (See Figure 2B&C of (Shin et al., 2016)). This observation highlights how specific oligomerization domains can act cooperatively with IDRs to promote LLPS in cells, and how some IDRs may be insufficient to undergo LLPS without additional oligomerization elements. As an example of the importance of non-specific interactions in promoting cellular LLPS, the C-terminal IDR of yeast Lsm4 can enhance yeast P-body formation, but it can be functionally replaced in this role by other IDRs (Decker et al., 2007). Moreover, polyQ rich tracts, which are disordered IDRs capable of diverse interactions, are prevalent in P-body components and RNA binding proteins (Decker et al., 2007; Reijns et al., 2008), and can function in RNP granule assembly in *A. gossypii* (C. Lee, Occhipinti, & Gladfelter,

2015). Taken together, we suggest that many IDRs on RNA binding proteins provide an additional layer of nonspecific interactions, and those interactions can contribute to granule formation when they synergize with more specific interactions to stabilize the macroscopic structure.

An important point is that, even when insufficient in themselves to promote LLPS, promiscuous IDRs can decrease the critical concentration for phase separation driven by more specific interactions. We demonstrate this phenomenon for phase separation of PTB and RNA *in vitro* (**Figure 22**), and for P-body assembly *in vivo* (**Figure 24**). This highlights that in a phase diagram describing an assembly based on specific and promiscuous interactions, the addition of promiscuous interactions can shift the system from an unassembled state to an assembled state (**Figure 26A,B**).

Not all IDRs will influence RNP granule formation in the same molecular manner. Some IDRs will provide specific interactions through SLiMs (Jonas & Izaurralde, 2013). Some IDRs may also afford interaction specificity through formation of local structure, including amyloid-like cross-beta interactions, that could be important in biological contexts where RNP granules need to be long-lived or mechanically stable (Boke & Mitchison, 2017; Kato et al., 2012) or α-helices (Conicella et al., 2016), both of which should show some sequence specificity. Charge patterning can also afford sequence specificity, although likely to a lower degree (Nott et al., 2015; Pak et al., 2016). Finally, as suggested here, some IDRs will provide promiscuous interactions that can enhance RNP granule assembly. Therefore, interactions undergone by any individual IDR that can contribute to intracellular LLPS likely lay on a scale from low affinity and highly promiscuous, to moderate affinity and selective.

A priori, there are three general classes of promiscuous interactions that IDRs could contribute to granule assembly. First, IDRs could interact with themselves or with other IDRs through weak interactions, which is suggested by observations that both IDR-based hydrogels and phase separated liquid droplets can recruit proteins with different IDRs (Kato et al., 2012; Lin et al., 2015). Second, IDRs could have promiscuous interactions with RNAs, which is suggested by observations that some IDRs cross-link to RNA *in*

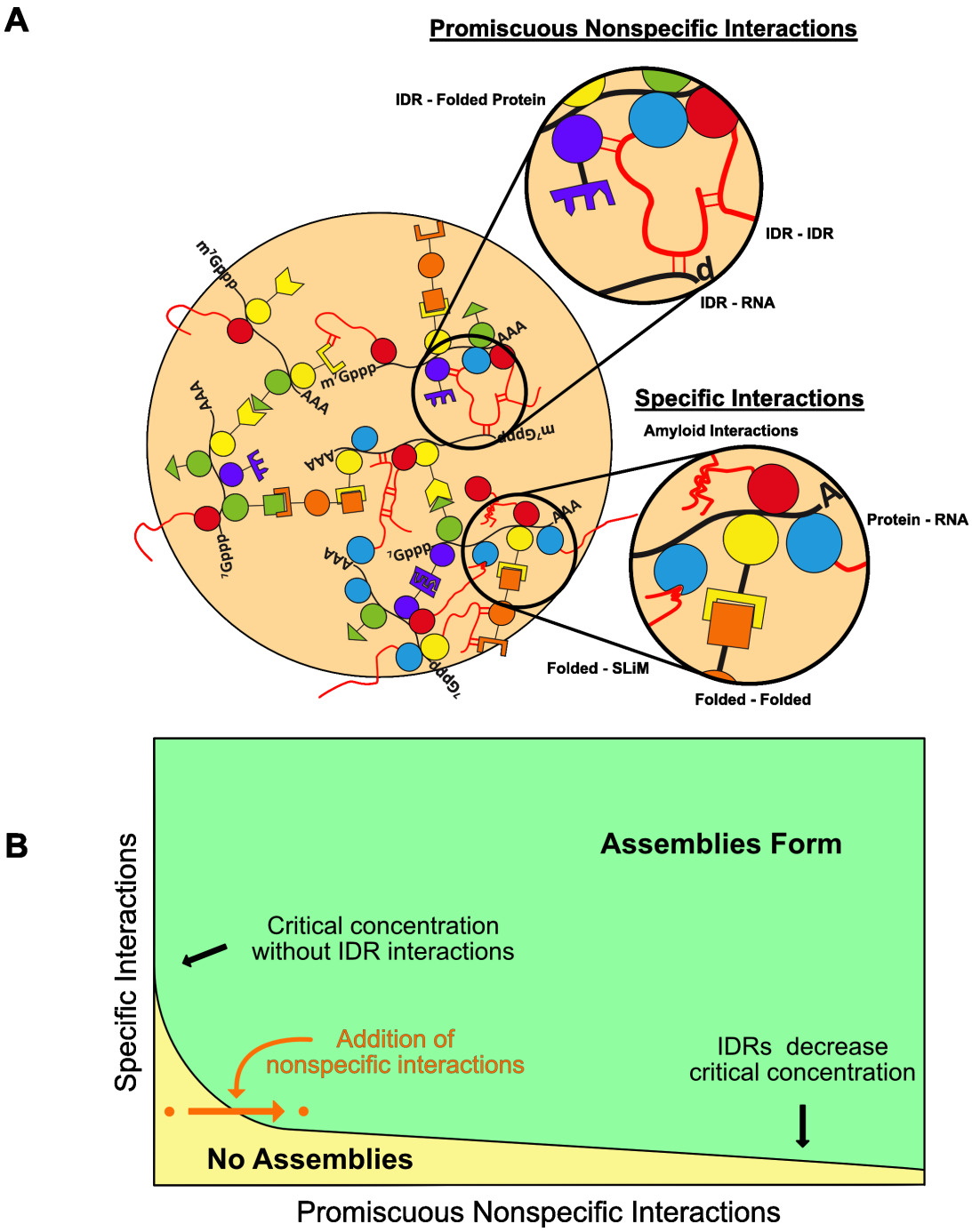

Figure 26: **Model of RNP granule assembly and contributions of IDRs**

(A) RNP granules assembly by a wide variety of specific and nonspecific interactions.

(B) A theoretical phase diagram depicting how the addition of nonspecific, IDR-driven interactions could decrease the critical concentration of assembly for higher-order structures.

vivo (Castello et al., 2016) and some IDRs bind RNA *in vitro* (Lin et al., 2015; Molliex et al., 2015). Finally, IDRs could make promiscuous interactions with other well-folded domains of granule components. Note that promiscuous interactions of IDRs with well-folded domains of proteins could provide an evolutionary starting point for the formation of SLiMs, which are often found in IDRs. An important future goal will be in determining how IDRs utilize each of these interaction types to contribution to granule formation.

Utilizing promiscuous nonspecific interactions of IDRs to modulate the assembly of macro-scale complexes has unique advantages. First, since such nonspecific interactions are not limited to defined components or stereospecific arrangements, they can interact promiscuously with any number of individual components to enhance assembly. For example, in RNP granules, a diversity of mRNPs with different RNA binding proteins can be components of the granule. Promiscuous IDRs on RNA-binding proteins could interact with any of these mRNPs to enhance granule assembly. Moreover, IDRs can be subject to rapid evolution, and control by post-translational modifications, thus making them ideal components to change granule assembly parameters under selective pressure and in response to signaling pathways. Finally, we note that because higher-order assemblies are large with respect to a single IDR, promiscuous interactions of IDRs will mostly occur within the quinary space of the assembly, rather than with proteins outside of the assembly. This makes large assemblies particularly well suited to enhancement by IDRs.

Macromolecular assembly and concomitant LLPS mediated by combinations of specific and promiscuous interactions is a general mechanism for forming dynamic, meso-scale structures in eukaryotic cells. Eukaryotic cells contain many such assemblies including RNP granules, signaling complexes, DNA damage repair foci, and transcription complexes. It is notable that components of all of these assemblies are enriched in IDRs (Banani et al., 2016; Hegde, Hazra, & Mitra, 2010; Jain et al., 2016; Hnisz, Shrinivas, Young, Chakraborty, & Sharp, 2017; Iakoucheva, Brown, Lawson, Obradovi, & Dunker, 2002; Kai, 2016; Minezaki, Homma, Kinjo, & Nishikawa, 2006). Thus, we suggest that higher order complexes will often be assembled by a combination of specific interactions that drive assembly, reinforced by a network of promiscuous nonspecific IDR based

interactions, which stabilize the complex because of their physical coupling to specific assembly components. Such assemblies will be easily modified over time via evolution, or in a dynamic sense by signaling pathways and post-translational modification. This would occur without having to change the underlying specific assembly interactions, thus allowing both rapid evolution of and immediate control over intracellular assemblies.

3.7 Materials and Methods

Protein Purification and Labeling

Proteins were expressed and purified as previously reported (Lin et al., 2015). Proteins were expressed from the pMal-c2 vector (NEB), except for full length hnRNPA1 and related mutants, which were cloned into a modified pet11a vector (Novagen). Proteins were expressed in *E. coli* BL21(DE3) and purified with Ni-NTA and/or amylose resin under standard conditions. SNAP-PTB-IDRs were further purified through a Superdex200 column (GE Healthcare). Proteins were fluorescently-labeled with SNAP-Surface 488 or SNAP-Surface 649 (NEB) according to the manufacturer's protocols. Unincorporated dye was removed using Zeba Spin Desalting Columns, 7K MWCO (Thermo Fisher). Proteins were concentrated using Amicon Ultra 10K MWCO centrifugal filters (Milipore) and aggregates removed by ultra-centrifugation at 4C for 30' at 50K RPM in a Beckman-Coulter TLA 100.2 rotor.

Fluorescence Microscopy

All yeast experiments and all images of SNAP-IDR and SNAP-hnRNPA1 were acquired on a DeltaVision epi-fluorescence microscope, equipped with an SCMOS camera. All images of SNAP-PTB-IDR were acquired on a Leica-based spinning disk confocal microscope (EMCCD digital camera, ImagEM X2, Hamamatsu; confocal scanner unit, CSU-X1, Yokogawa).

Droplet Assembly

For SNAP-IDRs and SNAP-hnRNPA1 (˜2% fluorescently labeled), droplet assembly was initiated by diluting solutions to 37.5 mM NaCl, 20 mM Tris pH 7.4, 1 mM DTT. For

SNAP-PTB-IDRs, proteins and RNA, $(UCUCUAAAAA)_5$, were mixed at the indicated concentrations (including 100 nM SNAP-PTB-IDRs labeled with SNAP-Surface 649) in 100 mM NaCl, 20 mM imidazole pH 7.0, 1 mM DTT, 10% glycerol. N-terminal purification tags of SNAP-hnRNPA1 were removed by HRV C3 protease (EMD Milipore) during the dye conjugation step (Lin et al., 2015). N-terminal MBP and C-terminal His tags of SNAP-IDRs and SNAP-PTB-IDRs were cleaved just prior to droplet assembly with TEV protease (Promega ProTEV). Reactions were performed in glass-bottom chambers passivated with 3% BSA. FITC-conjugated Lysozyme (Nanocs) and FITC-BSA (Thermo Fisher Scientific) were mixed with SNAP fusion proteins prior to droplet assembly at concentrations of 100 nM and 10 nM, respectively. BSA impairment at 100 mg/ml was repeated >3 times.

Droplet Quantification

Images were analyzed in FIJI as follows. Images were imported, flattened with a maximal intensity projection when applicable (hnRNPA1Δhexa droplets), and then thresholded using either the Default method (hnRNPA1 Δhexa droplets) or the Otsu method (PTB droplets) ('Threshold'). Binary images were eroded ('Erode) once to remove single pixels, then dialated ('Dialate') once to return droplets to their original size. This was followed by watershedding ('Watershed') to separate proximal droplets. FIJIs 'Analyze Particles' was used to generate ROIs, which were used to measure the maximal intensity projection, generating area and mean intensity values for each assembly. Three independent fields of view from each condition were used.

Microscopy and Quantification for P-body Colocalization

Cells were grown at 30C to OD_{600} of 0.3-0.5 in minimal media with 2% glucose as a carbon source and with necessary amino acid dropout to maintain plasmids and express constructs (See Supplemental File "Strains Plasmids and Antibodies"). Cells were stressed by glucose deprivation for 15 minutes before cells were concentrated for immediate microscopic examination at room temperature. All images underwent deconvolution using DeltaVision's algorithm.

Images were quantified using FIJI. To optimize yeast colocalization accuracy, single plane images were used and analysis were done in a blind manner. P-bodies were identified using protein markers (either Dcp2-GFP, Edc3-mCherry). Corresponding enrichment of the construct within the P bodies was then assessed manually. Manual assessment was required due to differential strengths of cytoplasmic signals between cells arising from stochastic variation and/or potentially different copy numbers of plasmids between cells.

Growth and Microscopy of Dhh1 Variants

To test the effect of Dhh1-IDR chimera on P-body recovery in the edc3Δ lsm4ΔC yeast (Strain yRP2338), yeast were transformed with vector only or vectors containing GFP fusions of Dhh1 wt, Dhh1-1-427 and Dhh1-IDR chimera using standard yeast transformation protocols. Two individual transformants were selected as biological replicates. The replicates were grown overnight to saturation at 30 °C with shaking in SD-Ura media (minimal media), containing 2% dextrose. The saturated cultures were re-inoculated into fresh SD-Ura media and grown to OD = 0.4-0.5. The cells were pelleted and transferred to S-Ura media lacking dextrose and shaken at 30 °C for 10 min prior to microscopic analysis. For the unstressed conditions, the cells were pelleted without glucose starvation.

Yeast were analyzed via fluorescence microscopy on the DeltaVision Elite microscope with a 100 X objective using a PCO Edge sCMOS camera. 2 images comprising of 9 Z-sections were obtained for each replicate. Images were analyzed using Image J. Z-projections derived from summation of the Z-sections with constant thresholding were used to count the number of yeast cells with 1 GFP-positive granule, and the percentage of cells with at least 1 granule was calculated.

Plasmid construction

The Dhh1-GFP gene fragment containing the Dhh1 promoter was PCR amplified using the genomic DNA from the Dhh1-GFP yeast strain (yeast GFP collection) and BSR_DhhGFP416NF and BSR_DhhGFP416NR primers. The Adh1 terminator fragment was clone using the primers BSR_Adh1SacF and BSR_Adh1SacR. The Dhh1-

GFP and Adh1 terminator fragments were inserted sequentially into the XhoI and SacI digested pRS416 vector, respectively, via Infusion cloning (Takara). The poly P/Q residues of Dhh1 (428-506 were deleted from the Dhh1-GFP containing vector using primers, Dhh11-427F and Dhh11-427R via the Phusion mutagenesis protocol (Thermo Fisher). Lastly, the intron-less IDR sequence for HsLsm4 was synthesized using gBLOCK technology from IDT technologies. The IDRs were PCR amplified using primers, BSR_427FUSF and BSR_427FUSR, BSR_427A1F and BSR_427A1R, BSR_427HsLsm4F and BSR_427HsLsm4R, for FUS, hnRNPA1 and HsLsm4, respectively and cloned into the linearized Dhh1-1-427-GFP vector using Infusion cloning.

4 Unpublished Observations

4.1 IDRs do not enhance LLPS of the SUMO-SIM system

Our observations above suggest LLPS assemblies in cells could form by a dual set of interactions with assembly being driven by a set of specific interactions, and then the prevalence of IDR regions in such assemblies contributing a second set of both homotypic and heterotypic interactions. These IDR-based interactions could potentially enhance the LLPS formation and give it unique properties . A prediction of this model is that the addition of an IDR to proteins capable of LLPS may increase the partition coefficient of the LLPS capable protein in droplets by increasing the binding energy that contributes to the droplet state. To test this prediction we compared the LLPS parameters of an EGFP-SUMO-SIM system in U2OS cells, a well studied model of LLPS both *in vitro* and in cells (Banani et al., 2016). Briefly, SUMO is a Ubiquitin-like protein that binds a peptide sequence known as SIM (SUMO Interaction Motif). Linking 10 SUMO motifs and 6 SIM peptides into a single polypeptide creates a protein that readily undergoes LLPS. Further, a GFP tagged version of $SUMO_{10}SIM_6$ undergoes LLPS in mammalian cells (Banani et al., 2016).

To test how IDRs could affect the LLPS behavior of the SUMO-SIM system we added IDRs from several RNA binding proteins that can undergo LLPS in vitro. Fusion of the yeast IDRs from Pub1, Lsm4, and eIF4GII to the N-terminus of $SUMO_{10}$-SIM_6 led to poor expression (**Figure 27A**). However, fusion of the hnRNPA1 IDR (including its pathological D262V, and Δhexapeptide variants) did not impair expression and droplets were readily formed in cells (**Figure 27B**).

A key observation is that addition of the hnRNPA1 IDR to $SUMO_{10}$-SIM_6 did not markedly change the concentration of the construct within droplets. The absolute fluorescence of EGFP within droplets may be used as a proxy for concentration. Therefore, we measured the intensity of droplets within cells. Droplets of diameter 2.8 microns to 6.4 microns were analyzed because all four constructs had statistically similar popula-

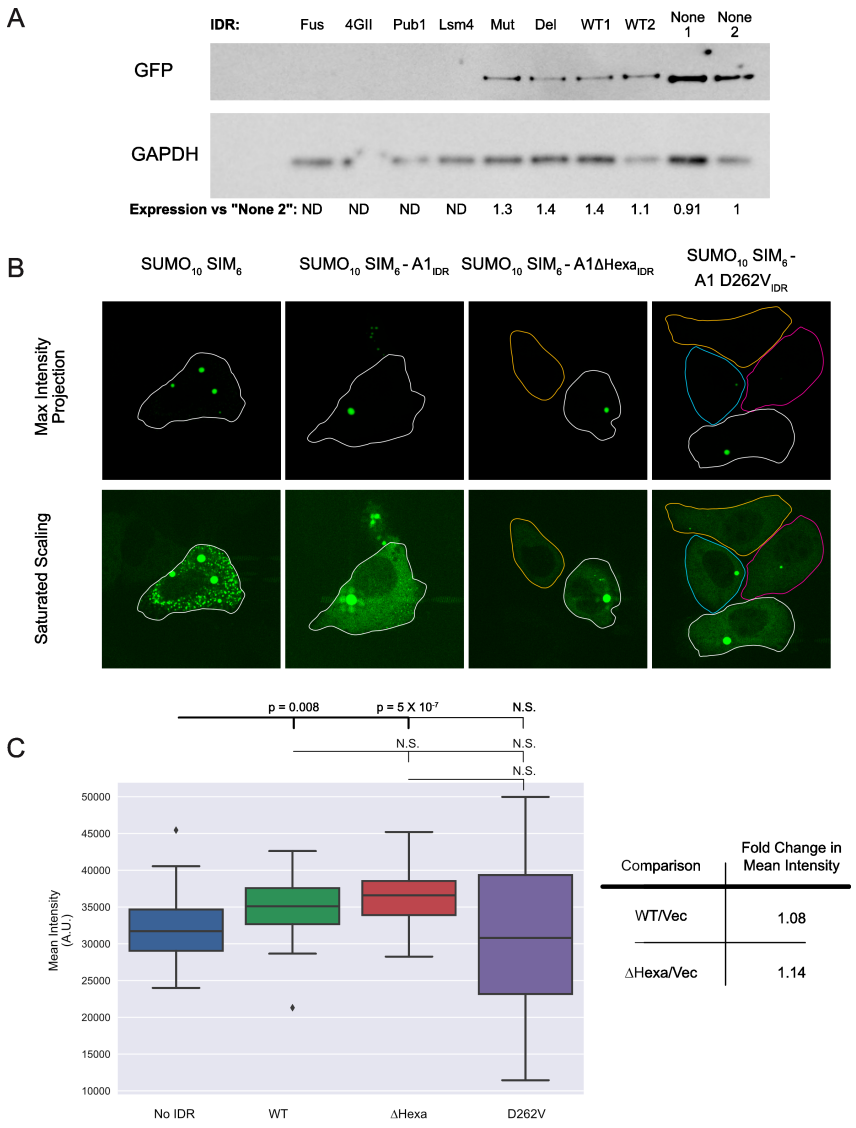

Figure 27: **Addition of IDRs to $SUMO_{10}SIM_6$ does not lead to large changes in droplet assembly**

(A) Western Blot showing decreased expression of $Lsm4_{IDR}$, FUS_{IDR}, and $eIF4GII_{IDR}$ tagged $SUMO_{10}SIM_6$, and comprable expression of untagged, $hnRNPA1_{IDR}$, $hnRNPA1\Delta Hexa_{IDR}$, and hnRNPA1 $D262V_{IDR}$

(B) Fluorescence microscopy images of GFP-$SUMO_{10}SIM_6$ variants, automatically scaled (above), and with saturated scaling to highlight morphological differences.

(C) Box plots of the raw intensity values for droplets between 2.8 and 6.4 µM, and fold-changes of mean intensities for significantly different populations

tions of droplets within this range. While the addition of the hnRNPA1 IDR (either WT, Δhexapeptide, or D262V) does significantly change the intensity of droplets after 49 hrs of expression (**Figure 27C**), the magnitude of change is very small (**Figure 27C**). We

interpret these observations to mean that addition of an IDR to a protein that undergoes LLPS does not necessarily lead to a dramatic increase in partitioning as might be expected.

It is important to note that while the detector was not saturated by signal, the leaking of light between pinholes that is especially evident in the hnRNPA1 WT, saturated scaling panel shows that technical artifacts may be affecting the results seen here. In this case, the incident light exposure and camera exposure were likely too high and too long for optimal imaging. In the future, attempts should be made to image at parameters where the microscope is working within optimal parameters.

Materials and Methods

U2OS cells were seeded on glass coverslips and transfected using JetPrime transfection reagent. 49 hours post-transfection cells were washed 3X with 37C PBS and fixed in 4% PFA at 37C for 20 min. Coverslips were mounted using VectaShield Antifade with DAPI. 15 0.3um slices were taken on a spinning disk confocal microscope with a 60X NA 1.4 objective. Maximum intensity projections of these z-stacks were generated to collapse the brightest section of each droplet into a single slice. ImageJs 3D object counter was then used to segment and measure the area and max intensity of each droplet.

4.2 Many small molecules alter LLPS of hnRNPA1Δhexa and IDR

Liquid-liquid phase separated droplets have interesting physical properties thanks to the weak nature of the interactions that hold them together. This could make them especially sensitive to small molecules that can interact with domains that mediate droplet formation. To see if LLPS of hnRNP A1 is sensitive to a variety of small molecules we prepared droplets of hnRNPA1Δhexa or hnRNPA1$_{\mathrm{IDR}}$ (as described above), in the presence or absence of a range of small molecules. 1,6 hexanediol is commonly used to delineate

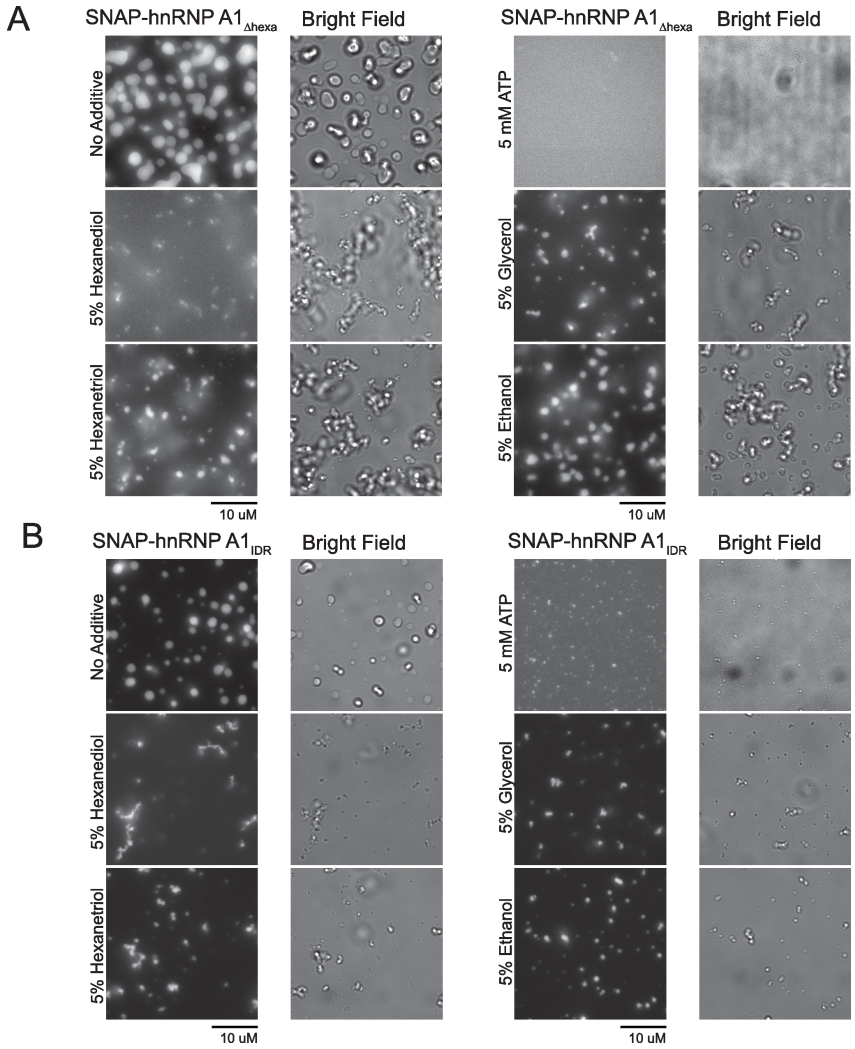

Figure 28: **Diverse small molecules disrupt IDR-driven LLPS**

(A) Solublizing effects of small molecules on hnRNPA1Δhexa

(B) Solubilizing effects of small molecules on $\text{hnRNPA1}_{\text{IDR}}$

liquid droplets from other assembles. Indeed, 1,6 hexanediol disrupts droplet assembly of both hnRNPA1Δhexa and the IDR of hnRNPA1 (**Figure 28A,B**). However, we also find that a number of other small molecules also impact droplets. Glycerol, ethanol, and 1,2,3 hexanetriol all impair droplet assembly to various degrees. Most surprisingly, we see that just 5mM ATP completely prevents droplet assembly and the other small aggregates observed in the presence of other small molecules. We interpret these results to mean that a wide variety of compounds are effective at disrupting droplets by competing with the protein-protein interactions that drive assembly. Ethanol, glycerol, and

hexanetriol likely interact with charged side chains through their polar moieties, competing with electrostatic interactions that are generally favored by the low ionic strength of the conditions used to drive assembly. ATP may also compete for electrostatics due to its highly charged nature, as well as hydrophobic interactions with it's planar π orbital system. This hydrotropic effect of ATP has been observed for other LLPS systems, as well as solid protein aggregation (Patel et al., 2017).

5 Conclusions

Since RNP granules were discovered these unusual, non-membrane-bound organelles have interested scientists for their unusual nature. Despite having no membrane and being quite large, they contain specific components. They exchange many components with the cytoplasm on fast time scales (half-life < 30s). Further, they appear to be conserved from yeast to mammals. However, an as-yet unresolved question is: how do RNP granules assemble?

Over the course of my studies I have explored how disordered regions of proteins might contribute to this assembly. I have found that IDRs are often sufficient for higher-order assembly through liquid-liquid phase separation (LLPS) *in vitro*. These assemblies change over time, losing their highly dynamic nature. This field has grown quickly from when I first started experimenting with proteins undergoing LLPS at the Woods Hole Marine Biology Laboratory in 2014. Many papers delving into LLPS of IDRs and folded proteins have been published, as the observation that these dynamic assemblies mature into static or gel assemblies has been observed repeatedly. However, strong *in vivo* evidence showing how IDRs contribute to granule assembly has been lacking.

Importantly, however, I have seen that the presence of other proteins or cell lysates has a major deleterious impact on assembly of IDRs *in vitro*. This suggests that, contrary to the models often described in the literature at the time of this writing, IDRs are not the primary drivers of granule assembly in cells. This observation is an important contribution to the field of RNP granule study, and hopefully will push other researchers to be more cautions in interpreting the fact that their particular protein of interest undergoes LLPS *in vitro*.

In collaboration with other researchers in the Parker and Rosen labs we have observed that often other interactions are important to granule assembly, such as specific protein-protein interactions and protein-RNA interactions, as well as potentially promiscuous RNA-RNA interactions (not discussed within this thesis). We have seen that IDRs can help a system cross a barrier from the non-assembled state to the assembled state, even if

they dont appear to be sufficient for higher order assembly in a cellular context. While the exact mechanism by which this occurs is not known, we believe it is due to IDR-based promiscuous interactions that synergize with more stereotypically understood protein-protein and protein-RNA interactions.

Together, these observations point to an inclusive model of granule assembly, wherein many different interactions (including IDR-based interactions) are important for granule assembly, and it is the sum-total of these interaction strengths that determines whether or not a granule assembles. These include traditional protein-protein and protein-RNA interactions, relying on well-folded domains with relatively fixed three-dimensional structure. Also involved are promiscuous interactions between IDRs and other IDRs, as well as IDRs and RNA. These interactions likely do not have fixed three-dimensional structures or constraints, giving them unique properties. Additionally, amyloid-like interactions may also play a role in granule assembly, as many IDRs seem to contain sequences that undergo transitions from poorly-structured to super-stable cross-beta sheet fibrils.

It is my hope that the research contained within this thesis will convince other researchers within the field to consider the impact of not just IDR-based interactions, but other protein-protein and protein-RNA interactions when considering the mechanisms by which RNP granules assemble.

References

Adjibade, P., Valrie Grenier St-Sauveur, Miguel Quevillion Huberdeau, Marie-Jose Furnier, Andreanne Savard, Laetitia Coudert, Mazroui, R. (2015, August). Sorafenib, a multikinase inhibitor, induces formation of stress granules in hepatocarcinoma cells. *Oncotarget*, *6*(41), 43927–43943. doi: 10.18632/oncotarget.5980

Aizer, A., Kalo, A., Kafri, P., Shraga, A., Ben-Yishay, R., Jacob, A., Shav-Tal, Y. (2014, October). Quantifying mRNA targeting to P-bodies in living human cells reveals their dual role in mRNA decay and storage. *Journal of Cell Science*, *127*(20), 4443–4456. Retrieved 2016-02-18, from `http://jcs.biologists.org/cgi/doi/10.1242/jcs.152975` doi: 10.1242/jcs.152975

Anderson, P., & Kedersha, N. (2009). RNA granules: post-transcriptional and epigenetic modulators of gene expression. *Nature Reviews Molecular Cell biology*, *10*(6), 430–436. Retrieved 2016-02-18, from

Anderson, P., Kedersha, N., & Ivanov, P. (2015, July). Stress granules, P-bodies and cancer. *Biochimica et Biophysica Acta (BBA) - Gene Regulatory Mechanisms*, *1849*(7), 861–870. Retrieved 2016-02-26, from `http://linkinghub.elsevier.com/retrieve/pii/S1874939914002946` doi: 10.1016/j.bbagrm.2014.11.009

Arimoto, K., Fukuda, H., Imajoh-Ohmi, S., Saito, H., & Takekawa, M. (2008, November). Formation of stress granules inhibits apoptosis by suppressing stress-responsive MAPK pathways. *Nature Cell Biology*, *10*(11), 1324–1332. Retrieved 2015-04-07, from `http://www.nature.com/doifinder/10.1038/ncb1791` doi: 10.1038/ncb1791

Banani, S., Rice, A., Peeples, W., Lin, Y., Jain, S., Parker, R., & Rosen, M. (2016, July). Compositional Control of Phase-Separated Cellular Bodies. *Cell*, *166*(3), 651–663. Retrieved 2016-09-16, from `http://linkinghub.elsevier.com/retrieve/pii/S0092867416307395` doi: 10.1016/j.cell.2016.06.010

Barbarese, E., Ifrim, M. F., Hsieh, L., Guo, C., Tatavarty, V., Maggipinto, M. J., Carson, J. H. (2013, August). Conditional Knockout of Tumor Overexpressed Gene in Mouse Neurons Affects RNA Granule Assembly, Granule Translation, LTP and Short Term Habituation. *PLoS One*, *8*(8), e69989. Retrieved from `http://dx.plos.org/10.1371/journal.pone.0069989` doi: 10.1371/journal.pone.0069989

Barbee, S. A., Estes, P. S., Cziko, A.-M., Hillebrand, J., Luedeman, R. A., Coller, J. M., Ramaswami, M. (2006, December). Staufen- and FMRP-Containing Neuronal RNPs Are Structurally and Functionally Related to Somatic P Bodies. *Neuron*, *52*(6), 997–1009. Retrieved 2015-10-06, from `http://linkinghub.elsevier.com/retrieve/pii/S0896627306008270` doi: 10.1016/j.neuron.2006.10.028

Beck, M., Schmidt, A., Malmstroem, J., Claassen, M., Ori, A., Szymborska, A., Aebersold, R. (2011, August). The quantitative proteome of a human cell line. *Molecular Systems Biology*, *7*(1), 549–549. Retrieved 2016-08-24, from http://msb.embopress.org/cgi/doi/10.1038/msb.2011.82 doi: 10.1038/msb.2011.82

Bell, S. D., & Botchan, M. R. (2013, November). The Minichromosome Maintenance Replicative Helicase. *Cold Spring Harbor Perspectives in Biology*, *5*(11), a012807–a012807. doi: 10.1101/cshperspect.a012807

Bhattacharyya, S. N., Habermacher, R., Martine, U., Closs, E. I., & Filipowicz, W. (2006, June). Relief of microRNA-Mediated Translational Repression in Human Cells Subjected to Stress. *Cell*, *125*(6), 1111–1124. Retrieved 2016-02-18, from http://linkinghub.elsevier.com/retrieve/pii/S0092867406005800 doi: 10.1016/j.cell.2006.04.031

Boke, E., & Mitchison, T. J. (2017, January). The balbiani body and the concept of physiological amyloids. *Cell Cycle*, *16*(2), 153–154. Retrieved 2017-02-13, from https://www.tandfonline.com/doi/full/10.1080/15384101.2016.1241605 doi: 10.1080/15384101.2016.1241605

Brangwynne, C., Tompa, P., & Pappu, R. (2015, November). Polymer physics of intracellular phase transitions. *Nature Physics*, *11*(11), 899–904. Retrieved 2016-08-30, from http://www.nature.com/doifinder/10.1038/nphys3532 doi: 10.1038/nphys3532

Brangwynne, C. P. (2013, December). Phase transitions and size scaling of membrane-less organelles. *The Journal of Cell Biology*, *203*(6), 875–881. Retrieved from http://jcb.rupress.org/content/203/6/875.full doi: 10.1083/jcb.201308087

Brangwynne, C. P., Eckmann, C. R., Courson, D. S., Rybarska, A., Hoege, C., Gharakhani, J., Hyman, A. A. (2009, June). Germline P granules are liquid droplets that localize by controlled dissolution/condensation. *Science*, *324*(5935), 1729–1732. Retrieved from http://www.sciencemag.org/content/324/5935/1729.full doi: 10.1126/science.1172046

Brangwynne, C. P., Mitchison, T. J., & Hyman, A. A. (2011, March). Active liquid-like behavior of nucleoli determines their size and shape in Xenopus laevis oocytes. *Proceedings of the National Academy of Sciences*, *108*(11), 4334–4339. Retrieved 2015-08-26, from http://www.pnas.org/cgi/doi/10.1073/pnas.1017150108 doi: 10.1073/pnas.1017150108

Brengues, M., Teixeira, D., & Parker, R. (2005). Movement of eukaryotic mRNAs between polysomes and cytoplasmic processing bodies. *Science*, *310*(5747), 486–489. Retrieved 2015-07-20, from http://www.sciencemag.org/content/310/5747/486.short

Buchan, J., Kolaitis, R.-M., Taylor, J., & Parker, R. (2013, June). Eukaryotic Stress Granules Are Cleared by Autophagy and Cdc48/VCP

Function. *Cell*, *153*(7), 1461–1474. Retrieved 2015-09-14, from http://linkinghub.elsevier.com/retrieve/pii/S0092867413006430 doi: 10.1016/j.cell.2013.05.037

Buchan, J. R. (2014, August). mRNP granules: Assembly, function, and connections with disease. *RNA Biology*, *11*(8), 1019–1030. Retrieved 2015-09-01, from http://www.tandfonline.com/doi/abs/10.4161/15476286.2014.972208 doi: 10.4161/15476286.2014.972208

Buchan, J. R., Muhlrad, D., & Parker, R. (2008, November). P bodies promote stress granule assembly in Saccharomyces cerevisiae. *The Journal of Cell Biology*, *183*(3), 441–455. Retrieved from http://www.jcb.org/cgi/doi/10.1083/jcb.200807043 doi: 10.1083/jcb.200807043

Buchan, J. R., & Parker, R. (2009, December). Eukaryotic Stress Granules: The Ins and Outs of Translation. *Molecular Cell*, *36*(6), 932–941. Retrieved from http://linkinghub.elsevier.com/retrieve/pii/S1097276509008612 doi: 10.1016/j.molcel.2009.11.020

Castello, A., Fischer, B., Frese, C., Horos, R., Alleaume, A.-M., Foehr, S., Hentze, M. (2016, August). Comprehensive Identification of RNA-Binding Domains in Human Cells. *Molecular Cell*, *63*(4), 696–710. Retrieved 2017-02-03, from http://linkinghub.elsevier.com/retrieve/pii/S1097276516302878 doi: 10.1016/j.molcel.2016.06.029

Chalupnikova, K., Lattmann, S., Selak, N., Iwamoto, F., Fujiki, Y., & Nagamine, Y. (2008, December). Recruitment of the RNA Helicase RHAU to Stress Granules via a Unique RNA-binding Domain. *Journal of Biological Chemistry*, *283*(50), 35186–35198. Retrieved 2016-02-19, from http://www.jbc.org/cgi/doi/10.1074/jbc.M804857200 doi: 10.1074/jbc.M804857200

Cherkasov, V., Grousl, T., Theer, P., Vainshtein, Y., Gler, C., Mongis, C., Bukau, B. (2015, November). Systemic control of protein synthesis through sequestration of translation and ribosome biogenesis factors during severe heat stress. *FEBS Letters*, *589*(23), 3654–3664. Retrieved 2016-04-25, from http://doi.wiley.com/10.1016/j.febslet.2015.10.010 doi: 10.1016/j.febslet.2015.10.010

Cherkasov, V., Hofmann, S., Druffel-Augustin, S., Mogk, A., Tyedmers, J., Stoecklin, G., & Bukau, B. (2013, December). Coordination of Translational Control and Protein Homeostasis during Severe Heat Stress. *Current Biology*, *23*(24), 2452–2462. Retrieved 2016-02-18, from http://linkinghub.elsevier.com/retrieve/pii/S0960982213012475 doi: 10.1016/j.cub.2013.09.058

Chernov, K. G., Barbet, A., Hamon, L., Ovchinnikov, L. P., Curmi, P. A., & Pastre, D. (2009, December). Role of Microtubules in Stress Granule Assembly: MICROTUBULE DYNAMICAL INSTABILITY FAVORS THE FORMATION OF MICROMETRIC STRESS GRANULES IN CELLS. *Jour-*

nal of Biological Chemistry, *284*(52), 36569–36580. Retrieved 2015-10-13, from http://www.jbc.org/cgi/doi/10.1074/jbc.M109.042879 doi: 10.1074/jbc.M109.042879

Cipolat Mis, M. S., Brajkovic, S., Frattini, E., Di Fonzo, A., & Corti, S. (2016, April). Autophagy in motor neuron disease: Key pathogenetic mechanisms and therapeutic targets. *Molecular and Cellular Neuroscience*, *72*, 84–90. Retrieved 2016-02-19, from http://linkinghub.elsevier.com/retrieve/pii/S1044743116300124 doi: 10.1016/j.mcn.2016.01.012

Conicella, A., Zerze, G., Mittal, J., & Fawzi, N. (2016, September). ALS Mutations Disrupt Phase Separation Mediated by -Helical Structure in the TDP-43 Low-Complexity C-Terminal Domain. *Structure*, *24*(9), 1537–1549. Retrieved 2017-05-09, from http://linkinghub.elsevier.com/retrieve/pii/S0969212616301927 doi: 10.1016/j.str.2016.07.007

Damgaard, C. K., & Lykke-Andersen, J. (2011, October). Translational coregulation of 5'TOP mRNAs by TIA-1 and TIAR. *Genes & Development*, *25*(19), 2057–2068. Retrieved 2016-02-18, from http://genesdev.cshlp.org/cgi/doi/10.1101/gad.17355911 doi: 10.1101/gad.17355911

Decker, C. J., Teixeira, D., & Parker, R. (2007, November). Edc3p and a glutamine/asparagine-rich domain of Lsm4p function in processing body assembly in Saccharomyces cerevisiae. *The Journal of Cell Biology*, *179*(3), 437–449. Retrieved from http://jcb.rupress.org/content/179/3/437.full doi: 10.1083/jcb.200704147

Elbaum-Garfinkle, S., Kim, Y., Szczepaniak, K., Chen, C. C.-H., Eckmann, C. R., Myong, S., & Brangwynne, C. P. (2015, June). The disordered P granule protein LAF-1 drives phase separation into droplets with tunable viscosity and dynamics. *Proceedings of the National Academy of Sciences*, *112*(23), 7189–7194. Retrieved 2015-09-08, from http://www.pnas.org/lookup/doi/10.1073/pnas.1504822112 doi: 10.1073/pnas.1504822112

Feric, M., Vaidya, N., Harmon, T., Mitrea, D., Zhu, L., Richardson, T., Brangwynne, C. (2016, May). Coexisting Liquid Phases Underlie Nucleolar Subcompartments. *Cell*. Retrieved 2016-06-11, from http://linkinghub.elsevier.com/retrieve/pii/S0092867416304925 doi: 10.1016/j.cell.2016.04.047

Freibaum, B. D., Lu, Y., Lopez-Gonzalez, R., Kim, N. C., Almeida, S., Lee, K.-H., Taylor, J. P. (2015, August). GGGGCC repeat expansion in C9orf72 compromises nucleocytoplasmic transport. *Nature*, *525*(7567), 129–133. Retrieved 2016-02-19, from http://www.nature.com/doifinder/10.1038/nature14974 doi: 10.1038/nature14974

Fromm, S. A., Kamenz, J., Nldeke, E. R., Neu, A., Zocher, G., & Sprangers, R. (2014, May). In Vitro Reconstitution of a Cellular Phase-Transition Process that Involves the mRNA Decapping Machinery. *Ange-*

wandte Chemie International Edition, *53*(28), 7354–7359. Retrieved from http://doi.wiley.com/10.1002/anie.201402885 doi: 10.1002/anie.201402885

Fromm, S. A., Truffault, V., Kamenz, J., Braun, J. E., Hoffmann, N. A., Izaurralde, E., & Sprangers, R. (2012). The structural basis of Edc3- and Scd6-mediated activation of the Dcp1: Dcp2 mRNA decapping complex. *The EMBO journal*, *31*(2), 279–290. Retrieved 2017-02-02, from http://emboj.embopress.org/content/31/2/279.abstract

Gilks, N., Kedersha, N., Ayodele, M., Shen, L., Stoecklin, G., Dember, L. M., & Anderson, P. (2004, December). Stress granule assembly is mediated by prion-like aggregation of TIA-1. *Molecular biology of the cell*, *15*(12), 5383–5398. Retrieved from http://www.molbiolcell.org/content/15/12/5383.short doi: 10.1091/mbc.E04-08-0715

Goulet, I., Boisvenue, S., Mokas, S., Mazroui, R., & Cote, J. (2008, July). TDRD3, a novel Tudor domain-containing protein, localizes to cytoplasmic stress granules. *Human Molecular Genetics*, *17*(19), 3055–3074. Retrieved 2015-09-07, from http://www.hmg.oxfordjournals.org/cgi/doi/10.1093/hmg/ddn203 doi: 10.1093/hmg/ddn203

Guil, S., Long, J. C., & Caceres, J. F. (2006, July). hnRNP A1 Relocalization to the Stress Granules Reflects a Role in the Stress Response. *Molecular and cellular biology*, *26*(15), 5744–5758. Retrieved from http://mcb.asm.org/cgi/doi/10.1128/MCB.00224-06 doi: 10.1128/MCB.00224-06

Guo, W., Chen, Y., Zhou, X., Kar, A., Ray, P., Chen, X., Wu, J. Y. (2011, June). An ALS-associated mutation affecting TDP-43 enhances protein aggregation, fibril formation and neurotoxicity. *Nature Structural & Molecular Biology*, *18*(7), 822–830. Retrieved 2016-02-23, from http://www.nature.com/doifinder/10.1038/nsmb.2053 doi: 10.1038/nsmb.2053

Han, T., Kato, M., Xie, S., Wu, L., Mirzaei, H., Pei, J., McKnight, S. (2012, May). Cell-free Formation of RNA Granules: Bound RNAs Identify Features and Components of Cellular Assemblies. *Cell*, *149*(4), 768–779. Retrieved 2017-06-29, from http://linkinghub.elsevier.com/retrieve/pii/S0092867412005132 doi: 10.1016/j.cell.2012.04.016

Hanazawa, M., Yonetani, M., & Sugimoto, A. (2011, March). PGL proteins self associate and bind RNPs to mediate germ granule assembly in C. elegans. *The Journal of Cell Biology*, *192*(6), 929–937. Retrieved from http://jcb.rupress.org/content/192/6/929.full doi: 10.1083/jcb.201010106

Hand, S. C., Menze, M. A., Toner, M., Boswell, L., & Moore, D. (2011, March). LEA Proteins During Water Stress: Not Just for Plants Anymore. *Annual Review of Physiology*, *73*(1), 115–134. doi: 10.1146/annurev-physiol-012110-142203

Handwerger, K. E., Cordero, J. A., & Gall, J. G. (2005). Cajal bodies, nucleoli,

and speckles in the Xenopus oocyte nucleus have a low-density, sponge-like structure. *Molecular biology of the cell*, *16*(1), 202–211. Retrieved 2017-06-29, from http://www.molbiolcell.org/content/16/1/202.short

Hegde, M. L., Hazra, T. K., & Mitra, S. (2010, November). Functions of disordered regions in mammalian early base excision repair proteins. *Cellular and Molecular Life Sciences*, *67*(21), 3573–3587. Retrieved 2017-02-03, from http://link.springer.com/10.1007/s00018-010-0485-5 doi: 10.1007/s00018-010-0485-5

Hennig, S., Kong, G., Mannen, T., Sadowska, A., Kobelke, S., Blythe, A., Fox, A. H. (2015, August). Prion-like domains in RNA binding proteins are essential for building subnuclear paraspeckles. *The Journal of Cell Biology*, *210*(4), 529–539. Retrieved 2015-08-28, from http://www.jcb.org/cgi/doi/10.1083/jcb.201504117 doi: 10.1083/jcb.201504117

Hilliker, A., Gao, Z., Jankowsky, E., & Parker, R. (2011, September). The DEAD-Box Protein Ded1 Modulates Translation by the Formation and Resolution of an eIF4f-mRNA Complex. *Molecular Cell*, *43*(6), 962–972. Retrieved 2015-09-30, from http://linkinghub.elsevier.com/retrieve/pii/S1097276511005855 doi: 10.1016/j.molcel.2011.08.008

Hnisz, D., Shrinivas, K., Young, R. A., Chakraborty, A. K., & Sharp, P. A. (2017, March). A Phase Separation Model for Transcriptional Control. *Cell*, *169*(1), 13–23. Retrieved 2017-05-19, from http://linkinghub.elsevier.com/retrieve/pii/S009286741730185X doi: 10.1016/j.cell.2017.02.007

Hubstenberger, A., Noble, S., Cameron, C., & Evans, T. (2013, October). Translation Repressors, an RNA Helicase, and Developmental Cues Control RNP Phase Transitions during Early Development. *Developmental Cell*, *27*(2), 161–173. Retrieved 2016-02-19, from http://linkinghub.elsevier.com/retrieve/pii/S1534580713005728 doi: 10.1016/j.devcel.2013.09.024

Iakoucheva, L. M., Brown, C. J., Lawson, J., Obradovi, Z., & Dunker, A. (2002, October). Intrinsic Disorder in Cell-signaling and Cancer-associated Proteins. *Journal of Molecular Biology*, *323*(3), 573–584. Retrieved 2017-02-03, from http://linkinghub.elsevier.com/retrieve/pii/S0022283602009695 doi: 10.1016/S0022-2836(02)00969-5

Jain, S., Wheeler, J., Walters, R., Agrawal, A., Barsic, A., & Parker, R. (2016, January). ATPase-Modulated Stress Granules Contain a Diverse Proteome and Substructure. *Cell*. Retrieved 2016-01-25, from http://linkinghub.elsevier.com/retrieve/pii/S009286741501702X doi: 10.1016/j.cell.2015.12.038

Jencks, W. P. (1981). On the attribution and additivity of binding energies. *Proceedings of the National Academy of Sciences*, *78*(7), 4046–4050. Retrieved 2017-05-19, from http://www.pnas.org/content/78/7/4046.short

Johnson, J. O., Mandrioli, J., Benatar, M., Abramzon, Y., Van Deerlin, V. M., Trojanowski, J. Q., Traynor, B. J. (2010, December). Exome Sequencing Reveals VCP Mutations as a Cause of Familial ALS. *Neuron*, *68*(5), 857–864. Retrieved 2016-02-19, from http://linkinghub.elsevier.com/retrieve/pii/S0896627310009785 doi: 10.1016/j.neuron.2010.11.036

Jonas, S., & Izaurralde, E. (2013, December). The role of disordered protein regions in the assembly of decapping complexes and RNP granules. *Genes & Development*, *27*(24), 2628–2641. Retrieved from http://genesdev.cshlp.org/content/27/24/2628.full doi: 10.1101/gad.227843.113

Kaehler, C., Isensee, J., Hucho, T., Lehrach, H., & Krobitsch, S. (2014, April). 5-Fluorouracil affects assembly of stress granules based on RNA incorporation. *Nucleic Acids Research*, gku264. Retrieved from http://nar.oxfordjournals.org/lookup/doi/10.1093/nar/gku264 doi: 10.1093/nar/gku264

Kai, M. (2016, February). Roles of RNA-Binding Proteins in DNA Damage Response. *International Journal of Molecular Sciences*, *17*(3), 310. Retrieved 2017-02-03, from http://www.mdpi.com/1422-0067/17/3/310 doi: 10.3390/ijms17030310

Kaiser, T. E., Intine, R. V., & Dundr, M. (2008, December). De Novo Formation of a Subnuclear Body. *Science*, *322*(5908), 1713–1717. Retrieved 2016-12-15, from http://www.sciencemag.org/cgi/doi/10.1126/science.1165322 doi: 10.1126/science.1165216

Kato, M., Han, T. W., Xie, S., Shi, K., Du, X., Wu, L. C., McKnight, S. L. (2012, May). Cell-free Formation of RNA Granules: Low Complexity Sequence Domains Form Dynamic Fibers within Hydrogels. *Cell*, *149*(4), 753–767. Retrieved from http://dx.doi.org/10.1016/j.cell.2012.04.017 doi: 10.1016/j.cell.2012.04.017

Kedersha, N., Ivanov, P., & Anderson, P. (2013, October). Stress granules and cell signaling: more than just a passing phase? *Trends in Biochemical Sciences*, *38*(10), 494–506. Retrieved 2017-02-03, from http://linkinghub.elsevier.com/retrieve/pii/S096800041300131X doi: 10.1016/j.tibs.2013.07.004

Kedersha, N., Panas, M. D., Achorn, C. A., Lyons, S., Tisdale, S., Hickman, T., Anderson, P. (2016, March). G3bpCaprin1USP10 complexes mediate stress granule condensation and associate with 40s subunits. *The Journal of Cell Biology*, *212*(7), 845–860. Retrieved 2016-04-05, from http://www.jcb.org/lookup/doi/10.1083/jcb.201508028 doi: 10.1083/jcb.201508028

Kedersha, N., Stoecklin, G., Ayodele, M., Yacono, P., Lykke-Andersen, J., Fritzler, M. J., Anderson, P. (2005, June). Stress granules and processing bodies are dynamically linked sites of mRNP remodeling. *The Journal of Cell Biology*, *169*(6), 871–884. Retrieved from http://www.jcb.org/cgi/doi/10.1083/jcb.200502088 doi:

10.1083/jcb.200502088

Kim, H. J., Kim, N. C., Wang, Y.-D., Scarborough, E. A., Moore, J., Diaz, Z., Taylor, J. P. (2013, March). Mutations in prion-like domains in hnRNPA2b1 and hnRNPA1 cause multisystem proteinopathy and ALS. *Nature*, *495*(7442), 467–473. Retrieved from http://dx.doi.org/10.1038/nature11922 doi: 10.1038/nature11922

Kim, W. J., Back, S. H., Kim, V., Ryu, I., & Jang, S. K. (2005, March). Sequestration of TRAF2 into Stress Granules Interrupts Tumor Necrosis Factor Signaling under Stress Conditions. *Molecular and Cellular Biology*, *25*(6), 2450–2462. Retrieved 2016-01-18, from http://mcb.asm.org/cgi/doi/10.1128/MCB.25.6.2450-2462.2005 doi: 10.1128/MCB.25.6.2450-2462.2005

Kimonis, V. E., Mehta, S. G., Fulchiero, E. C., Thomasova, D., Pasquali, M., Boycott, K., Watts, G. D. J. (2008, March). Clinical studies in familial VCP myopathy associated with Paget disease of bone and frontotemporal dementia. *American Journal of Medical Genetics Part A*, *146A*(6), 745–757. Retrieved 2016-02-19, from http://doi.wiley.com/10.1002/ajmg.a.31862 doi: 10.1002/ajmg.a.31862

King, O. D., Gitler, A. D., & Shorter, J. (2012, June). The tip of the iceberg: RNA-binding proteins with prion-like domains in neurodegenerative disease. *Brain Research*, *1462*, 61–80. Retrieved from http://www.sciencedirect.com/science/article/pii/S0006899312000546 doi: 10.1016/j.brainres.2012.01.016

Klar, J., Sobol, M., Melberg, A., Mbert, K., Ameur, A., Johansson, A. C., Dahl, N. (2013, January). Welander Distal Myopathy Caused by an Ancient Founder Mutation in *TIA1* Associated with Perturbed Splicing. *Human Mutation*, n/a–n/a. Retrieved 2016-02-19, from http://doi.wiley.com/10.1002/humu.22282 doi: 10.1002/humu.22282

Kroschwald, S., Maharana, S., Mateju, D., Malinovska, L., Nske, E., Poser, I., Alberti, S. (2015). Promiscuous interactions and protein disaggregases determine the material state of stress-inducible RNP granules. *eLife*, *4*, e06807. Retrieved 2015-09-04, from http://elifesciences.org/content/4/e06807.abstract

Kwon, S., Zhang, Y., & Matthias, P. (2007, December). The deacetylase HDAC6 is a novel critical component of stress granules involved in the stress response. *Genes & Development*, *21*(24), 3381–3394. Retrieved 2016-02-23, from http://www.genesdev.org/cgi/doi/10.1101/gad.461107 doi: 10.1101/gad.461107

Lee, C., Occhipinti, P., & Gladfelter, A. S. (2015, March). PolyQ-dependent RNAprotein assemblies control symmetry breaking. *The Journal of Cell Biology*, *208*(5), 533–544. Retrieved 2016-09-15, from http://www.jcb.org/lookup/doi/10.1083/jcb.201407105 doi: 10.1083/jcb.201407105

Lee, C. F., Brangwynne, C. P., Gharakhani, J., Hyman, A. A., & Jlicher, F. (2013, August). Spatial organization of the cell cytoplasm by position-dependent phase

separation. *Physical Review Letters*, *111*(8), 088101.

Leung, A. K. L., Vyas, S., Rood, J. E., Bhutkar, A., Sharp, P. A., & Chang, P. (2011, May). Poly(ADP-Ribose) Regulates Stress Responses and MicroRNA Activity in the Cytoplasm. *Molecular Cell*, *42*(4), 489–499. Retrieved from http://linkinghub.elsevier.com/retrieve/pii/S1097276511003194 doi: 10.1016/j.molcel.2011.04.015

Li, P., Banjade, S., Cheng, H.-C., Kim, S., Chen, B., Guo, L., Rosen, M. K. (2012, March). Phase transitions in the assembly of multivalent signalling proteins. *Nature*, *483*(7389), 336–340. Retrieved from http://dx.doi.org/10.1038/nature10879 doi: 10.1038/nature10879

Li, S., Zhang, P., Freibaum, B. D., Kim, N. C., Kolaitis, R.-M., Molliex, A., Kim, H. J. (2016, March). Genetic interaction of hnRNPA2b1 and DNAJB6 in a *Drosophila* model of multisystem proteinopathy. *Human Molecular Genetics*, *25*(5), 936–950. Retrieved 2016-04-27, from http://www.hmg.oxfordjournals.org/lookup/doi/10.1093/hmg/ddv627 doi: 10.1093/hmg/ddv627

Li, Y. R., King, O. D., Shorter, J., & Gitler, A. D. (2013, April). Stress granules as crucibles of ALS pathogenesis. *The Journal of Cell Biology*, *201*(3), 361–372. Retrieved 2016-02-18, from http://www.jcb.org/lookup/doi/10.1083/jcb.201302044 doi: 10.1083/jcb.201302044

Lin, Y., Protter, D., Rosen, M., & Parker, R. (2015, October). Formation and Maturation of Phase-Separated Liquid Droplets by RNA-Binding Proteins. *Molecular Cell*, *60*(2), 208–219. Retrieved 2015-10-19, from http://linkinghub.elsevier.com/retrieve/pii/S1097276515006644 doi: 10.1016/j.molcel.2015.08.018

Ling, S.-C., Polymenidou, M., & Cleveland, D. (2013, August). Converging Mechanisms in ALS and FTD: Disrupted RNA and Protein Homeostasis. *Neuron*, *79*(3), 416–438. Retrieved 2016-02-19, from http://linkinghub.elsevier.com/retrieve/pii/S0896627313006570 doi: 10.1016/j.neuron.2013.07.033

Ling, S. H. M., Decker, C. J., Walsh, M. A., She, M., Parker, R., & Song, H. (2008, October). Crystal Structure of Human Edc3 and Its Functional Implications. *Molecular and Cellular Biology*, *28*(19), 5965–5976. Retrieved 2015-07-15, from http://mcb.asm.org/cgi/doi/10.1128/MCB.00761-08 doi: 10.1128/MCB.00761-08

Little, S. C., Sinsimer, K. S., Lee, J. J., Wieschaus, E. F., & Gavis, E. R. (2015, April). Independent and coordinate trafficking of single Drosophila germ plasm mRNAs. *Nature Cell Biology*, *17*(5), 558–568. Retrieved 2015-09-29, from http://www.nature.com/doifinder/10.1038/ncb3143 doi: 10.1038/ncb3143

Loschi, M., Leishman, C. C., Berardone, N., & Boccaccio, G. L. (2009, November). Dynein and kinesin regulate stress-granule and P-body dynamics. *Journal of Cell Science*, *122*(21), 3973–3982. Retrieved 2015-09-

28, from http://jcs.biologists.org/cgi/doi/10.1242/jcs.051383 doi: 10.1242/jcs.051383

Lyons, S. M., Ricciardi, A. S., Guo, A. Y., Kambach, C., & Marzluff, W. F. (2014, January). The C-terminal extension of Lsm4 interacts directly with the 3' end of the histone mRNP and is required for efficient histone mRNA degradation. *RNA*, *20*(1), 88–102. Retrieved 2017-01-25, from http://rnajournal.cshlp.org/cgi/doi/10.1261/rna.042531.113 doi: 10.1261/rna.042531.113

Martin, K. C., & Ephrussi, A. (2009, February). mRNA Localization: Gene Expression in the Spatial Dimension. *Cell*, *136*(4), 719–730. Retrieved 2016-02-18, from http://linkinghub.elsevier.com/retrieve/pii/S0092867409001263 doi: 10.1016/j.cell.2009.01.044

Mayeda, A., Munroe, S. H., Cceres, J. F., & Krainer, A. R. (1994, November). Function of conserved domains of hnRNP A1 and other hnRNP A/B proteins. *The EMBO Journal*, *13*(22), 5483–5495. Retrieved from /pmc/articles/PMC395506/?report=abstract

Mazroui, R., Di Marco, S., Kaufman, R. J., & Gallouzi, I.-E. (2007). Inhibition of the ubiquitin-proteasome system induces stress granule formation. *Molecular Biology of the Cell*, *18*(7), 2603–2618.

Meyer, H., & Weihl, C. C. (2014, September). The VCP/p97 system at a glance: connecting cellular function to disease pathogenesis. *Journal of Cell Science*, *127*(18), 3877–3883. Retrieved 2016-02-19, from http://jcs.biologists.org/cgi/doi/10.1242/jcs.093831 doi: 10.1242/jcs.093831

Milo, R. (2013, December). What is the total number of protein molecules per cell volume? A call to rethink some published values: Insights & Perspectives. *BioEssays*, *35*(12), 1050–1055. Retrieved 2016-08-24, from http://doi.wiley.com/10.1002/bies.201300066 doi: 10.1002/bies.201300066

Minezaki, Y., Homma, K., Kinjo, A. R., & Nishikawa, K. (2006, June). Human Transcription Factors Contain a High Fraction of Intrinsically Disordered Regions Essential for Transcriptional Regulation. *Journal of Molecular Biology*, *359*(4), 1137–1149. Retrieved 2017-02-03, from http://linkinghub.elsevier.com/retrieve/pii/S0022283606004669 doi: 10.1016/j.jmb.2006.04.016

Mitrea, D. M., Cika, J. A., Guy, C. S., Ban, D., Banerjee, P. R., Stanley, C. B., Kriwacki, R. W. (2016). Nucleophosmin integrates within the nucleolus via multi-modal interactions with proteins displaying R-rich linear motifs and rRNA. *eLife*, *5*, e13571. Retrieved 2017-02-03, from https://elifesciences.org/content/5/e13571v3

Molliex, A., Temirov, J., Lee, J., Coughlin, M., Kanagaraj, A., Kim, H., Taylor, J. (2015, September). Phase Separation by Low Complexity Domains Promotes Stress Granule Assembly and Drives Pathological Fibrillization. *Cell*, *163*(1), 123–133. Retrieved 2016-02-19, from

http://linkinghub.elsevier.com/retrieve/pii/S0092867415011769 doi: 10.1016/j.cell.2015.09.015

Mu, X., Fu, Y., Zhu, Y., Wang, X., Xuan, Y., Shang, H., Gao, G. (2015, August). HIV-1 Exploits the Host Factor RuvB-like 2 to Balance Viral Protein Expression. *Cell Host & Microbe*, *18*(2), 233–242. Retrieved 2016-02-19, from http://linkinghub.elsevier.com/retrieve/pii/S1931312815002668 doi: 10.1016/j.chom.2015.06.018

Nadezhdina, E. S., Lomakin, A. J., Shpilman, A. A., Chudinova, E. M., & Ivanov, P. A. (2010, March). Microtubules govern stress granule mobility and dynamics. *Biochimica et Biophysica Acta (BBA) - Molecular Cell Research*, *1803*(3), 361–371. Retrieved 2015-09-29, from http://linkinghub.elsevier.com/retrieve/pii/S0167488909002985 doi: 10.1016/j.bbamcr.2009.12.004

Nott, T., Petsalaki, E., Farber, P., Jervis, D., Fussner, E., Plochowietz, A., Baldwin, A. (2015, March). Phase Transition of a Disordered Nuage Protein Generates Environmentally Responsive Membraneless Organelles. *Molecular Cell*, *57*(5), 936–947. Retrieved 2015-03-31, from http://linkinghub.elsevier.com/retrieve/pii/S1097276515000143 doi: 10.1016/j.molcel.2015.01.013

Ohn, T., Kedersha, N., Hickman, T., & Tisdale, S. (2008, January). A functional RNAi screen links O-GlcNAc modification of ribosomal proteins to stress granule and processing body assembly. *Nature Cell*. Retrieved from http://www.nature.com/ncb/journal/v10/n10/abs/ncb1783.html

Onomoto, K., Jogi, M., Yoo, J.-S., Narita, R., Morimoto, S., Takemura, A., Fujita, T. (2012, August). Critical Role of an Antiviral Stress Granule Containing RIG-I and PKR in Viral Detection and Innate Immunity. *PLoS ONE*, *7*(8), e43031. Retrieved 2016-02-19, from http://dx.plos.org/10.1371/journal.pone.0043031 doi: 10.1371/journal.pone.0043031

Pak, C., Kosno, M., Holehouse, A., Padrick, S., Mittal, A., Ali, R., Rosen, M. (2016, July). Sequence Determinants of Intracellular Phase Separation by Complex Coacervation of a Disordered Protein. *Molecular Cell*, *63*(1), 72–85. Retrieved 2016-07-11, from http://linkinghub.elsevier.com/retrieve/pii/S1097276516302283 doi: 10.1016/j.molcel.2016.05.042

Parker, R., & Sheth, U. (2007, March). P Bodies and the Control of mRNA Translation and Degradation. *Molecular Cell*, *25*(5), 635–646. Retrieved 2016-02-18, from http://linkinghub.elsevier.com/retrieve/pii/S1097276507001116 doi: 10.1016/j.molcel.2007.02.011

Patel, A., Lee, H., Jawerth, L., Maharana, S., Jahnel, M., Hein, M., Alberti, S. (2015, August). A Liquid-to-Solid Phase Transition of the ALS Protein FUS Accelerated by Disease Mutation. *Cell*, *162*(5), 1066–1077. Retrieved 2015-09-17, from http://linkinghub.elsevier.com/retrieve/pii/S0092867415009630 doi: 10.1016/j.cell.2015.07.047

Patel, A., Malinovska, L., Saha, S., Wang, J., Alberti, S., Krishnan, Y., & Hyman, A. A. (2017). ATP as a biological hydrotrope. *Science*, *356*(6339), 753–756. Retrieved 2017-07-16, from http://science.sciencemag.org/content/356/6339/753.abstract

Ramaswami, M., Taylor, J., & Parker, R. (2013, August). Altered Ribostasis: RNA-Protein Granules in Degenerative Disorders. *Cell*, *154*(4), 727–736. Retrieved 2015-08-12, from http://linkinghub.elsevier.com/retrieve/pii/S009286741300946X doi: 10.1016/j.cell.2013.07.038

Reijns, M. A. M., Alexander, R. D., Spiller, M. P., & Beggs, J. D. (2008, August). A role for Q/N-rich aggregation-prone regions in P-body localization. *Journal of Cell Science*, *121*(Pt 15), 2463–2472. Retrieved from http://jcs.biologists.org/cgi/doi/10.1242/jcs.024976 doi: 10.1242/jcs.024976

Reineke, L. C., Kedersha, N., Langereis, M. A., van Kuppeveld, F. J. M., & Lloyd, R. E. (2015, May). Stress Granules Regulate Double-Stranded RNA-Dependent Protein Kinase Activation through a Complex Containing G3bp1 and Caprin1. *mBio*, *6*(2), e02486–14. Retrieved 2015-05-05, from http://mbio.asm.org/lookup/doi/10.1128/mBio.02486-14 doi: 10.1128/mBio.02486-14

Reineke, L. C., & Lloyd, R. E. (2013, February). Diversion of stress granules and P-bodies during viral infection. *Virology*, *436*(2), 255–267. Retrieved 2016-02-19, from http://linkinghub.elsevier.com/retrieve/pii/S0042682212005909 doi: 10.1016/j.virol.2012.11.017

Reineke, L. C., & Lloyd, R. E. (2015, March). The Stress Granule Protein G3bp1 Recruits Protein Kinase R To Promote Multiple Innate Immune Antiviral Responses. *Journal of Virology*, *89*(5), 2575–2589. Retrieved 2016-02-19, from http://jvi.asm.org/lookup/doi/10.1128/JVI.02791-14 doi: 10.1128/JVI.02791-14

Riback, J. A., Katanski, C. D., Kear-Scott, J. L., Pilipenko, E. V., Rojek, A. E., Sosnick, T. R., & Drummond, D. A. (2017, March). Stress-Triggered Phase Separation Is an Adaptive, Evolutionarily Tuned Response. *Cell*, *168*(6), 1028–1040.e19. Retrieved 2017-05-09, from http://linkinghub.elsevier.com/retrieve/pii/S0092867417302428 doi: 10.1016/j.cell.2017.02.027

Schwartz, J. C., Wang, X., Podell, E. R., & Cech, T. R. (2013, November). RNA Seeds Higher-Order Assembly of FUS Protein. *Cell Reports*, *5*(4), 918–925. Retrieved from http://linkinghub.elsevier.com/retrieve/pii/S2211124713006840 doi: 10.1016/j.celrep.2013.11.017

Sheth, U., Pitt, J., Dennis, S., & Priess, J. R. (2010, April). Perinuclear P granules are the principal sites of mRNA export in adult C. elegans germ cells. *Development*, *137*(8), 1305–1314. Retrieved 2015-08-

24, from http://dev.biologists.org/cgi/doi/10.1242/dev.044255 doi: 10.1242/dev.044255

Shin, Y., Berry, J., Pannucci, N., Haataja, M. P., Toettcher, J. E., & Brangwynne, C. P. (2016, December). Spatiotemporal Control of Intracellular Phase Transitions Using Light-Activated optoDroplets. *Cell*. Retrieved 2017-01-10, from http://linkinghub.elsevier.com/retrieve/pii/S009286741631666X doi: 10.1016/j.cell.2016.11.054

Smith, J., Calidas, D., Schmidt, H., Lu, T., Rasoloson, D., & Seydoux, G. (2016, December). Spatioal patterning of P granules by RNA-induced phase separation of the intrinsically-disordered protein MEG-3. *eLife*. doi: 10.7554/eLife.21337

Solomon, S., Xu, Y., Wang, B., David, M. D., Schubert, P., Kennedy, D., & Schrader, J. W. (2007, March). Distinct Structural Features ofCaprin-1 Mediate Its Interaction with G3bp-1 and Its Induction of Phosphorylation of Eukaryotic Translation Initiation Factor 2 , Entry to Cytoplasmic Stress Granules, and Selective Interaction with a Subset of mRNAs. *Molecular and Cellular Biology*, *27*(6), 2324–2342. Retrieved 2016-02-18, from http://mcb.asm.org/cgi/doi/10.1128/MCB.02300-06 doi: 10.1128/MCB.02300-06

Somasekharan, S. P., El-Naggar, A., Leprivier, G., Cheng, H., Hajee, S., Grunewald, T. G. P., Sorensen, P. H. (2015, March). YB-1 regulates stress granule formation and tumor progression by translationally activating G3bp1. *The Journal of Cell Biology*, *208*(7), 913–929. Retrieved 2015-04-07, from http://www.jcb.org/cgi/doi/10.1083/jcb.201411047 doi: 10.1083/jcb.201411047

Souquere, S., Mollet, S., Kress, M., Dautry, F., Pierron, G., & Weil, D. (2009, October). Unravelling the ultrastructure of stress granules and associated P-bodies in human cells. *Journal of Cell Science*, *122*(20), 3619–3626. Retrieved 2015-08-20, from http://jcs.biologists.org/cgi/doi/10.1242/jcs.054437 doi: 10.1242/jcs.054437

Spector, D. L. (2006, December). SnapShot: Cellular Bodies. *Cell*, *127*(5), 1071.e1–1071.e2. Retrieved 2016-02-18, from http://linkinghub.elsevier.com/retrieve/pii/S0092867406015297 doi: 10.1016/j.cell.2006.11.026

Sun, Z., Diaz, Z., Fang, X., Hart, M. P., Chesi, A., Shorter, J., & Gitler, A. D. (2011, April). Molecular Determinants and Genetic Modifiers of Aggregation and Toxicity for the ALS Disease Protein FUS/TLS. *PLoS Biology*, *9*(4), e1000614. Retrieved 2017-06-29, from http://dx.plos.org/10.1371/journal.pbio.1000614 doi: 10.1371/journal.pbio.1000614

Takahara, T., & Maeda, T. (2012, July). Transient Sequestration of TORC1 into Stress Granules during Heat Stress. *Molecular Cell*, *47*(2), 242–252. Retrieved 2016-02-19, from http://linkinghub.elsevier.com/retrieve/pii/S1097276512004030 doi: 10.1016/j.molcel.2012.05.019

Teixeira, D., Sheth, U., Valencia-Sanchez, M. A., Brengues, M., & Parker,

R. (2005, April). Processing bodies require RNA for assembly and contain nontranslating mRNAs. *RNA*, *11*(4), 371–382. Retrieved from http://www.rnajournal.org/cgi/doi/10.1261/rna.7258505 doi: 10.1261/rna.7258505

Thedieck, K., Holzwarth, B., Prentzell, M., Boehlke, C., Klsener, K., Ruf, S., Baumeister, R. (2013, August). Inhibition of mTORC1 by Astrin and Stress Granules Prevents Apoptosis in Cancer Cells. *Cell*, *154*(4), 859–874. Retrieved 2016-02-19, from http://linkinghub.elsevier.com/retrieve/pii/S0092867413009021 doi: 10.1016/j.cell.2013.07.031

Tourriere, H. (2003, March). The RasGAP-associated endoribonuclease G3bp assembles stress granules. *The Journal of Cell Biology*, *160*(6), 823–831. Retrieved 2015-06-18, from http://www.jcb.org/cgi/doi/10.1083/jcb.200212128 doi: 10.1083/jcb.200212128

Tsai, N. P., Ho, P. C., & Wei, L. N. (2008, January). Regulation of stress granule dynamics by Grb7 and FAK signalling pathway. *The EMBO journal*, *27*(5), 715–726. Retrieved from http://onlinelibrary.wiley.com/doi/10.1038/emboj.2008.19/full doi: 10.1038/emboj.2008.19

Updike, D. L., Hachey, S. J., Kreher, J., & Strome, S. (2011, March). P granules extend the nuclear pore complex environment in the C. elegans germ line. *The Journal of Cell Biology*, *192*(6), 939–948. Retrieved 2015-06-18, from http://www.jcb.org/cgi/doi/10.1083/jcb.201010104 doi: 10.1083/jcb.201010104

Vanderweyde, T., Yu, H., Varnum, M., Liu-Yesucevitz, L., Citro, A., Ikezu, T., Wolozin, B. (2012, June). Contrasting Pathology of the Stress Granule Proteins TIA-1 and G3bp in Tauopathies. *Journal of Neuroscience*, *32*(24), 8270–8283. Retrieved 2015-10-15, from http://www.jneurosci.org/cgi/doi/10.1523/JNEUROSCI.1592-12.2012 doi: 10.1523/JNEUROSCI.1592-12.2012

Wallace, E., Kear-Scott, J., Pilipenko, E., Schwartz, M., Laskowski, P., Rojek, A., Drummond, D. (2015, September). Reversible, Specific, Active Aggregates of Endogenous Proteins Assemble upon Heat Stress. *Cell*, *162*(6), 1286–1298. Retrieved 2016-02-17, from http://linkinghub.elsevier.com/retrieve/pii/S0092867415010934 doi: 10.1016/j.cell.2015.08.041

Walters, R. W., Muhlrad, D., Garcia, J., & Parker, R. (2015, September). Differential effects of Ydj1 and Sis1 on Hsp70-mediated clearance of stress granules in *Saccharomyces cerevisiae*. *RNA*, *21*(9), 1660–1671. Retrieved 2015-09-14, from http://rnajournal.cshlp.org/lookup/doi/10.1261/rna.053116.115 doi: 10.1261/rna.053116.115

Wang, J. T., Smith, J., Chen, B.-C., Schmidt, H., Rasoloson, D., Paix, A., Seydoux, G. (2015). Regulation of RNA granule dynamics by phosphorylation of serine-rich, intrinsically disordered proteins in C. elegans. *Elife*, *3*, e04591. Retrieved

2015-06-18, from http://elifesciences.org/content/3/e04591.abstract

Wang, P., Xue, Y., Han, Y., Lin, L., Wu, C., Xu, S., Cao, X. (2014, April). The STAT3-binding long noncoding RNA lnc-DC controls human dendritic cell differentiation. *Science*, *344*(6181), 310–313. Retrieved from http://www.sciencemag.org/cgi/doi/10.1126/science.1251456 doi: 10.1126/science.1251456

Weber, S., & Brangwynne, C. (2015, March). Inverse Size Scaling of the Nucleolus by a Concentration-Dependent Phase Transition. *Current Biology*, *25*(5), 641–646. Retrieved 2016-12-15, from http://linkinghub.elsevier.com/retrieve/pii/S0960982215000147 doi: 10.1016/j.cub.2015.01.012

Weber, S. C., & Brangwynne, C. P. (2012, June). Getting RNA and protein in phase. *Cell*, *149*(6), 1188–1191. Retrieved from http://linkinghub.elsevier.com/retrieve/pii/S0092867412006344 doi: 10.1016/j.cell.2012.05.022

Wippich, F., Bodenmiller, B., Trajkovska, M., Wanka, S., Aebersold, R., & Pelkmans, L. (2013, February). Dual Specificity Kinase DYRK3 Couples Stress Granule Condensation/Dissolution to mTORC1 Signaling. *Cell*, *152*(4), 791–805. Retrieved 2016-02-18, from http://linkinghub.elsevier.com/retrieve/pii/S0092867413000858 doi: 10.1016/j.cell.2013.01.033

Xiang, S., Kato, M., Wu, L., Lin, Y., Ding, M., Zhang, Y., McKnight, S. (2015, November). The LC Domain of hnRNPA2 Adopts Similar Conformations in Hydrogel Polymers, Liquid-like Droplets, and Nuclei. *Cell*, *163*(4), 829–839. Retrieved 2015-11-06, from http://linkinghub.elsevier.com/retrieve/pii/S0092867415013549 doi: 10.1016/j.cell.2015.10.040

Yang, X., Shen, Y., Garre, E., Hao, X., Krumlinde, D., Cvijovi, M., Sunnerhagen, P. (2014, November). Stress Granule-Defective Mutants Deregulate Stress Responsive Transcripts. *PLoS Genetics*, *10*(11), e1004763. Retrieved 2016-02-18, from http://dx.plos.org/10.1371/journal.pgen.1004763 doi: 10.1371/journal.pgen.1004763

Yang, Z. (2004, November). GW182 is critical for the stability of GW bodies expressed during the cell cycle and cell proliferation. *Journal of Cell Science*, *117*(23), 5567–5578. Retrieved 2015-08-24, from http://jcs.biologists.org/cgi/doi/10.1242/jcs.01477 doi: 10.1242/jcs.01477

Yeo, G. C., Keeley, F. W., & Weiss, A. S. (2011, September). Coacervation of tropoelastin. *Advances in Colloid and Interface Science*, *167*(1-2), 94–103. Retrieved 2017-06-29, from http://linkinghub.elsevier.com/retrieve/pii/S0001868610001764 doi: 10.1016/j.cis.2010.10.003

Zhang, H., Elbaum-Garfinkle, S., Langdon, E. M., Taylor, N., Occhipinti, P.,

Bridges, A., Gladfelter, A. (2015, October). RNA Controls PolyQ Protein Phase Transitions. *Molecular Cell*, *60*(2), 220–230. Retrieved 2016-02-23, from http://linkinghub.elsevier.com/retrieve/pii/S1097276515007376 doi: 10.1016/j.molcel.2015.09.017

Zhang, K., Donnelly, C. J., Haeusler, A. R., Grima, J. C., Machamer, J. B., Steinwald, P., Rothstein, J. D. (2015, August). The C9orf72 repeat expansion disrupts nucleocytoplasmic transport. *Nature*, *525*(7567), 56–61. Retrieved 2016-02-19, from http://www.nature.com/doifinder/10.1038/nature14973 doi: 10.1038/nature14973